



POLITECNICO DI MILANO

FACOLTÀ DI INGEGNERIA INDUSTRIALE

CORSO DI LAUREA IN INGEGNERIA MECCANICA

**An automated method for the FE
analysis of 3D cracks under
mixed mode loading**

Supervisor:
Prof. Mario GUAGLIANO

Student:
Dimitar DANOV
Matr.: 722574

Academic Year 2010 – 2011

I would like to dedicate this work to my
parents,

Neda and Atanas

for their boundless patience and incredible
support!

Acknowledgements

I would like to thank my supervisor Prof. Guagliano, for his trust and for giving me both freedom and opportunity to explore fields, which I am interested in.

Contents

1	Introduction	1
1.1	Previous development and foundation of the present work	1
1.1.1	Background	1
1.1.2	Present work	1
1.2	Programming side	2
1.2.1	Abaqus structure and script execution	2
1.2.2	Python and Abaqus	2
1.2.3	On programming style	3
1.3	Motivation	3
1.3.1	Automation	3
1.3.2	Post-processing	3
1.3.3	Visualization	4
1.4	Significance of the work	4
1.4.1	Modeling	4
1.4.2	Automation	4
1.4.3	Post-processing	4
1.4.4	Scalability	5
1.4.5	Knowledge base	5
2	Theoretical overview	6
2.1	Introduction	6
2.2	Fracture mechanics overview	6
2.2.1	LEFM scope	6
2.2.2	Stress intensity factors K	6
2.2.3	Energy approach to Fracture Mechanics	12
2.2.4	Elliptic cracks	15
2.3	LEFM analysis with FEM	18
2.3.1	Special crack tip elements	18
2.3.2	Calculation of the stress intensity factors	18
2.4	XFEM	20
2.4.1	Introduction	20
2.4.2	<i>XFEM</i> concepts	21
2.4.3	Partition of unity based methods	23
2.4.4	XFEM formulation	24
2.4.5	<i>XFEM</i> crack definition in Abaqus	25
2.4.6	Crack analysis with <i>XFEM</i>	25
2.5	Fracture mechanics software	26
2.5.1	Zenocrack	26

2.5.2	FRANC2D and FRANC3D	26
2.5.3	NASGRO	27
2.5.4	AFGROW	27
2.5.5	ADAPCRACK3D	27
3	Methodology	28
3.1	Introduction	28
3.2	Description of the model types	28
3.2.1	FEM – <i>crackNormal</i> model type	28
3.2.2	Model types for XFEM analysis	34
3.2.3	XFEM <i>simple</i> model type	34
3.2.4	XFEM <i>crackPartition</i> model type	35
3.2.5	XFEM <i>multiplePartitions</i> model type	37
3.3	Visualization Odb	39
3.3.1	Node data	39
3.3.2	Element data	40
3.3.3	Field output data	40
3.4	GUI and Abaqus integration	40
3.4.1	First dialog box	40
3.4.2	Second dialog box	41
3.5	Organization of the application	42
3.5.1	Structure by function	43
3.5.2	Directory structure and modules	44
3.6	Description of classes	45
3.6.1	Classes interaction	45
3.6.2	DataStr classes	46
3.6.3	Model database classes	53
3.6.4	ReadOdb() class	66
3.6.5	PersistentData() class	67
3.6.6	DbDataStr() class	68
3.6.7	AnalyticalData classes	69
3.6.8	XYPlotDataFromDbEntry() class	72
3.6.9	VisualizationOdbFromDbEntry() class	72
3.6.10	GUI classes	75
3.6.11	CreateID function family	79
3.6.12	Execute gui commands functions	79
3.6.13	Main loop	80
4	Results	82
4.1	Introduction	82
4.2	Procedure	82
4.3	Delimitations	83
4.4	Element type comparison	83
4.5	Analysis of the influence of the cylinder dimensions	87
4.6	Mesh convergence analysis	90
4.6.1	Mesh convergence analysis with quadratic reduced integration elements	90
4.6.2	Mesh convergence analysis with linear reduced integration elements	93
4.7	Comparison between mesh transformations	95

4.7.1	Comparison between <i>elliptic</i> and <i>simpleScale</i> mesh transformations	95
4.7.2	<i>advancedScale</i> mesh transformation	102
4.8	XFEM results	103
4.8.1	Mesh and singularity radius convergence study	103
4.8.2	Comparison of the values and errors of the calculated stress intensity factors by <i>XFEM</i>	111
4.8.3	Comparison between <i>FEM</i> and <i>XFEM</i> results	114
4.9	Visualization of the stress intensity factors	119
5	Conclusion	123
5.1	Introduction	123
5.2	Summary of results	123
5.3	Implications for practice and recommendations	124
5.4	Implications for further development	124
5.4.1	Modeling automation	124
5.4.2	Results processing and optimization	124
5.4.3	Other functionality	124
5.5	Conclusion	125

List of Figures

1.1	Execution of script commands	2
2.1	Polar coordinate system at the crack tip	7
2.2	The three load type modes of a crack	8
2.3	Crack with blunted tip	11
2.4	Crack in biaxially loaded plate	11
2.5	Stress distribution in the vicinity of the crack tip	13
2.6	Visualization of the yield stress boundaries of the crack tip plastic zone	13
2.7	Total energy of a plate as a function of the crack length a	14
2.8	Potential energy release rate for <i>EPFM</i> and <i>LEFM</i> for different loads	15
2.9	Elliptic crack types	16
2.10	Elliptic crack plane	16
2.11	Orientation of an elliptic crack	17
2.12	Special crack tip elements	19
2.13	Zones of elements around a crack tip	21
2.14	Standard, enriched and blending elements in a domain	23
2.15	Level set functions for a flat crack	24
2.16	Crack flanks and crack tip	25
2.17	Crack domain and crack geometry	26
3.1	Cross section of the crackNormal model	29
3.2	crackNormal model	32
3.3	<i>WEDGE</i> elements of the inner cylinder of the crackNormal model	34
3.4	<i>crack domain</i> of the <i>crackPartition</i> model	36
3.5	<i>crack domain</i> of the <i>multiplePartitions</i> model	38
3.6	Visualization output database	39
3.7	First dialog box of the program user interface	41
3.8	Second dialog box of the program user interface	43
3.9	Classes interaction	46
4.1	Comparison of values for K_I obtained for <i>crackNormal</i> model type with different element types and <i>elliptic</i> transformation	84
4.2	Comparison of values for K_{II} obtained for <i>crackNormal</i> model type with different element types and <i>elliptic</i> transformation	84
4.3	Comparison of values for K_I obtained for <i>crackNormal</i> model type with different element types and <i>elliptic</i> transformation	85

4.4	Comparison of errors for K_I obtained for <i>crackNormal</i> model type with different element types and <i>elliptic</i> transformation . . .	85
4.5	Comparison of errors for K_{II} obtained for <i>crackNormal</i> model type with different element types and <i>elliptic</i> transformation . . .	86
4.6	Comparison of errors for K_{III} obtained for <i>crackNormal</i> model type with different element types and <i>elliptic</i> transformation . . .	86
4.7	Convergence study for cylinder dimensions against the maximum errors for K_I	87
4.8	Convergence study for cylinder dimensions against the maximum errors for K_{II}	88
4.9	Convergence study for cylinder dimensions against the maximum errors for K_{III}	88
4.10	Comparison of errors for K_I along the crack front for different cylinder dimensions	89
4.11	Comparison of errors for K_{II} along the crack front for different cylinder dimensions	89
4.12	Comparison of errors for K_{III} along the crack front for different cylinder dimensions	90
4.13	Comparison of errors for K_I along the crack front for different mesh densities of <i>quadratic reduced integration</i> elements	91
4.14	Comparison of errors for K_{II} along the crack front for different mesh densities of <i>quadratic reduced integration</i> elements	92
4.15	Comparison of errors for K_{III} along the crack front for different mesh densities of <i>quadratic reduced integration</i> elements	92
4.16	Comparison of errors for K_I along the crack front for different mesh densities of <i>linear reduced integration</i> elements	94
4.17	Comparison of errors for K_{II} along the crack front for different mesh densities of <i>linear reduced integration</i> elements	94
4.18	Comparison of errors for K_{III} along the crack front for different mesh densities of <i>linear reduced integration</i> elements	95
4.19	Comparison of errors for K_I for <i>elliptic</i> and <i>simpleScale</i> mesh transformation along the crack front for crack with aspect ratio of 3	96
4.20	Comparison of errors for K_{II} for <i>elliptic</i> and <i>simpleScale</i> mesh transformation along the crack front for crack with aspect ratio of 3	96
4.21	Comparison of errors for K_{III} for <i>elliptic</i> and <i>simpleScale</i> mesh transformation along the crack front for crack with aspect ratio of 3	97
4.22	Comparison of errors for K_I for <i>elliptic</i> and <i>simpleScale</i> mesh transformation along the crack front for crack with aspect ratio of 5	97
4.23	Comparison of errors for K_{II} for <i>elliptic</i> and <i>simpleScale</i> mesh transformation along the crack front for crack with aspect ratio of 5	98
4.24	Comparison of errors for K_{III} for <i>elliptic</i> and <i>simpleScale</i> mesh transformation along the crack front for crack with aspect ratio of 5	98

4.25	Comparison of errors for K_I for <i>elliptic</i> and <i>simpleScale</i> mesh transformation along the crack front for crack with aspect ratio of 10	99
4.26	Comparison of errors for K_{II} for <i>elliptic</i> and <i>simpleScale</i> mesh transformation along the crack front for crack with aspect ratio of 10	99
4.27	Comparison of errors for K_{III} for <i>elliptic</i> and <i>simpleScale</i> mesh transformation along the crack front for crack with aspect ratio of 10	100
4.28	Comparison of the maximum errors for K_I for <i>elliptic</i> and <i>simpleScale</i> mesh transformations for crack with aspect ratios of 3, 5 and 10	101
4.29	Comparison of the maximum errors for K_{II} for <i>elliptic</i> and <i>simpleScale</i> mesh transformations for crack with aspect ratios of 3, 5 and 10	101
4.30	Comparison of the maximum errors for K_{III} for <i>elliptic</i> and <i>simpleScale</i> mesh transformations for crack with aspect ratios of 3, 5 and 10	102
4.31	Convergence study for <i>crackPartition</i> XFEM model for K_I stress intensity factor	103
4.32	Convergence study for <i>crackPartition</i> XFEM model for K_{II} stress intensity factor	104
4.33	Convergence study for <i>crackPartition</i> XFEM model for K_{III} stress intensity factor	104
4.34	Convergence study for <i>multiplePartitions</i> XFEM model for K_I stress intensity factor	107
4.35	Convergence study for <i>multiplePartitions</i> XFEM model for K_{II} stress intensity factor	107
4.36	Convergence study for <i>multiplePartitions</i> XFEM model for K_{III} stress intensity factor	108
4.37	Mesh and singularity radius convergence for K_I	109
4.38	Mesh and singularity radius convergence for K_{II}	110
4.39	Mesh and singularity radius convergence for K_{III}	110
4.40	Comparison of the calculated values for K_I along the crack front for the different <i>XFEM</i> model types	111
4.41	Comparison of the calculated values for K_{II} along the crack front for the different <i>XFEM</i> model types	112
4.42	Comparison of the calculated values for K_{III} along the crack front for the different <i>XFEM</i> model types	112
4.43	Errors of the calculated values for K_I along the crack front for the different <i>XFEM</i> model types	113
4.44	Errors of the calculated values for K_{II} along the crack front for the different <i>XFEM</i> model types	113
4.45	Errors of the calculated values for K_{III} along the crack front for the different <i>XFEM</i> model types	114
4.46	Comparison between the calculated values for K_I by <i>FEM</i> and <i>XFEM</i> along the crack front for crack with aspect ratio of 3 . . .	115
4.47	Comparison between the calculated values for K_{III} by <i>FEM</i> and <i>XFEM</i> along the crack front for crack with aspect ratio of 3 . . .	115

4.48	Comparison between the calculated errors for K_{III} by <i>FEM</i> and <i>XFEM</i> along the crack front for crack with aspect ratio of 3 . . .	116
4.49	Comparison between the calculated values for K_I by <i>FEM</i> and <i>XFEM</i> along the crack front for crack with aspect ratio of 5 . . .	116
4.50	Comparison between the calculated values for K_{III} by <i>FEM</i> and <i>XFEM</i> along the crack front for crack with aspect ratio of 3 . . .	117
4.51	Comparison between the calculated errors for K_{III} by <i>FEM</i> and <i>XFEM</i> along the crack front for crack with aspect ratio of 5 . . .	117
4.52	Comparison between the calculated values for K_I by <i>FEM</i> and <i>XFEM</i> along the crack front for crack with aspect ratio of 10 . .	118
4.53	Comparison between the calculated values for K_{III} by <i>FEM</i> and <i>XFEM</i> along the crack front for crack with aspect ratio of 10 . .	118
4.54	Comparison between the calculated errors for K_{III} by <i>FEM</i> and <i>XFEM</i> along the crack front for crack with aspect ratio of 10 . .	119
4.55	Visualization of the <i>1309848923dot31 FEM</i> model with crack aspect ratio 3	120
4.56	Visualization of the <i>1309869569dot74 XFEM</i> model with crack aspect ratio 3	120
4.57	Visualization of the <i>1310240764dot87 XFEM</i> model with crack aspect ratio 5	121
4.58	Visualization of the <i>1310240980dot74 XFEM</i> model with crack aspect ratio 10	121
4.59	Visualization of the <i>1309907898dot52 XFEM</i> model with crack aspect ratio 3	122

List of Tables

3.1	GUI tree abbreviation key	42
4.1	Models included in the element type study	84
4.2	Models in figures 4.10, 4.11 and 4.12	89
4.3	Models with <i>quadratic reduced integration</i> elements included in the mesh convergence study	91
4.4	Models with <i>linear reduced integration</i> elements included in the mesh convergence study	93
4.5	Models included in the comparison of mesh transformations . . .	100
4.6	Models of type <i>crackPartition</i> included in the convergence study	105
4.7	Models of type <i>multiplePartitions</i> included in the convergence study	106
4.8	Models of type <i>simple</i> included in the convergence study	109
4.9	Models included in the comparison of the accuracy of the different <i>XFEM</i> model types	112
4.10	<i>FEM</i> models included in the comparison of the accuracy with <i>XFEM</i> models	115
4.11	<i>XFEM</i> models included in the comparison of the accuracy with <i>FEM</i> models	116
4.12	Visualization of models	119

Abstract

Analysis of elliptic cracks under mixed mode loading is a challenging aspect of the design and life assessment of mechanical components. Nevertheless, perpetually increasing requirements in terms of safety and performance, demand an efficient procedure for accurate crack analysis.

A computer program is developed in the scope of the current project, aiming to address both efficiency and accuracy of analysis. The program is a plug-in to Abaqus finite element analysis program and automates significantly the modeling and analysis of stress intensity factors of elliptic cracks.

Elliptic cracks are analyzed with *FEM* and *XFEM*, and several mesh configurations are compared. A visualization technique is proposed for representation of stress intensity factors and results from the analyses are stored in custom database, providing a foundation for accumulating a large knowledge base including all analyzed crack configurations.

Results from the performed analyses prove that depending on the analysis type and mesh design, evaluated stress intensity factors may vary significantly.

Chapter 1

Introduction

1.1 Previous development and foundation of the present work

1.1.1 Background

Background of the current project is ref [7], which is focused on evaluation of stress intensity factors of elliptic cracks by *FEM*. For the purpose a model with the shape of a cylinder is introduced, which accommodates the analyzed crack. Cracks with axes aspect ratio between 0.01 and 100 are analyzed and the results are compared with analytical solutions. The geometry of the analyzed cracks is obtained from a circular shape by means of either *elliptic* or *linear scale* transformation. Comparison is performed between the two transformations and both linear and quadratic finite elements are used. Results prove that the *elliptic* transformation is superior to the *linear scale* one. In addition to stress intensity factors, the work also derives the strain energy factor for the analyzed cracks from which the crack propagation direction is obtained.

In addition, the methodology presented in ref [7], has been utilized in ref [13] for analysis of sub-surface cracks in hypoid gears and in ref [12] for analysis of sub-surface cracks in railway wheels.

1.1.2 Present work

The present work recreates and builds upon the developments in ref [7]. The model introduced by Guagliano et al corresponds to the *crackNormal* model, in terms of geometric features, also the transformations *elliptic* and *simpleScale* correspond to the transformations used in ref [7]. In addition, strain energy density is not considered in this project.

The present project, however, extends ref [7] with the following key developments:

- analysis of elliptic cracks with *XFEM*;
- automated history output extraction from the Abaqus output database;
- storing stress intensity factors data in a custom *shelve* database;

- automated report generation;
- visualization of the stress intensity factors;
- integrated into Abaqus browser with tree representation of the custom *shelve* database;
- functionality for analysis of *surface* and *edge* elliptic cracks.

1.2 Programming side

1.2.1 Abaqus structure and script execution

Abaqus has a modular structure, with components addressing various fields and providing complementary functionality. Abaqus/CAE provides the scripting extensions and graphical user interface for Abaqus/Standard, Abaqus/Explicit, Abaqus/CFD or Abaqus/Design. It is therefore an optional component. All of the analyses in the current project are performed with Abaqus/Standard.

The structure and workflow of execution of script commands by Abaqus is illustrated in figure 1.1. First, the script commands are executed by Abaqus/CAE, which generates the model database. When the model database is submitted for analysis Abaqus/CAE generates an input file which is passed to Abaqus/Standard, which executes the analysis and generates an output database with the results.

It follows that there are two way to approach an Abaqus analysis, one with Abaqus/CAE, and other without, by manually generating the input file. This applies to scripting as well, one way is to use the Abaqus scripting API and the other is to generate an input file by string manipulation. For the project scripts are designed to work with the Abaqus scripting API. This has the considerable advantage that, commands, in their majority, are of higher level of abstraction. The drawback is that commands are translated multiple times until the input file is generated and this makes them implicit. Interacting with the input file directly, eliminates that drawback. However, interaction is at a very low level and is mostly reduced to counting node and element labels.

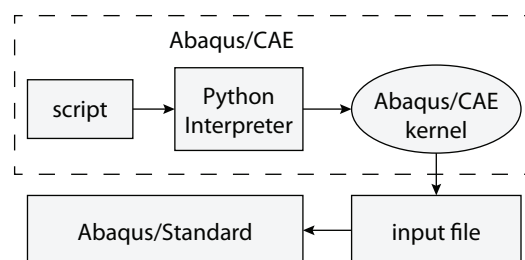


Figure 1.1: Execution of script commands

1.2.2 Python and Abaqus

Python ref [20] and ref [30] is the scripting language used in Abaqus. It is used both for kernel commands and GUI. In addition to the standard features of Python, the implementation in Abaqus incorporates the API, which are the

particular to Abaqus commands. The graphical user interface of Abaqus/CAE is a custom implementation of the FOXtoolkit in Python. The graphical interface of Abaqus/CAE is can be customized in a variety of ways from building dialog boxes to modifying the default user interface or creating a custom from scratch.

1.2.3 On programming style

At a certain point during the development of the program for the project, it the issue of maintainability of the code has surfaced. According to ref [21] time spent reading code exceeds the time writing code nine fold. Therefore, maintaining a certain coding style is crucial component of programming and has been consciously reinforced. It took several trials, each iteration including a complete redesign to develop the program at its present version. The main features from a programming point of view include:

- scalability,
- object oriented,
- multiple inheritance,
- encapsulation,

Little of the functionality of the current version, would have been achieved unless a particular effort has been made during its development to adhere to the programming practices stated in ref [21].

1.3 Motivation

Abaqus native tools for fracture analysis, as of time of writing, require significant effort. Therefore, an automated framework for modeling, analysis and post-processing of the results is welcome. Nevertheless, fracture mechanics problems are becoming increasingly important and to make matters worse, a fracture mechanics analysis involves numerous parameters, which means that numerous analysis iterations must be performed.

1.3.1 Automation

The developed program in the project addresses these issues by automating the modeling a cylindric model with embedded elliptic crack. The model, can be utilized either as a submodel for a larger analysis, or it can be used in a convergence study to determine the optimal parameters and expected accuracy for a larger model including a crack definition.

1.3.2 Post-processing

Post-processing of stress intensity factors may also prove challenging, as at present it requires a significant interaction between the analyst and Abaqus. This issue is also addressed by automated extraction of the stress intensity factors from the Abaqus output database and creating plot data for convenience.

The post-processing is taken even a step further by storing crack analysis results in a custom database to create a knowledge base of all of the performed analyses.

1.3.3 Visualization

Visualization is introduced to improve the understanding of the analyzed crack. It represents stress intensity factors in a three dimensional space mapped to the crack geometry. The technique can also be utilized as a diagnostic tool for *XFEM* to improve understanding and thus quality of the analysis.

1.4 Significance of the work

The project and framework significance can be evaluated in the following aspects:

- modeling,
- automation,
- post-processing,
- scalability,
- knowledge base.

1.4.1 Modeling

The modeling aspect contribution is mostly in regard of time-saving and consistency. The framework is capable of generating several model databases by given parameters. In addition, *FEM* models, including mesh transformations cannot be created without scripting.

1.4.2 Automation

The automation aspect contribution extends beyond time-saving. It is also enabling to evaluate multiple scenarios, a challenging and error prone task if performed manually. For instance, creating a plot for the stress intensity factors may require selecting manually up to or over 300 points in succession for some *XFEM* analyses performed in chapter 4. The framework does this automatically, without user input.

1.4.3 Post-processing

The chief contribution in the post-processing aspect is the visualization technique, utilized for representation of the stress intensity factors and as a diagnostic tool.

1.4.4 Scalability

This scalability aspect is a measure of the framework ability to be extended, either by new model types or further post-processing techniques. At present the framework can create models for quarter and semi-elliptic cracks for all model types, though the project scope is limited only to embedded.

1.4.5 Knowledge base

The knowledge base is one of the most significant features of the framework. It provides access through a browser to the custom database with all the calculated cracks. At the moment of writing the *shelve* database has 484 entries, or in other words, the knowledge base contains input parameters and results for stress intensity factors for 484 different cracks, which can be easily accessed. The number can increase in the future and the framework can be extended by optimization algorithms.

Chapter 2

Theoretical overview

2.1 Introduction

The theoretical yield strength of materials is of one to three orders of magnitude higher than the one observed in practice. The discrepancy is attributed to imperfections of the structure of the material, resulting in stress concentrations, which drastically reduce the material properties. Furthermore, such defects – *cracks* may occur when a component is in service. Cracks may either stay dormant and not influence the function of the component, or may grow reaching a critical size and resulting in fast and often catastrophic fracture of the component. A list of some of the most prominent disasters, due to fracture are listed in ref [2].

Therefore, to prevent future catastrophic failures, it is crucial to evaluate the strength of a critical component and estimate its remaining service life and design future components to be damage tolerant.

2.2 Fracture mechanics overview

2.2.1 LEFM scope

Whether LEFM is applicable to a specific problem depends on the extent of the applied stress and the local stress field in the vicinity of the crack. For instance, if a sharp crack is considered, the linear stress at the crack tip is singular and therefore, the material will yield. The size of this plastic zone determines the applicability of LEFM i.e. conditions must be essentially linear. It is applicable mostly to high strength materials. In case stresses are high and the yielding in the vicinity of the crack zone cannot be neglected, or the material is relatively more ductile, the problem should be addressed with EPFM.

2.2.2 Stress intensity factors K

The stress intensity factors define the stress field in the vicinity of the crack tip. The stress intensity factors are valid only for LEFM. The stress field is defined in a polar coordinate system with coordinates r and θ at the crack tip, as shown

in figure 2.1. The stress is defined by:

$$\sigma_{ij} = \frac{K}{\sqrt{2\pi r}} \cdot f_{ij}(\theta) + \dots,$$

where K is the stress intensity factor, which defines the magnitude of the stress. K is defined by: $K = \sigma\sqrt{\pi a} \cdot f(a/W)$, where:

- a is the half length of the crack,
- $f(a/W)$ is a dimensionless coefficient, depending on the crack geometry,
- σ is the remotely applied stress.

The so defined σ_{ij} becomes infinite when $r \rightarrow 0$, thus there is singularity in the stress field when plasticity is not considered. The σ_{ij} also tends to 0, when $r \rightarrow \infty$. Therefore, the equation is valid only for $r \ll a$.

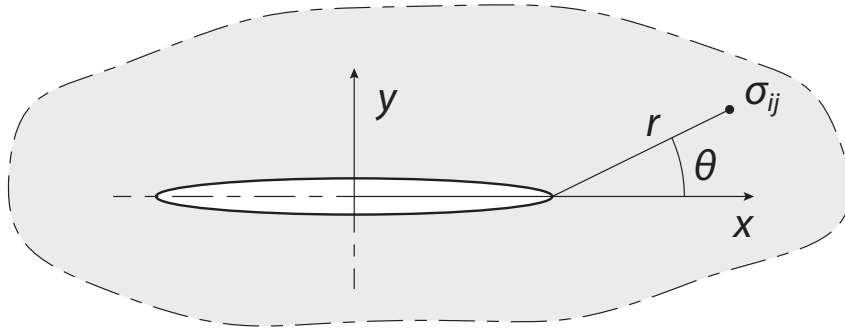


Figure 2.1: Polar coordinate system at the crack tip

Modes of loading

Stresses in the vicinity of the crack can be decomposed into a combination of modes of crack surface displacements, shown in figure 2.2:

Mode I opening mode

Mode II sliding mode

Mode III tearing mode

A stress intensity factor corresponds to each mode of crack surface displacement, K_I , K_{II} and K_{III} . This decomposition allows to estimate an arbitrary load conditions around a crack with only three parameters.

Airy stress functions

A function describing the elastic stress field must fulfill both the equilibrium and compatibility of strain requirements. Let such a function be $\Phi(x, y)$, an Airy stress function for a two dimensional problem.

The equilibrium equations are satisfied if:

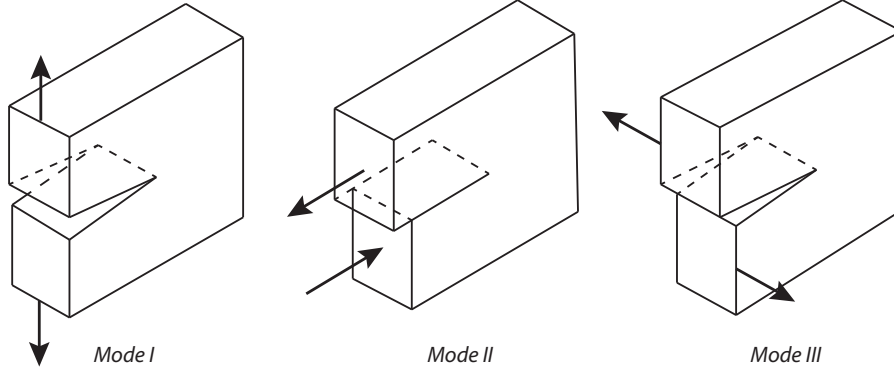


Figure 2.2: The three load type modes of a crack

$$\sigma_x = \frac{\partial^2 \Phi}{\partial y^2} \quad (2.1)$$

$$\sigma_y = \frac{\partial^2 \Phi}{\partial x^2} \quad (2.2)$$

$$\tau_{xy} = -\frac{\partial^2 \Phi}{\partial x \partial y} \quad (2.3)$$

The compatibility of strain is satisfied if:

$$\frac{\partial^4 \Phi}{\partial x^4} + \frac{2\partial^4 \Phi}{\partial x^2 \partial y^2} + \frac{\partial^4 \Phi}{\partial y^4} = 0$$

Westergaard stress equations

A Westergaard stress function relates the geometry, stress intensity factors, stress and displacement. It is a specific type of an Airy stress function Φ , defined by a complex stress function $\phi(z)$. For $\phi(z)$ is assumed that its derivative and first $\bar{\phi}(z)$ and second $\bar{\bar{\phi}}(z)$ order integrals exist. Therefore:

$$\Phi = \text{Re}(\bar{\phi}(z)) + y \cdot \text{Im}(\bar{\bar{\phi}}(z))$$

where $z = x + i \cdot y$. Thus defined the function Φ , leads to the Cauchy-Riemann conditions:

$$\frac{\partial \text{Re}(\Phi)}{\partial x} = \frac{\partial \text{Im}(\Phi)}{\partial y} = \frac{\text{Re}(\partial \Phi)}{\partial z} \quad (2.4)$$

$$\frac{\partial \text{Im}(\Phi)}{\partial x} = -\frac{\partial \text{Re}(\Phi)}{\partial y} = \frac{\text{Im}(\partial \Phi)}{\partial z} \quad (2.5)$$

Using equations 2.3 for the stresses, we obtain:

$$\sigma_x = \text{Re}(\phi(z)) - \text{Im}(\phi'(z)) \quad (2.6)$$

$$\sigma_y = \text{Re}(\phi(z)) + y \cdot \text{Im}(\phi'(z)) \quad (2.7)$$

$$\tau_{xy} = -y \cdot \text{Re}(\phi'(z)) \quad (2.8)$$

The $\phi(z)$ function is a generalization and for each particular case it should be defined to correspond to the boundary conditions. The Westergaard complex stress function limits the problems to $\sigma_x = \sigma_y$ and $\tau_{xy} = 0$.

Biaxially loaded plate

The case of a crack in a biaxially loaded infinite plate is shown in figure 2.4. Load σ is applied in the plate both directions along X axis and Y axis. The complex function for this case is:

$$\phi(z) = \frac{\sigma}{\sqrt{1 - a^2/z^2}}$$

Results for the stresses are obtained by substituting $\phi(z)$ in equations 2.8 and considering the following cases:

- $y = 0$ and $|x| < a$, which corresponds to the stresses on the crack flanks,

$$\phi(z) = \phi(x) = \frac{-i\sigma}{\sqrt{a^2/x^2 - 1}}$$

and therefore, $\phi(z)$ is purely imaginary, resulting in $\sigma_y = 0$.

- $x \rightarrow \infty$ and/or $y \rightarrow \infty$ results in $\phi(z) = \sigma$.
- $x = \pm a$ and $y = 0$, which corresponds to the crack tips, $\phi(z) \rightarrow \infty$.

For the derivation of the stress intensity factor K_I it is convenient to move the origin of the coordinate system to coincide with the crack tip. The $\phi(z)$ then becomes:

$$\phi(\eta) = \frac{\sigma}{\sqrt{1 - \left(\frac{a}{a+\eta}\right)^2}} = \frac{\sigma(a+\eta)}{\sqrt{(a+\eta)^2 - a^2}}$$

where $\eta = z - a$. Then $\phi(\eta)$ can be approximated as:

$$\phi(\eta) \approx \frac{\sigma a}{\sqrt{2a\eta}} = \sigma \sqrt{\frac{a}{2}} \eta^{-\frac{1}{2}}$$

In polar coordinates $\eta = re^{i\theta}$, and therefore:

$$\phi(\eta) = \frac{\sigma\sqrt{\pi a}}{\sqrt{2\pi r}} e^{-\frac{1}{2}i\theta}$$

Finally, the results for the stress components are:

$$\sigma_x = \frac{\sigma\sqrt{\pi a}}{\sqrt{2\pi r}} \cos \frac{\theta}{2} \cdot \left(1 - \sin \frac{\theta}{2} \sin \frac{3\theta}{2}\right) \quad (2.9)$$

$$\sigma_y = \frac{\sigma\sqrt{\pi a}}{\sqrt{2\pi r}} \cos \frac{\theta}{2} \cdot \left(1 + \sin \frac{\theta}{2} \sin \frac{3\theta}{2}\right) \quad (2.10)$$

$$\tau_{xy} = \frac{\sigma\sqrt{\pi a}}{\sqrt{2\pi r}} \sin \frac{\theta}{2} \cos \frac{\theta}{2} \cos \frac{3\theta}{2} \quad (2.11)$$

For a biaxially loaded infinite plate the factor $f(a/W) = 1$ and therefore, $K_I = \sigma\sqrt{\pi a}$, depends only on the applied stress and crack length. The derivations apply for infinitely sharp tips, for cracks with blunted tips, the blunting radius ρ should be accounted for in the stress equations.

Superposition principle

The principle of superposition can be applied in linear elastic fracture mechanics to calculate stress components and stress intensity factors as follows:

$$(\sigma_{ij})_{total} = (\sigma_{ij})_1 + (\sigma_{ij})_2 + \dots + (\sigma_{ij})_n \quad (2.12)$$

and from equation 2.2.2 follows:

$$(\sigma_{ij})_{total} = (K_I)_1 \cdot f_{ij}(r, \theta) + (K_I)_2 \cdot f_{ij}(r, \theta) + \dots + (K_I)_n \cdot f_{ij}(r, \theta)$$

Finally, the following result is obtained:

$$(\sigma_{ij})_{total} = (K_I)_{total} \cdot f_{ij}(r, \theta)$$

where

$$(K_I)_{total} = (K_I)_1 + (K_I)_2 + \dots + (K_I)_n$$

where $(K_I)_n$ corresponds to a the load σ_n , applied to the specimen.

Although the principle of superposition is illustrated for *mode I* of crack surface displacement, it is applicable to *mode II* and *mode III* as well.

Crack tip blunting

For cracks with blunted tips, shown in figure 2.3, stress field is not singular as it is the case with sharp crack tip. The near crack tip stress field is defined by:

$$\sigma_x = \frac{K_I}{\sqrt{2\pi r}} \cos \frac{\theta}{2} \cdot \left(1 - \sin \frac{\theta}{2} \sin \frac{3\theta}{2} \right) - \frac{K_I}{\sqrt{2\pi r}} \frac{\rho}{2r} \cos \frac{3\theta}{2} \quad (2.13)$$

$$\sigma_y = \frac{K_I}{\sqrt{2\pi r}} \cos \frac{\theta}{2} \cdot \left(1 + \sin \frac{\theta}{2} \sin \frac{3\theta}{2} \right) + \frac{K_I}{\sqrt{2\pi r}} \frac{\rho}{2r} \cos \frac{3\theta}{2} \quad (2.14)$$

$$\tau_{xy} = \frac{K_I}{\sqrt{2\pi r}} \sin \frac{\theta}{2} \cos \frac{\theta}{2} \cos \frac{3\theta}{2} - \frac{K_I}{\sqrt{2\pi r}} \frac{\rho}{2r} \sin \frac{3\theta}{2} \quad (2.15)$$

Stress intensity and stress concentration factors

Stress intensity factors K define the stress field near the crack tip and have dimension $[MPa\sqrt{m}]$. Stress concentration factor, on the other hand, define the ratio between the remotely applied stress and the local stress increase due to a geometric feature and it is dimensionless value. Considering a blunted crack tip the following results are obtained for a stress concentration factor:

$$\sigma_y = \frac{2K_I}{\sqrt{\pi\rho}} = \frac{2\sigma\sqrt{\pi a}}{\sqrt{\pi\rho}}$$

and therefore, for the *stress concentration factor*:

$$\frac{\sigma_y}{\sigma} = 2\sqrt{\frac{a}{\rho}}$$

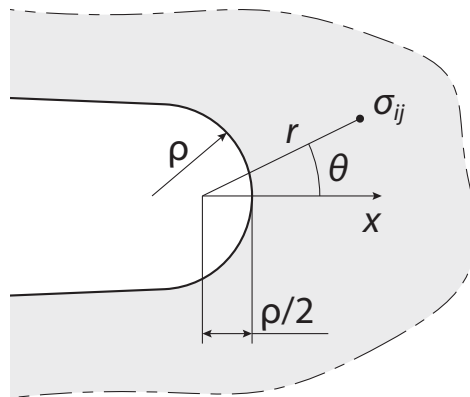


Figure 2.3: Crack with blunted tip

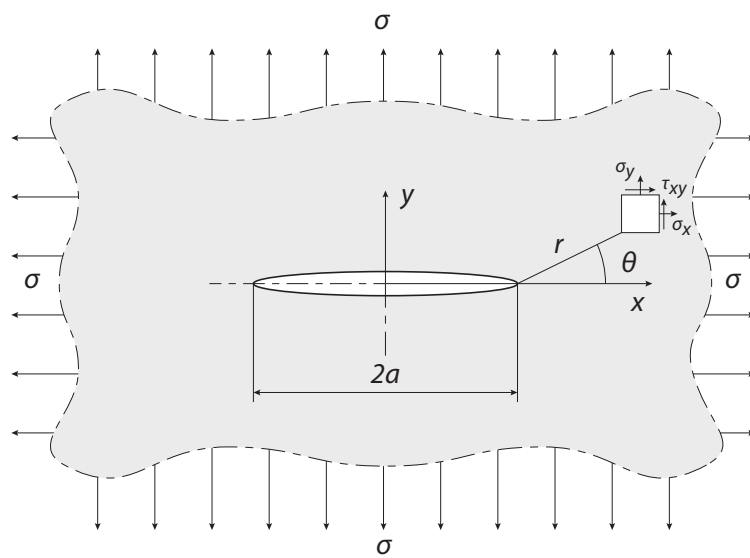


Figure 2.4: Crack in biaxially loaded plate

Finite specimen size

Prior derivations of the stress intensity factors are valid strictly for an infinite plate. If the size of the plate is finite, it must be taken into account using correction coefficients C and $f(a/W)$. The general form a stress intensity factor is:

$$K_I = C\sigma\sqrt{\pi a}.f(a/W),$$

where C and $f(a/W)$ are to be determined most often by stress analysis or analytically.

Crack tip plasticity

The linear stress field at the vicinity of the crack tip tends to infinity at the crack tip for a sharp crack. If, however, a real material is considered, there would be a zone, where the calculated linear stress field would be higher than the yield strength σ_y of the material. Therefore, the material would plastically deform in that zone. Exact representation of the plastic zone at the crack tip has proved to be extremely challenging. Therefore, representations are either for the size of the crack tip plastic zone with assumed arbitrary shape, or approximation of the shape. For instance if the crack tip plastic zone is assumed to be of a circular shape with diameter r_y , then by substituting the yield strength σ_y for the stress the following result is obtained:

$$\sigma_y = \frac{\sigma\sqrt{\pi a}}{\sqrt{2\pi r}} = \frac{K_I}{\sqrt{2\pi r}}$$

and therefore for the plastic zone diameter:

$$r_y = \frac{1}{2}\pi \left(\frac{K_I}{\sigma_y} \right)^2$$

The equation 2.2.2 is a rough approximation, due to the selection of the shape of the plastic zone is arbitrary and the stress field is limited to the σ_y and the higher calculated linear stress field in that region is not accounted for. The approximation is shown in figure 2.5.

More accurate representations of the crack tip plastic zone are derived by Irwin and Dugdale.

Representations of the shape of the crack tip plastic zone of first order are obtained by utilizing the yield criteria by von Mises or Tresca. In that way only the boundaries, where the material starts to yield are obtained. Furthermore, it is not accounted for the area, where the linear elastic stress exceeds the yield stress. A visualization based on the von Mises yield criteria for plane stress and plane strain is shown in figure 2.6.

2.2.3 Energy approach to Fracture Mechanics

Total energy

Consider an infinite plate with a through thickness crack with length $2a$, subjected stress σ . Therefore, for unit thickness of the plate the following quantities

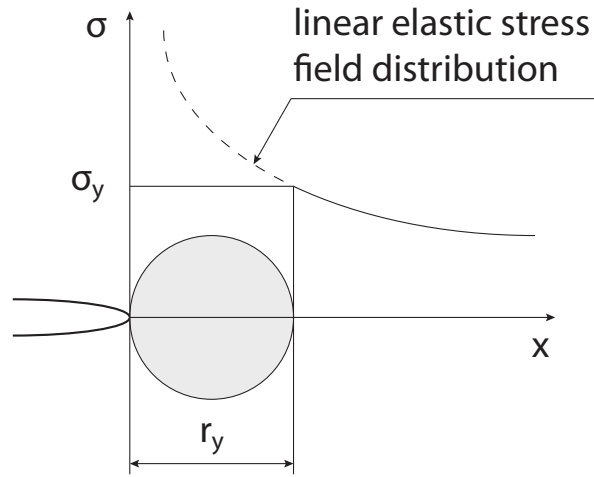


Figure 2.5: Stress distribution in the vicinity of the crack tip

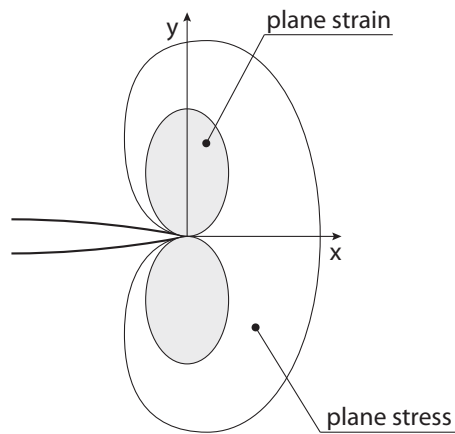


Figure 2.6: Visualization of the yield stress boundaries of the crack tip plastic zone

are defined: U_0 total energy of the plate and its loading system before introducing the crack, U_a change in the elastic energy of the plate, caused by introducing a crack, U_γ change in the plate surface energy due to the crack, F work performed by the loading system during the introduction of the crack. Therefore, the total energy of the plate is:

$$U = U_0 + U_a + U_\gamma - F$$

Potential energy

The part of equation 2.2.3 that can perform work is defined as *potential energy*:

$$U_p = U_0 + U_a - F \quad (2.16)$$

Energy balance

For the considered case, the *total energy* changes with the crack length a as shown in figure 2.7. The *total energy* has a maximum at point O , where crack growth becomes unstable. The condition for instability is given by:

$$\frac{\partial U}{\partial a} < 0$$

substituting equation 2.16:

$$\frac{\partial(U_0 + U_a - F)}{\partial a} < 0$$

and therefore:

$$-\frac{\partial U_p}{\partial a} > \frac{\partial U_\gamma}{\partial a}$$

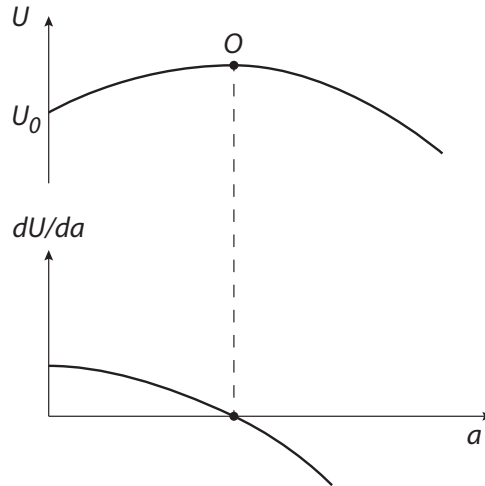


Figure 2.7: Total energy of a plate as a function of the crack length a

Potential energy release rate

The potential energy release rate G is the energy per unit thickness available per crack extension increment:

$$G = -\frac{\partial U_p}{\partial 2a}$$

LEFM and EPFM

An approximate graph comparing the potential energy release rate calculated with *EPFM* and *LEFM* methods against load magnitude σ and yield strength σ_y is shown in figure 2.8. The discrepancy $A - A'$ at small stresses is small, however, when the loads increase, the crack tip plastic zone increases and the values start to diverge $B - B'$.

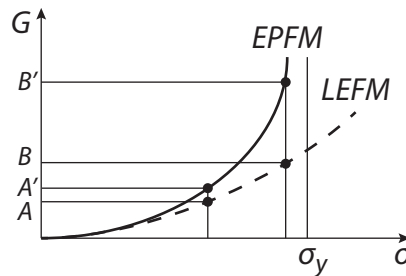


Figure 2.8: Potential energy release rate for *EPFM* and *LEFM* for different loads

2.2.4 Elliptic cracks

Cracks considered up to this point are *through thickness* cracks. However, in practice for bulk components, elliptic cracks are observed. Elliptic cracks are of three types, depending on the relative position of the crack with respect to the component:

embedded or full elliptic crack is located inside the component.

surface or semi- elliptic crack is an elliptic notch on the surface of the component.

edge or quarter elliptic crack is an elliptic notch on two intersecting surfaces.

Cross sections of the crack plane of the elliptic crack types are shown in figure 2.9.

Analytical solutions for embedded elliptic cracks

The first analytical solution for embedded elliptic crack is derived by Irwin and is for K_I crack mode:

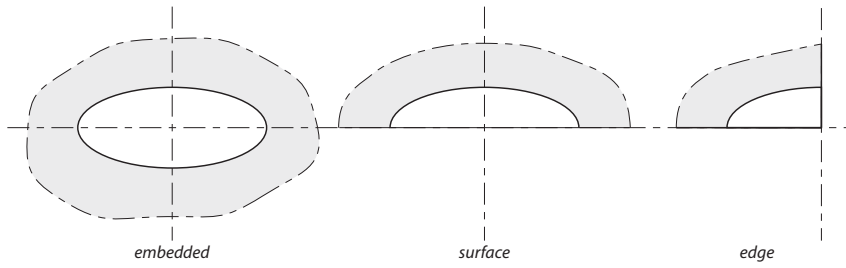


Figure 2.9: Elliptic crack types

$$K_I = \sigma \frac{\sqrt{\pi b}}{E(k)} \left(\sin^2 \phi + \frac{b^2}{a^2} \cos^2 \phi \right)^{1/4}$$

where $E(k)$ is an elliptic integral of the second kind and ϕ is the angle of the point on the crack front. A cross section of the elliptic crack plane is shown in figure 2.10

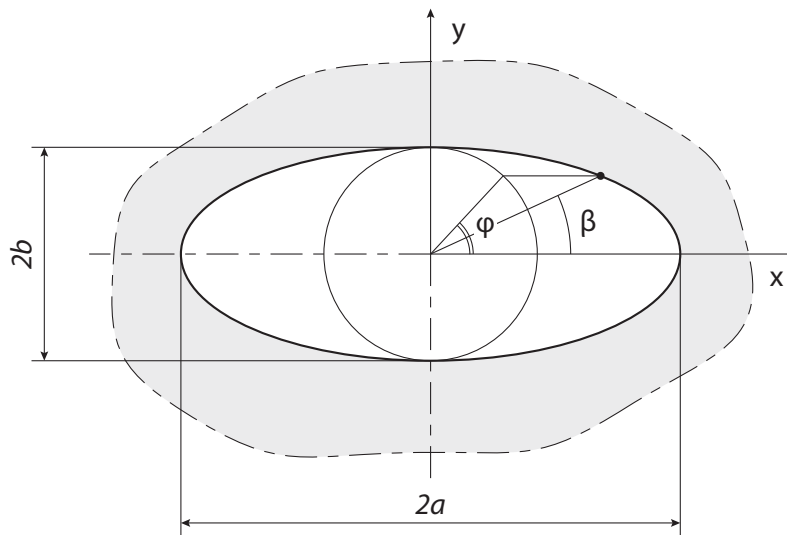


Figure 2.10: Elliptic crack plane

Orientation of an embedded elliptic crack

The orientation of an embedded elliptic crack in an infinite cylinder subjected to tensile stress σ_t is visualized in figure 2.11. The orientation of the crack is completely defined by two angles γ and ω . Rotation of the crack around the axis of the cylinder is determined by the ω angle. Whereas, γ is the angle between the axis of the cylinder and the normal to the crack plane.

Therefore, the stresses for the analytical solutions of the stress intensity factors are:

$$\sigma = \sigma_t \cos^2 \gamma$$

and

$$\tau = \sigma_t \cos \gamma \sin \gamma$$

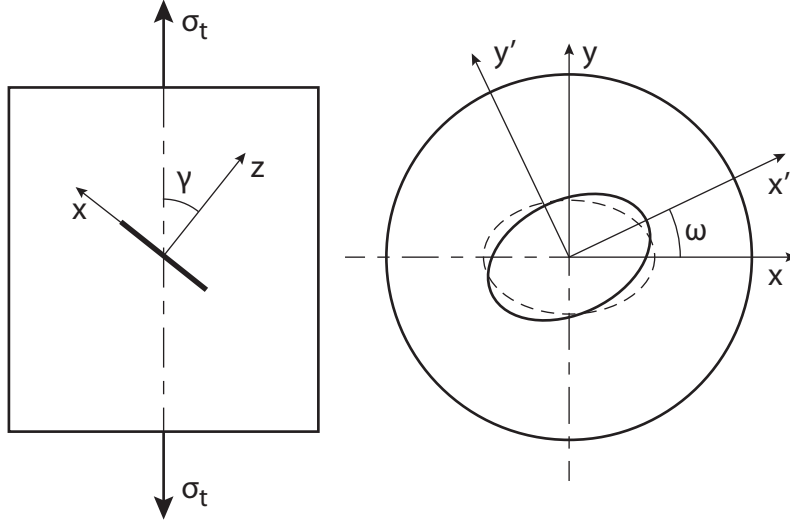


Figure 2.11: Orientation of an elliptic crack

Analytical solutions for mixed mode loading of elliptic cracks

Analytical solutions for K_I , K_{II} and K_{III} for embedded elliptic crack are obtained in ref [18] and are as follows:

$$K_I(\beta) = \sigma \frac{\sqrt{\pi(b/a)}}{E(k)} (a^2 \sin^2 \beta + b^2 \cos^2 \beta)^{1/4} \quad (2.17a)$$

$$K_{II}(\beta) = -\tau \left(\frac{\pi b}{a} \right)^{1/2} \frac{bR(K, v) \cos \beta \cos \omega + aQ(k, v) \sin \beta \sin \omega}{(a^2 \sin^2 \beta + b^2 \cos^2 \beta)^{1/4}} \quad (2.17b)$$

$$K_{III}(\beta) = \tau(1-v) \left(\frac{\pi b}{a} \right)^{1/2} \frac{aR(k, v) \sin \beta \cos \omega - bQ(k, v) \cos \beta \sin \omega}{(a^2 \sin^2 \beta + b^2 \cos^2 \beta)^{1/4}} \quad (2.17c)$$

where β and ω are the angles defining a point on the crack front and the angle determining the orientation of the crack in the crack plane, as illustrated in figure 2.10, a and b are the major and minor ellipse axes, v is the Poisson's ratio, $K(k)$ and $E(k)$ are the complete elliptic integrals of first and second kind, $k = \sqrt{1 - b/a}$, $k_1^2 = 1 - k^2$ and

$$R(k, v) = \frac{k^2}{[(k^2 - v)E(k) + vk_1^2 K(k)]}$$

$$Q(k, v) = \frac{k^2}{[(k^2 + vk_1^2)E(k) - vk_1^2 K(k)]}$$

In ref [10] an error in equations 2.17 is discovered that has gone unnoticed, namely that instead of β , angle ϕ should be used figure 2.10. Observations in ref [10] are later confirmed in ref [24] and the following equations are proposed and used in the project as reference analytical solutions:

$$K_I(\beta) = \sigma \frac{\sqrt{\pi b/a}}{E(k)} \frac{(a^4 \sin^2 \beta + b^4 \cos^2 \beta)}{(a^2 \sin^2 \beta + b^2 \cos^2 \beta)^{1/4}} \quad (2.18a)$$

$$K_{II}(\beta) = -\tau \left(\frac{\pi b}{a}\right)^{1/2} \frac{b^2 R(k, v) \cos \beta \cos \omega + a^2 Q(k, v) \sin \beta \sin \omega}{(a^2 \sin^2 \beta + b^2 \cos^2 \beta)^{1/4} (a^4 \sin^2 \beta + b^4 \cos^2 \beta)^{1/4}} \quad (2.18b)$$

$$K_{III}(\beta) = \tau(1 - v) \left(\frac{\pi b}{a}\right)^{1/2} \frac{a^2 R(k, v) \sin \beta \cos \omega - b^2 Q(k, v) \cos \beta \sin \omega}{(a^2 \sin^2 \beta + b^2 \cos^2 \beta)^{1/4} (a^4 \sin^2 \beta + b^4 \cos^2 \beta)^{1/4}} \quad (2.18c)$$

2.3 LEFM analysis with FEM

2.3.1 Special crack tip elements

The stress field in the vicinity of the crack requires special attention, due to its singularity. Higher mesh density is necessary to approximate properly the stress field. In addition to this requirement, the stress singularity may be accounted for in two ways, either approximating it with very dense mesh or using special crack tip elements.

For instance the required quadratic displacement function of a triangular element is:

$$u(\xi, \eta) = a_1 + \frac{a_2 \xi + a_3 \eta}{\sqrt{\eta + \xi}} + \frac{a_4 \xi \eta}{\xi + \eta} + a_5 \xi + a_6 \eta$$

which corresponds to the standard quadratic polynomial displacement function:

$$u(\xi, \eta) = a_1 + a_2 \xi + a_3 \eta + a_4 \xi \eta + a_5 \xi^2 + a_6 \eta^2$$

The effect is achieved by translation the mid-side nodes for quadratic elements to the crack tip, figure 2.12.

The \sqrt{r} singularity is achieved by coalescence of the nodes, as shown in figure 2.12.

2.3.2 Calculation of the stress intensity factors

Methods of calculating stress intensity factors fall into two main categories *substitution* and *energy* methods.

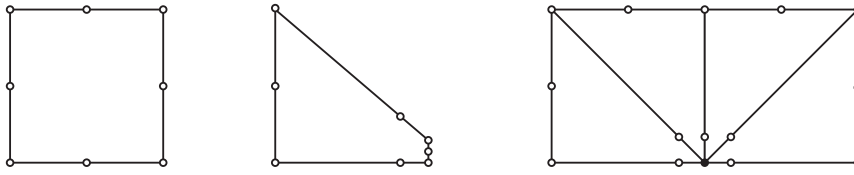


Figure 2.12: Special crack tip elements

Substitution methods

Substitution methods are post-processing procedures and uses the calculated values for stress and displacement by the FEM analysis. They are of two types *displacement* and *stress*. Stress intensity factors are obtained by substituting the values for either stress or displacement in the Westergaard's equations. For the substitution, also the (r, θ) coordinates of either Gauss points or nodes for stress and displacement respectively are required and can be easily calculated.

Energy methods

Numerous energy methods have been developed, they calculate directly only G . Subsequently the stress intensity factors are obtained from G . Some of the most common energy methods are ref [14]:

- energy difference technique
- virtual crack extension methods
- J - integral
- crack closure/opening work
- weight functions

From the above methods, only the *energy difference technique* and *virtual crack extension methods* are reviewed.

Energy difference technique

The energy difference technique for two dimensional analysis is composed of three steps:

- Perform analysis and calculate the potential energy P_1 of the crack with given length a .
- Move the position of the crack tip with δa , where δa is much smaller than the size of the crack tip elements, and perform analysis to calculate the potential energy P_2 .
- Finally, calculate G by:

$$G = \frac{dP}{da} = -\frac{P_2 - P_1}{\delta a}$$

The accuracy of G is dependent on the value of δa , in a way that G values may be inaccurate if δa is either too small or too large. The technique can be extended to three dimensional analyses by performing the procedure for each node of the crack. This, however, leads to multiple runs, of the analysis.

Virtual crack extension methods

Virtual crack extension methods are equivalent to the energy difference method, however, they eliminate the need for multiple simulations. Virtual crack extension methods are of two types *discrete* and *continuum*.

Discrete virtual crack extension methods

This section is a review of some of the first virtual crack extension methods.

The *stiffness derivative method* was introduced in ref [25] The method uses the strain energy expression:

$$U = -\frac{1}{2}\{u\}^T[K]\{u\} \quad (2.19)$$

where $[K]$ is the stiffness matrices over the crack tip region. The method takes the derivative of the equation 2.19 with respect to the crack length a . The matrix $\delta[K]$ is calculated as difference of the stiffness matrices for crack lengths a and $a+\delta a$. Then vector products of $\delta[K]$ and the crack tip local displacements give the energy change.

A method developed in ref [15] calculates $\delta[K]$ only for elements affected by the crack extension.

Continuum virtual crack extension methods

In continuum virtual crack extension methods δa is defined algebraically, rather than explicitly. In ref [8] is shown that the potential energy release rate can be derived as:

$$G = \int_V \left\{ \left(\sigma_{ij} \frac{\partial u_i}{\partial X_i} - W \delta_{jk} \right) \frac{\partial \Delta X_k}{\partial X_j} - f_i \frac{\partial u_i}{\partial X_k} \Delta X_k \right\} dV \quad (2.20)$$

where W is the strain energy density, σ_{ij} and u_i are the stress and displacement tensors,

$$\delta_{jk} = \begin{cases} 0, & \text{if } j \neq k \\ 1, & \text{if } j = k \end{cases}$$

is the Kronecker delta, and X_k are the Cartesian geometric values. The gradient ΔX_k varies linearly with δa in the region B , figure 2.13, is equal to δa in region C and is zero in the region A .

2.4 XFEM

2.4.1 Introduction

XFEM or *eXtended Finite Element Method* is a technique to analyze discontinuities, independently of the of the mesh of the part. This is contrary to *FEM*,

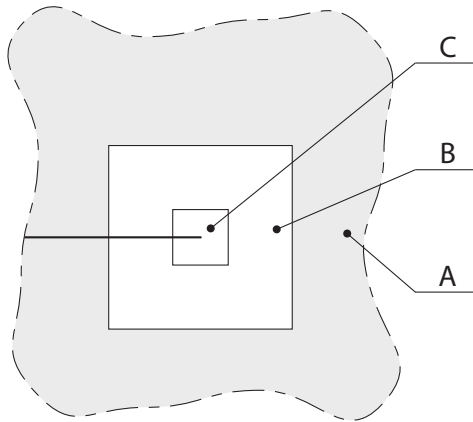


Figure 2.13: Zones of elements around a crack tip

which requires the mesh to conform to the crack geometry. A major feature of *XFEM* is that it builds upon the classic *FEM* and is an extension of the method, rather than a completely different methodology. For further details on *XFEM* can be found in ref [23], [5] and [1].

2.4.2 *XFEM* concepts

The basic concept of *XFEM* is to incorporate modeling of discontinuities into the element definition, and therefore, the mesh does not need to conform to the geometry of the crack. This is implemented by local *enrichment* of the elements surrounding the crack.

Partition of unity

Partition of unity is defined as a set of m functions $f_k(x)$ in a domain Ω , such that:

$$\sum_{k=1}^m f_k(x) = 1$$

and therefore it is true that:

$$\sum_{k=1}^m f_k(x) \cdot \psi(x) = \psi(x)$$

The shape functions N_j of isoparametric elements also satisfy the condition:

$$\sum_{k=1}^n N_j(x) = 1$$

where n is the number of nodes in an element.

Enrichment

One way to consider *enrichment* is by incorporating analytical solutions for crack tip stress field for fracture analysis and thus increasing the accuracy of the solution. A starting point, when considering enrichment is the approximation function of a field variable:

$$u = \sum_{j=1}^n N_j \cdot u_j$$

The same expression can be rewritten in terms of the m basis functions p_k :

$$u = \sum_{k=1}^m p_k \cdot a_k \quad (2.21)$$

where a_k can be determined from approximation at nodal points.

Enrichment is of two types:

intrinsic enrichment is achieved by modification of the basis function

extrinsic enrichment is achieved by adding new basis functions to the approximation.

Intrinsic enrichment

Intrinsic enrichment is achieved by modification of the basis function p_k , so that it includes additional terms, which meet a requirement. For instance in equation 2.21, $p_k = \{1, x, y\}$ for a linear two dimensional case. However, for the enriched basis for representation of the near crack tip strain field is:

$$p^T(x) = \left[1, x, y, \sqrt{r} \sin \frac{\theta}{2}, \sqrt{r} \cos \frac{\theta}{2}, \sqrt{r} \sin \theta \sin \frac{\theta}{2}, \sqrt{r} \sin \theta \cos \frac{\theta}{2} \right]$$

where θ and r are the polar coordinates of the system at the crack tip, shown in figure 2.1. And finally the strain field is:

$$u(x) = p^T(x)a(x)$$

where $a(x)$ is a vector of coefficients.

Extrinsic enrichment

Extrinsic enrichment uses external basis functions p_k , so that the equation for the strain field becomes:

$$u(x) = \sum_{j=1}^n N_j(x)u_j + \sum_{k=1}^m p_k(x)a_k$$

2.4.3 Partition of unity based methods

Partition of unity finite element method – *PUFEM*

The *PUFEM* is one of the key developments, which eventually lead to the *XFEM*. Its main features ref [22] are the capability to incorporate knowledge about a certain behavior in the finite element definition. The *PUFEM* is a generalization of the *h*, *p* and *hp* versions of *FEM* ref [4].

The displacement interpolation function for *PUFEM* is:

$$u(x) = \sum_{j=1}^n N_j(x) \left(u_j + \sum_{k=1}^n (p_k(x) - p_k(x_j)) a_j \right)$$

Generalized finite element method – *GFEM*

The *GFEM* utilizes different shape functions for the *FEM* and the *enriched* interpolation. Therefore, the generalized form of the displacement field is:

$$u(x) = \sum_{j=1}^n N_j(x) u_j + \sum_{j=1}^n \bar{N}_j(x) \left(\sum_{k=1}^m p_k(x) a_{jk} \right)$$

eXtended finite element method – *XFEM*

The *XFEM* uses local enrichment, opposed to global as is the case with *PUFEM* and *GFEM*. Local enrichment may, however, lead to incompatible solution between the local enriched region and the rest of the analyzed domain. Therefore, a transition zone, composed of blending elements is introduced on the boundary between the two regions of the domain, figure 2.14.

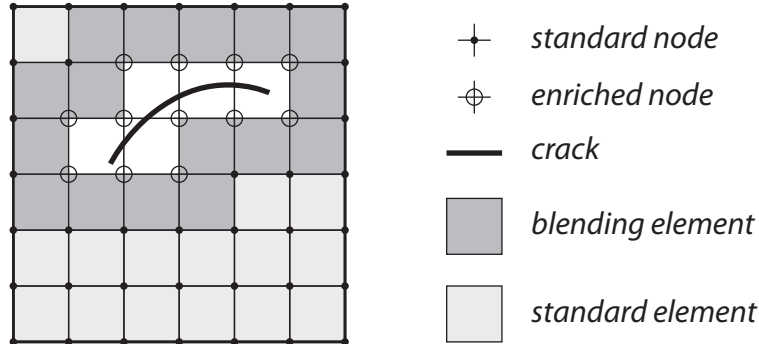


Figure 2.14: Standard, enriched and blending elements in a domain

The displacement field of the transition zone is described by:

$$u(x) = (1 - R(x)) u(x) + R(x) u_{enr}(x)$$

where $R(x)$ is a ramp function so that it is 1 at the enriched boundary and 0 at the standard element boundary.

2.4.4 XFEM formulation

Approximation I

The general approximation function for displacement $u(x)$ has the form:

$$u(x) = \sum_{j=1}^n N_j(x)u_j(x) + \sum_{j=1}^n N_j(x)\psi(x)a_k$$

where u_j is the vector of the nodal degrees of freedom, a_k is the added set of degrees of freedom added to the standard finite element model, $\psi(x)$ is the enrichment function for the discontinuity.

Level set method for tracking boundary

Level set functions are utilized to define the location of the crack in the domain. A case for a flat crack is illustrated in figure 2.15.

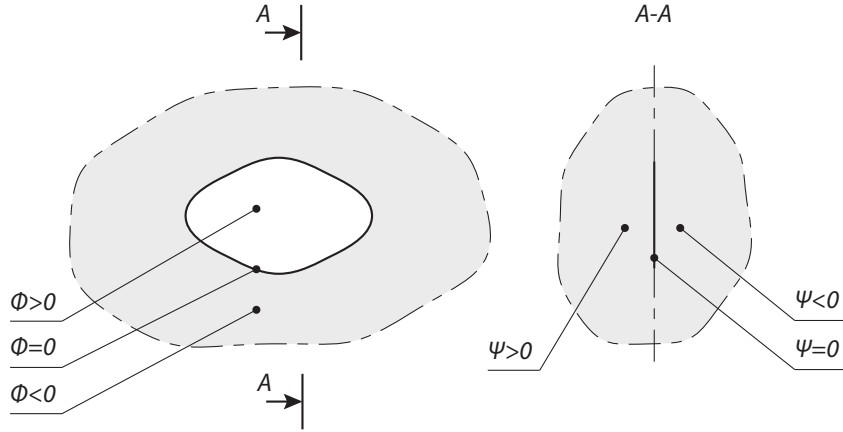


Figure 2.15: Level set functions for a flat crack

The functions Ψ and Φ completely define the crack location in the domain. For instance the boundary of the crack corresponds to $\Psi = 0$ and $\Phi = 0$. In addition, $\Phi > 0$ inside the crack contour and $\Phi < 0$ outside. The Ψ function defines the *top* and *bottom* of the crack, and $\Psi = 0$ at the crack plane.

Heaviside function

Consider a crack and a point x' on the crack flank in figure 2.16. The Heaviside function $H(x)$ is defined as:

$$H(x) = \begin{cases} 1, & \text{if } (x - x')n \geq 0 \\ -1, & \text{otherwise} \end{cases}$$

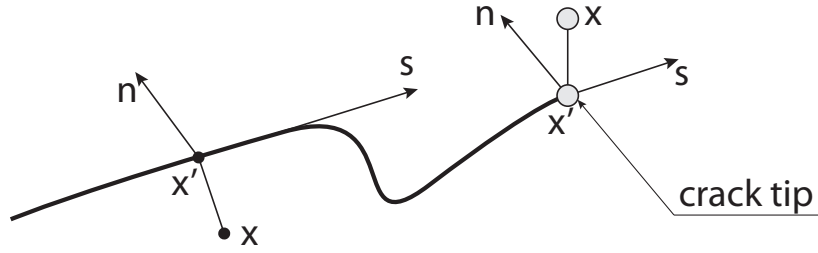


Figure 2.16: Crack flanks and crack tip

Approximation II

Finally the approximation for the displacement field has the form:

$$u(x) = \sum_{j=1}^n N_j(x) \left(u_j + H(x)a_j + \sum_{k=1}^m F_k(x)b_j^k \right)$$

where

$$\begin{aligned} \sum_{k=1}^m F_k(x)b_j^k & \text{ is the crack tip enrichment term,} \\ H(x)a_j & \text{ is the Heaviside enrichment term,} \\ u_j & \text{ are the nodal degrees of freedom and} \\ m & \text{ is the number of the enriched nodes of the element and} \\ F_k & = \left[\sqrt{r} \sin \frac{\theta}{2}, \sqrt{r} \cos \frac{\theta}{2}, \sqrt{r} \sin \theta \sin \frac{\theta}{2}, \sqrt{r} \sin \theta \cos \frac{\theta}{2} \right] \end{aligned}$$

2.4.5 XFEM crack definition in Abaqus

With *XFEM* both stationary crack and crack growth may be defined ref [29]. For stationary crack the initial geometry and location of the crack is defined by *faces* one, two or three dimensional – figure 2.17. In addition, the crack can also intersect the elements of the *crack domain* arbitrarily.

Conversely, in the case of a non-stationary crack, its location and geometry may not be specified explicitly, in which case is calculated on the basis of damage initiation and evolution law.

2.4.6 Crack analysis with XFEM

Analysis of stress intensity factors with *XFEM* and *tetrahedral* elements is presented in ref [3]. *XFEM* solutions have noise and therefore, techniques are developed to reduce the noise in the solution. A technique proposed in ref [26] is based on using selective data from the solution. A "moving average" technique, employed in ref [3].

The capability of *XFEM* to include priori knowledge about a discontinuity facilitates multiscale analysis. In this case multiscale refers to combining *FEM* to model the whole component and a modeling technique to simulate

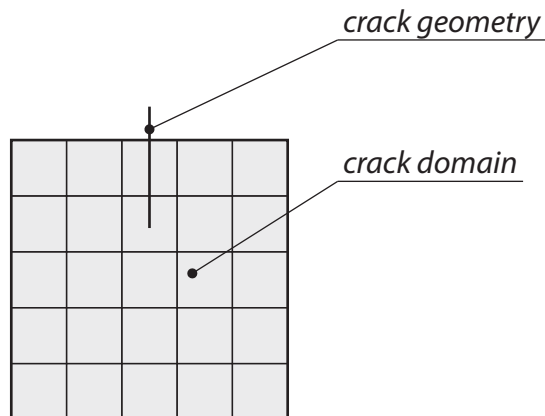


Figure 2.17: Crack domain and crack geometry

the microstructure locally. Further information is available in ref [16], [9], [6] and [27].

2.5 Fracture mechanics software

General purpose FEM software like Abaqus and Ansys are not specifically designed to meet the needs of fracture mechanics. Therefore, fracture mechanics oriented software has been developed. This section is a brief review of some of the most widely used fracture mechanics software. In particular, the review is limited to *ZenCrack*, *FRANC2D* and *FRANC3D*, *NASGO*, *AFGROW* and *ADAPCRACK3D*.

2.5.1 ZenCrack

ZenCrack is a *FEM* 3D fracture mechanics software. It uses automated mesh generation according to the crack geometry. ZenCrack runs along side a general finite element program and requires either Abaqus, Ansys or MSC Marc. ZenCrack also is available in two versions *Standard* and *Professional*. The *Standard* version is able to calculate fracture parameters for stationary cracks, while the *Professional* version includes capabilities for crack growth analysis. ZenCrack works by defining a standard element block, which contains the crack geometry. The standard element block is then included in the analysis, by replacing corresponding elements of the mesh ref [19].

2.5.2 FRANC2D and FRANC3D

FRANC3D is a 3D fracture mechanics software developed by Cornell university, ref [17]. It is a *FEM* and *BEM* based. *FRANC2D* is a two dimensional version of *FRANC3D*.

2.5.3 NASGRO

NASGRO is a software developed by NASA for fracture analysis. It is NASA's standard software package used by all NASA Centers ref [11]. It is utilized for fracture control and damage tolerance assessment.

2.5.4 AFGROW

AFGROW is a fracture mechanics software for analysis of crack initiation and crack growth.

2.5.5 ADAPCRACK3D

ADAPCRACK3D is a fracture mechanics software for fatigue crack growth of 3D cracks under arbitrary loading. A main purpose of the program is to determine crack path and surfaces and remaining life of a component ref [28].

Chapter 3

Methodology

3.1 Introduction

The procedures of building the models in Abaqus are implemented by Abaqus kernel commands. These commands are organized onto custom classes and functions, comprising the program. This organization enables scalability, further automation, reduces code duplication and facilitates further development and maintainability.

3.2 Description of the model types

The program is able to analyze 4 model types for each crack type. In addition to that, the *FEM* analysis type model, has 3 mesh transformation types. This results in total of 18 different model databases. For *FEM* analysis type, the model type is one – *crackNormal*, however, the model is capable of 3 mesh transformations, which can be considered as a model sub-types. For *XFEM* analysis type the model types are 3 – *simple*, *crackPartition* and *multiplePartitions*.

3.2.1 FEM – *crackNormal* model type

The *crackNormal* model type is the most complex of all model types. The complete analysis of a crack with this model type is performed at two stages. First, building a model with a circular crack and associative to the geometry mesh. Second, importing the input file from the first to create an orphan mesh, applying a transformation to the mesh to obtain the desired crack shape and creating boundary conditions.

Geometry of the model

Geometry of the model is a cylinder and at its center is located the crack. Initially the crack is modeled as circular. The geometric parameters are shown in fig 3.1. The model is composed of multiple parts, which define the majority of the internal edges of the model. For instance, edges of the crack zone and crack tip are the intersection between a cylinder and two washer-shaped solid parts with square cross section. In similar fashion, slanted edges connecting the

vertices of the crack zone edges and the cylinder are created by the intersection of the cylinder with 4 shell parts. Additional edges and partitions are created by subsequent partitioning of the cylinder by datum planes. The cross section of the model is shown in figure 3.1. Thus created edges, faces and cells are organized into sets and utilized in the definition of the features of the model.

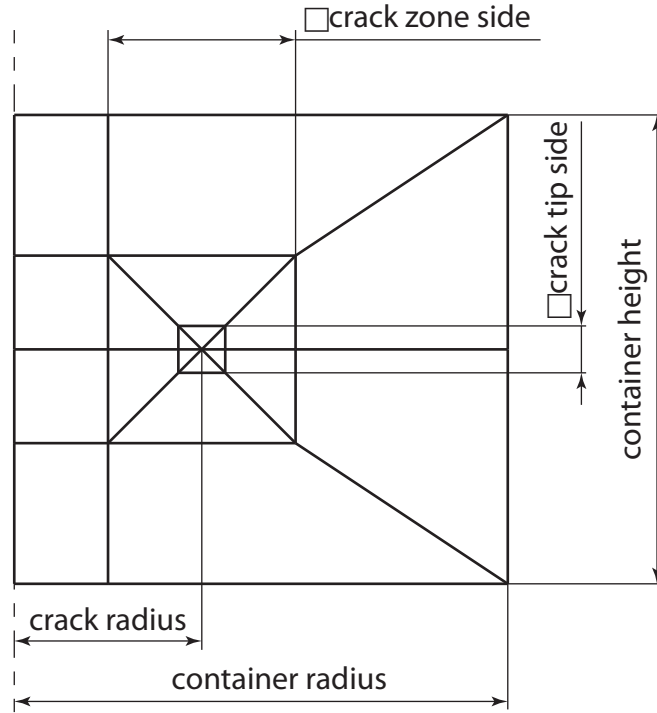


Figure 3.1: Cross section of the crackNormal model

Geometric parameters

The geometry of the model is completely defined by the following parameters, as shown in figure 3.1:

crackRadius is the radius of the crack as modeled. The radius is either equal the elliptic crack minor axis, for *elliptic* and *simpleScale* transformations or \sqrt{ab} for the *advancedScale* transformation, where a and b are the elliptic crack axes. The value of the *crackRadius* is calculated by the **FEM-dataStr.calculateCrackRadiusBeforeTransformation()** method.

crackZoneSide defines the crack zone area of the model, has a square cross section and is an area of higher mesh density to accommodate the stress field around the crack front. The *crackZoneSide*, though independent parameter, is set to be equal the *crackRadius*.

crackTipSide defines the zone directly surrounding the crack front. It has a square cross section and is meshed with *WEDGE* elements. The value of

the parameter can be set either explicitly or as a fraction of the *crackZoneSide* by the **FEMdataStr.calculateCrackTipSide()** method.

containerHeight parameter defines the height of the cylinder containing the crack.

containerRadius parameter defines the radius of the cylinder containing the crack. Both *containerHeight* and *containerRadius* should be sufficiently large to accommodate the crack. They should also define a cylinder, large enough volume to ensure that the stress field is homogeneous and thus not affect the stress intensity factors.

In total the geometry of the model is defined by four parameters *containerHeight*, *containerRadius*, *crackZoneSide* and *crackTipSide*.

Crack parameters

The crack parameters define the geometry of the crack *a* and *b* and the type of the crack. The crack geometry parameters *a* and *b* are the ellipse axes, corresponding to the *X* and *Z* coordinate axes. The *crackType* parameter defines the what crack would be analyzed. Possible values are *embedded*, *surface* and *edge*. The *crackType* determines the geometry of the model. For *embedded* crack the container is a full cylinder and for *surface* and *edge*, it is a cylinder section of 180 and 90 degrees respectively.

Geometric sets

Thus partitioned, the geometry of the model is organized into sets, which are subsequently utilized in the definition of the features of the model. *Cell* sets are defined to facilitate assignment of mesh controls. *Face* set is defined to facilitate contact definition between the crack flanks. *Edge* sets are created to facilitate seeding of the model and definition of the crack front.

The following edge sets are defined:

allArcEdges set, includes all concentric internal and external circumferential edges. The edge seeds of the set define the angular density of the mesh and the number of elements along the crack front.

containerRefinementEdges set, includes edges connecting the vertices of the crack zone and the cylinder. The seeds of these edges define the density of the mesh surrounding the crack zone. This area is of secondary interest, as the stress field is mostly constant.

crackFrontEdges set, includes the edges of the crack front. It is utilized to define the crack.

crackTipRefinementEdges set, includes the edges, having one of their ends on the crack front. These edges are utilized to constrain the number of seeds, so that the crackTipCells are meshed with *WEDGE* elements only.

crackZoneHorizontalEdges set, includes edges of the crack zone and edges from the cylinder top and bottom surface. The edges have equal number of seeds and define the number of elements around the crack front and thus

are one of main parameters influencing the accuracy of the evaluation of the contour integral.

crackZoneRefinementEdges set, includes edges going radially from the crack tip zone. Seed number is related to the seeds of the *crackZoneHorizontalEdges* and also influences accuracy.

crackZoneVerticalEdges set includes edges of the crack zone, are partitioned by the *XY* plane, edges of the cylinder wall and inner cylinder. The seeds of the edges are calculated as half of the seeds assigned to the *crackZoneHorizontalEdges*.

innerCylinderHorizontalEdges set includes the radial edges of the inner cylinder.

Cell sets are utilized to facilitate the assignment of the mesh controls. The following cell sets are defined:

crackTipCells set is utilized to assign *SWEEP* meshing technique and *WEDGE* element shape to the cells surrounding the crack front.

innerCylinderCells set is utilized to assign *SWEEP* meshing technique and *Medial axis* algorithm to the cells. This meshing technique guarantees, that the cells contain *WEDGE* elements along the *Z* axis. These *WEDGE* elements may become severely distorted during mesh transformation and may fail if the crack aspect ratio becomes large. Therefore, the **FEMorphMesh()** class provides method to delete these elements and close the resulting hole, by moving and merging the nodes of the adjacent *Hex* elements.

Seeds

Seeds of the model are defined as by number, corresponding to edges of the model. The model seeds are completely defined by 4 parameters as follows:

crackZoneMainSeeds define the number of seeds and respectively the mesh density around the crack front. The *crackZoneMainSeeds* are assigned to the *crackZoneHorizontalEdges* edge set. Half of the *crackZoneMainSeeds* are assigned to the *crackZoneVerticalEdges* edge set.

crackZoneRefinementSeeds defines the mesh density in radial direction of the crack front. The seeds are assigned to the *crackZoneRefinementEdges*.

arcSeeds define the number of elements along the crack front. Seeds are assigned to the *allArcEdges* edge set.

containerRefinementSeeds define the mesh density of the container. The seeds are assigned to the *containerRefinementEdges* edge set.

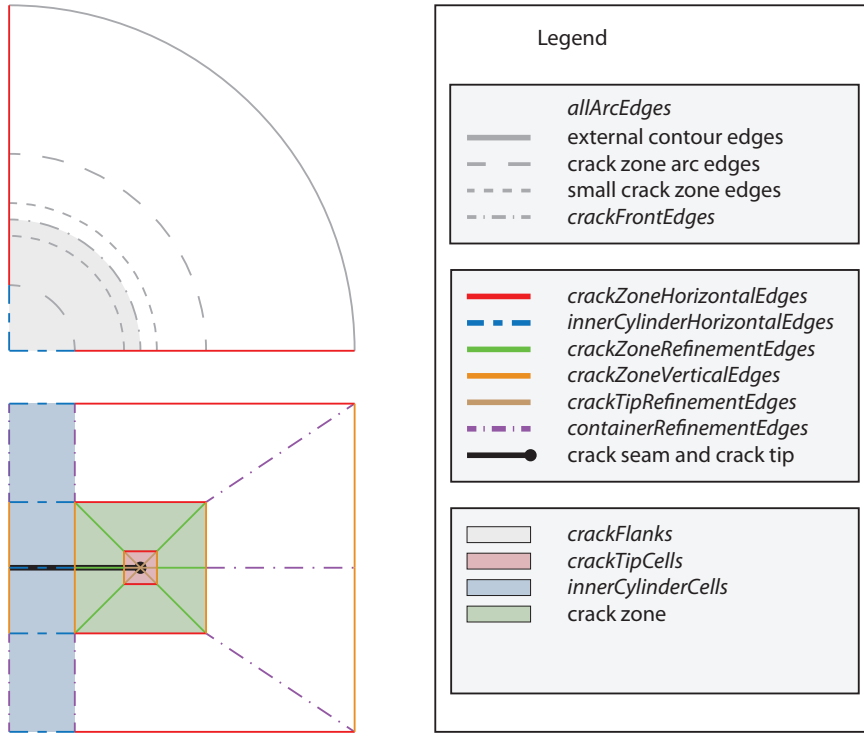


Figure 3.2: crackNormal model

Mesh parameters

The model can be meshed with linear and quadratic, both full and reduced integration elements. Mesh transformation is utilized to obtain a crack shape corresponding to the a and b parameters from the initial circular crack. Mesh transformation is applied to the orphan mesh model and is of three types:

simpleScale transformation multiplies either X or Y coordinate of each node, depending on the ratio a/b , by a factor equal to the *major Axis/minor Axis* of the crack. Then the node is moved to the new coordinate.

advancedScale transformation multiplies both X and Y coordinates of each node, by *expansion* and *contraction* factor, depending on the crack ellipse axes. The both factors are as follows:

$$expansion = \frac{majorAxis}{crackRadius}$$

and

$$contraction = \frac{minorAxis}{crackRadius}$$

elliptic transformation multiplies either the X or Y axis, depending on the

crack parameters by:

$$x = x \sqrt{1 + \frac{a^2 - b^2}{x^2 + y^2}}$$

or

$$y = y \sqrt{1 + \frac{a^2 - b^2}{x^2 + y^2}}$$

depending on the crack ratio.

Analysis parameters

Analysis parameters define the boundary conditions for the model. Analysis parameters for *embedded* crack are as follows:

σ is the applied tension to the an infinite cylinder.

γ angle, defines the rotation of the crack with respect to the applied tension.

ω angle, defines the rotation of the crack in the XY plane.

Material

Material is linear isotropic with Poisson ration $\nu = 0.3$ and Young's modulus $E = 200 \text{ GPa}$.

Interaction properties

Interaction properties include the contour integral definition and contact between the crack flanks.

Contact is defines as frictionless as *Tangential behavior* and *HARD* as *Normal behavior*. Firstly the contact is defined as *SurfaceToSurface* and in the orphan mesh is redefined as *General*, using all surfaces of the model.

Crack interaction is defined using the *crackFrontEdges* edge set a dummy direction of the *qVectors*, *Midside node parameter* as set by the **FEMdataStr.-setMidNodePosition()** and singularity – collapsed element side, single node. The crack interaction is subsequently redefined in the orphan mesh model, with *crackNormal* as extension direction.

Inner cylinder operation

The *WEDGE* elements in the inner cylinder, become severely distorted during mesh transformation and may corrupt the mesh and analysis. Therefore, in case of a crack with large or small ratio of the ellipse axes, these elements are deleted and the resulting hole closed. The difference, in the model is illustrated by figure 3.3. The *WEDGE* elements of the model on the left have been removed and the resulting hole closed by moving the nodes of the hole wall to the axis of transformation and then merging the nodes. On the right side of the figure, however, the *WEDGE* elements have been left, and show severe *skewness*.

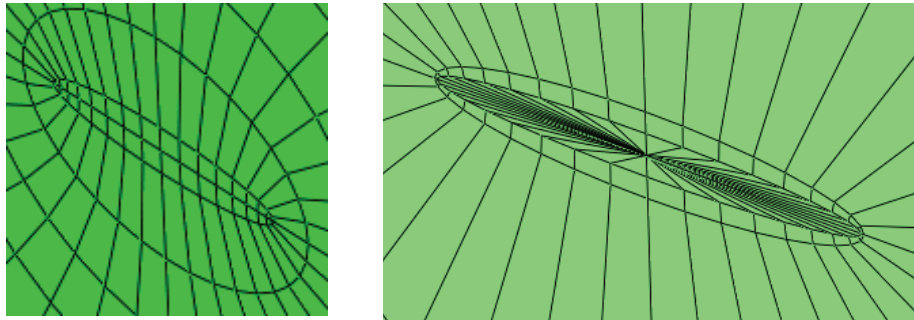


Figure 3.3: *WEDGE* elements of the inner cylinder of the *crackNormal* model

3.2.2 Model types for XFEM analysis

For *XFEM* analysis of cracks, mesh is not required to comply with the crack geometry and this leads to a considerable simplification of the model geometry. However, finer mesh is required for more accurate results. Further, the *XFEM* implementation in Abaqus is available for linear elements only. For the *XFEM* analysis type, three model types are designed: *crackPartition*, *multiplePartitions* and *simple*. The *XFEM* model types share the *analysis*, *crack* and *material* parameters with the *crackNormal* model type. Crack definition for *XFEM* is defined by a *crack geometry* part and *crack domain*. The *crack geometry* part is a *shell* part of an elliptic shape with major and minor axes corresponding to the crack parameters. The *crack domain* represents the part, which contains the crack. Both *crack geometry* part and *crack domain* are independent from each other. Therefore, identical *crack geometry* part, with the corresponding minor and major axes can be utilized, regardless of the crack type and model type. *Crack domain*, however, changes from full cylinder for *embedded* crack to 180 and 90 degree sector for *surface* and *edge* cracks. The model types for the *XFEM* analysis differ only in their respective *crack domains*. This allows experimentation with different meshing techniques and elements.

3.2.3 XFEM *simple* model type

The *simple* modelType uses a cylinder as a *crack domain* without any partitions. Therefore, the mesh size is even in the volume.

Geometric parameters

The *crack domain* is completely defined by the **containerHeight** and **containerRadius**.

Geometric sets

The model has one edge set *allEdges*, containing the edges of the *crack domain*.

Mesh parameters

The *crack domain* can be meshed with *Tetrahedral* or *Hexahedral* elements. The seed size is assigned to the edges of the *allEdges* edge set.

Interaction properties

Contact between the crack flanks is defined in the *XFEM* definition, by specifying contact interaction properties, which are identical to those of the *crackNormal*.

3.2.4 XFEM *crackPartition* model type

The *crackPartition* model type is shown in figure 3.4. The model has a partition in the shape of the crack at its location in the *crack domain*. This permits defining a finer mesh in the vicinity of the crack, and therefore, more accurate estimation of the stress field. A limitation of the this model type is that the *crack domain* can be meshed with linear *tetrahedral* elements only.

Crack partition part

The partitioning of the *crack domain* performed by a part with elliptic shape and minor and major axes equal to the axes of the crack. The part geometry depends also on the *crackType*. For *embedded* crack the part is a full ellipse, while for *surface* and *edge* crack type, the part is a sector of an ellipse of 180 and 90 angle.

Geometric parameters

The parameters defining the *crack domain* and the *partition part* are shown in figure 3.4 are as follows:

- a** the ellipse axis of the crack corresponding to the *X* coordinate axis.
- b** the ellipse axis of the crack corresponding to the *Y* coordinate axis.
- containerRadius** radius of the *crack domain*.
- containerHeight** height of the *crack domain*.

Geometric sets

Two geometric sets are defined in the model. The first, *allEdges* includes all the edges of the *crack domain*. The second, *crackEdges* includes the edges created by the partitioning, and which coincide with the edges of the *crack geometry* part.

Seeds

Seeds are assigned first to the edges of the *allEdges* set, this operation seeds all edges. However, to obtain finer mesh in the vicinity of the crack, edges from the *crackEdges* are seed after the *allEdges*, which ensures that the seed size assigned by the first operation is overwritten.

Mesh parameters

The *crack domain* for this model type can be meshed only with *Tetrahedral* elements.

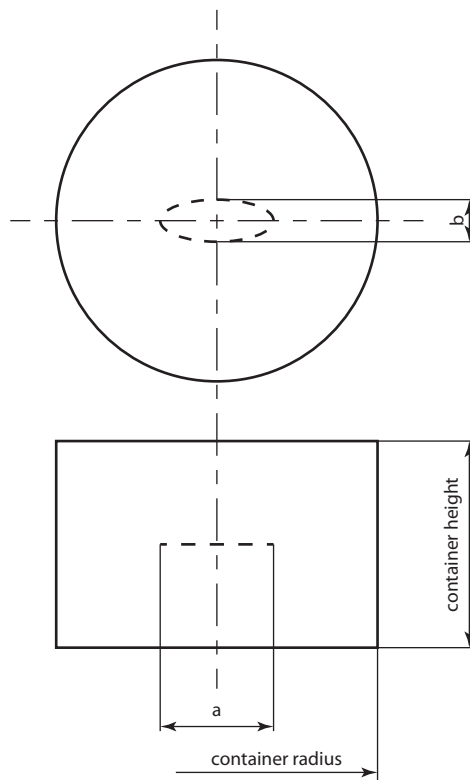


Figure 3.4: *crack domain* of the *crackPartition* model

3.2.5 XFEM *multiplePartitions* model type

The *multiplePartitions* model type is shown in figure 3.5. The *crack domain* is partitioned by an elliptic cylinder around the crack. This creates cells, which can be finely meshed to increase the accuracy of the solution. The model can be meshed with both *Tetrahedral* and *Hexahedral* elements. However, successful meshing mostly with *tetrahedral* elements may prove unpredictable. Therefore, the model is meshed with *Hexahedral* elements only.

Geometric parameters

The model is defined by the following parameters:

a is the ellipse axis of the crack corresponding to the *X* coordinate axis.

b is the ellipse axis of the crack corresponding to the *Y* coordinate axis.

offset parameter, defines the cross section of the elliptic cylinder, which is equidistant to the crack ellipse.

smallContainerHeight defines the height of the elliptic cylinder.

containerRadius radius of the *crack domain*.

containerHeight height of the *crack domain*.

Partition part and lofts

The *crack domain* is partitioned first by an elliptic cylinder, then loft surfaces are created between the elliptic cylinder partition edges and the crack domain circumferential edges and finally by datum planes.

The elliptic cylinder is defined by the *offset* parameter and the crack axes. Its geometry, also depends on the crack type. For *embedded* crack it is a full cylinder and for *surface* and *edge* it is a sector of an elliptic cylinder.

Loft surfaces partition additionally the *crack domain*, to enable and improve meshing of the model.

Finally, the *crack domain* is partitioned by *XZ* and *YZ* planes in case of an *embedded* crack, by *YZ* plane in case of *surface* crack.

Geometric sets

Two geometric sets are defined in the model: *allEdges* and *crackContEdges*. The first contains all the edges of the *crack domain* and the second only edges defined by the partitioning with the elliptic cylinder.

Seeds

Two seed sizes are assigned to the edges of the *crack domain*. First, larger seed size is assigned to the edges of the *allEdges* edge set. Then smaller seed size is assigned to the edges of the *crackContEdges*, overwriting the previous seed size.

Mesh parameters

The *crack domain* is meshed with linear *Hexahedral* elements.

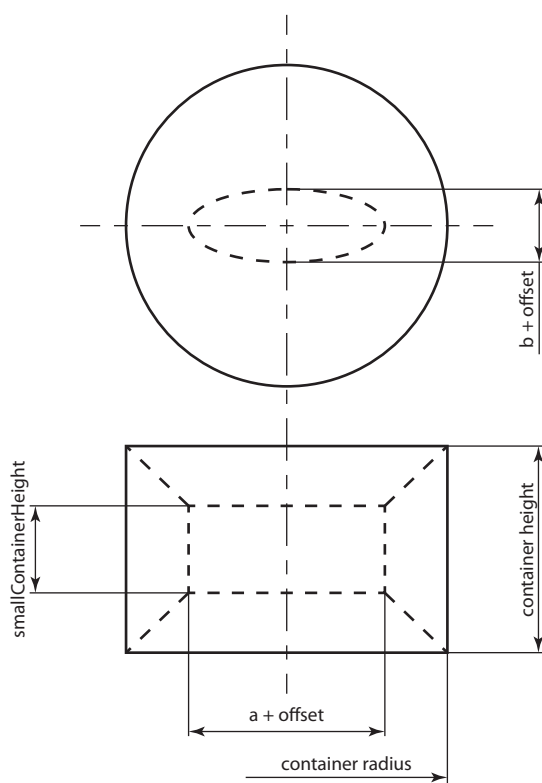


Figure 3.5: *crack domain* of the *multiplePartitions* model

3.3 Visualization Odb

The *visualization output database* is generated to represent the stress intensity factors. A visualization output database is shown in figure 3.6. The objective of the visualization is to provide a clear representation of the stress intensity factors and how they relate with the crack geometry. The visualization is created, by generating nodal, element and field output data, based on the results of the analysis. Stress intensity factor values are written as scalar nodal quantities. The crack front is represented by *truss* elements connecting the nodes of the crack. On the figure 3.6, they are the thin elliptic line and represent the **K3** values. **K1** values are represented by the elements of the two elliptic cylinders located above and below the crack plane. **K2** values are represented by the elements in the crack plane.

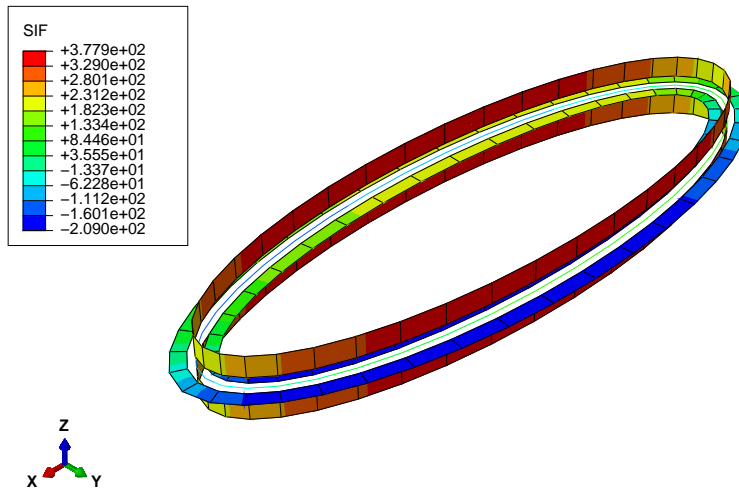


Figure 3.6: Visualization output database

3.3.1 Node data

Nodes are created on the basis of the crack geometry and mesh refinement of the corresponding model database. Nodes can be divided into three groups, on the basis of the elements, which they define and the values the elements represent.

K3 – nodes . These nodes are used to define the *truss* elements and have identical coordinates with the nodes of the modeled crack in the model database.

K1 – nodes . The K1 – nodes are used to define the *shell* elements of elliptic cylinder. They are created by offsetting the *Z* coordinate of each of the K3 – nodes. These nodes lie on four planes, offset from the crack plane. Two of them are above the crack plane and the other two are below it. Each of the two pairs of nodes are used to create the *shell* elements representing the **K1** values.

K2 – nodes . The **K2 – nodes** are used to define the *shell* elements, in the crack plane. They are created as equidistant from the **K3 – nodes**. The offset is measured on the normal to the ellipse at each **K3 – node**. The created nodes form two pair of nodes, one inside the crack, and one outside. Each pair of nodes is used to create *shell* elements, which represent the **K2** values.

3.3.2 Element data

Elements of the visualization output database are used to interpolate the field output, which is the stress intensity factors. According to the stress intensity factor, they represent, elements can be divided into three groups:

K3 – elements are the *truss* elements representing the crack front.

K1 – elements are the *shell* elements on the elliptic cylinders located above and below the crack plane.

K2 – elements are the *shell* elements in the crack plane, located inside and outside the crack contour.

3.3.3 Field output data

Field output data represents the stress intensity factors for the analyzed crack. The values are averaged over specified contours from the user. The field data is *NODAL* and of type *SCALAR*. The stress intensity factors field output is the only available field output for the output database. The data is written for each node, respecting the node label, which identifies the which stress intensity factor value is written.

Regarding **K1** and **K2**, nodes are four times the number of the crack nodes (two pairs of nodes for each), therefore, the data is repeated to comply with the number of nodes. The result for **K1** is that nodes with the same *x* and *y* coordinates are assigned identical values. For **K2**, the nodes with identical values, lie on the normal to the crack contour. As for the **K3 nodes** number corresponds to the number of the crack nodes and, therefore, no further processing is required.

3.4 GUI and Abaqus integration

The program features a graphical user interface to browse the *shelve* databases, which contain results, input parameters and statistics about every analysis run with the program. The graphical user interface of the program is accessed through the menu *Plug_ins* → *cracks* → *DB ACCESS*.

3.4.1 First dialog box

The interface consists of two dialog boxes. The *first dialog* box, shown in figure 3.7 asks user to select the crack type to analyze. The program uses this information to determine the *shelve* database, read its contents and use it to prepare the *second dialog* box.

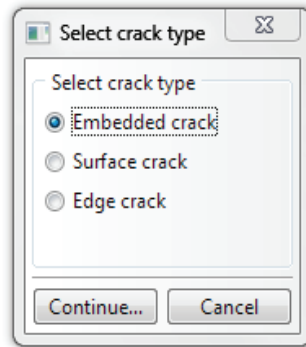


Figure 3.7: First dialog box of the program user interface

3.4.2 Second dialog box

The *second dialog* box is shown in figure 3.8 for *embedded* crack type, though the dialog box is identical for the *surface* and *edge* crack types. The dialog box is separated into four sections:

- Database records
- Results selection
- Contours
- Items to create

Database records

The **Database records** is the browser section of the dialog box, it contains all the entries of the corresponding *shelve* database. The database records are organized in a tree representation based on the input parameters of each entry, narrowing down the selection to the *modelName* of the analysis, which corresponds to the *shelve* key of the entry. Only the *modelNames* of the successful analyses are selectable and selection of multiple entries is possible.

To preserve space logical groups of parameters are abbreviated and concatenated with their respective value. For instance *h200r120* denotes a cylinder with *height* = 200 and *radius* = 120. The complete list of abbreviations is given in table 3.1.

Results selection

The **Results selection** section contains Two subsections **Analytical solutions** and **Analysis results**. Both are composed of check boxes to specify which of the stress intensity factors should be included in the analysis.

Contours

The **Contours** section is composed of two subsections **Contours to average** and **Include contour data**. The **Contours to average** contains a list of

abbreviation example	explanation	
h200r120		
	h	height
	r	radius
czm5czt5ar5cr5		
	czm	crack zone main seeds
	czt	crack zone refinement seeds
	ar	arch seeds
	cr	container refinement
czs10cts3mn0.27		
	czs	crack zone side
	cts	crack tip side
	mn	mid node position
ae5		
	ae	all edges
ae5ce1		
	ae	all edges
	ce	crack / container edges

Table 3.1: GUI tree abbreviation key

five contours, from which the specified stress intensity factors are averaged. The **Separate contours** includes the check box **Include contour data**. The check box is applicable for the creation of *XYPlotData* only. It specifies that *XYPlotData* to be created for the each contour of the analysis, otherwise, *XYPlotData* is created for the averaged data only.

Items to create

The **Items to create** section contains the following check boxes, specifying what actions to perform with the selected data:

XYPlotData creates *XYPlotData* with the selected options.

Print data structure prints the data contained in the *shelve* database including the averaged contours, for the selected entries in the *tree*.

Visualization Odb creates a visualization output databases for the selected entries in the *tree* and the results from the averaging of the contours.

3.5 Organization of the application

The afore described functionality and model, output and *shelve* databases are created by a number of scripts, organized in modules and packages, which compose the complete program, which closes the cycle of analysis, providing the following functionality:

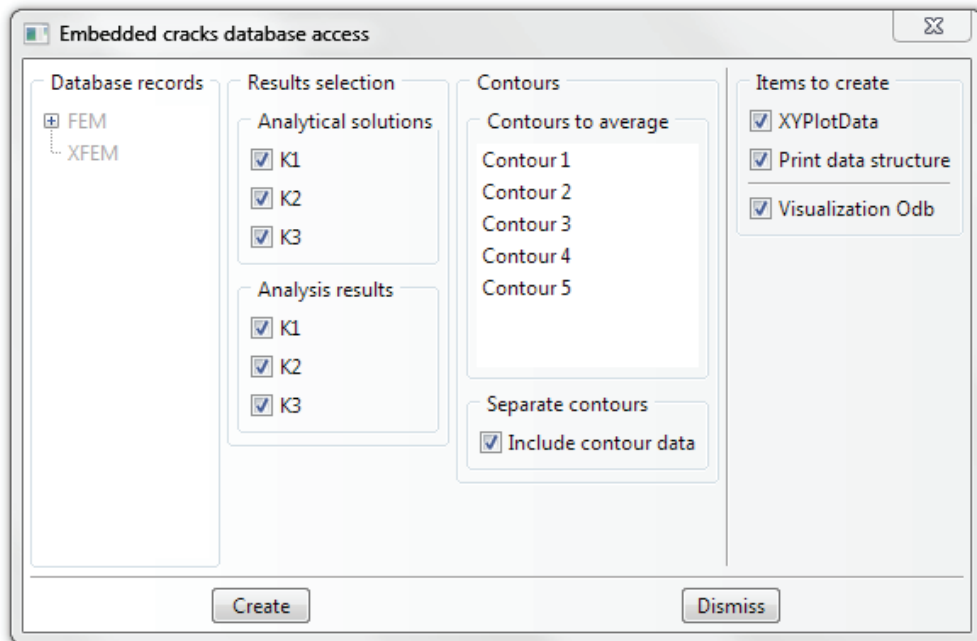


Figure 3.8: Second dialog box of the program user interface

- creation of model databases for the different crack and analysis types.
- submitting the model databases.
- post processing and results extraction.
- storing the extracted results to a *shelve* database.
- creation of visualization.
- providing a graphical user interface to browse the data in the *shelve* database and selecting the desired operations and data combination.

3.5.1 Structure by function

The program can provisionally be divided into two independent components:

- Running analyses
 1. building of Abaqus model databases,
 2. executing the subsequent analysis,
 3. extraction of the required values from the Abaqus output database
 4. saving the results into a custom *shelve* database;
- Post processing and visualization
 1. graphical user interface to read the custom database entries

2. creation of plots from the analysis results, and analytical solutions,
3. building of visualization Abaqus output database for stress intensity factors

3.5.2 Directory structure and modules

Both functional components share the same directory structure for convenience and portability. Program classes and functions are organized in files, called *modules*. *Modules* are organized in directories, called *packages*. The directory structure of the program is as follows:

```

dir simpleGui
    module createEntryID.py
    module dbAccessDialogs.py
    module dbAccessDialogs_plugin.py
    module executeDbAccessCommands.py
    dir db
    dir scripts
        dir analyticalSolutions
            module analyticalData.py
            module baseAE.py
            module edgeAE.py
            module embeddedAE.py
            module surfaceAE.py
            module miscFunctions.py
        dir dataStr
            module baseDataStr.py
            module femDataStr.py
            module xfemBaseDataStr.py
            module xfemDataStrMP.py
            module xfemSimpleDataStr.py
            module xfemTETdataStr.py
        dir modelDb
            module baseCrack.py
        dir fem
            module femCrack.py
            module orphanMesh.py
        dir xfem
            module xfemBaseCrack.py
            module xfemCrackMP.py
            module xfemSimpleCrack.py
            module xfemTETcrack.py
    dir persistence

```



```

    module dbDataStr.py
    module persistence.py
dir processOdb
    module readOdb.py
    module xyPlotDataFromDbEntry.py
dir visualizationOdb
    module visualizationOdb.py

```

The program directory should be located in a directory named *abaqus_plugins*, which should be located in either:

- user home directory,
- abaqus directory,
- current directory,
- or *plugin_dir*, specified in the abaqus environment file.

Installing the program in one of these directories, enables Abaqus to identify the program and make it available in the *Plug-ins* menu, as a *DB ACCESS* entry item.

3.6 Description of classes

3.6.1 Classes interaction

Each class has a strictly defined role and interaction among classes is provided by interfaces (*accessor* methods) implementing the important concept of *encapsulation*. *Encapsulation* is to isolate the internal operations of an object from the other interacting objects and code one operation only once.

In addition, by *encapsulation* internal logic and operations of classes are decoupled from each other, which makes them separate units. Moreover, any modifications to the class methods and algorithms of the class do not affect the rest of the program.

A simplified representation of the program structure is shown in figure 3.9. Blocks are given generic names, referring to families of classes or functions, serving equivalent purposes. Therefore, the particular name of the class and implementation depends on the model and analysis type.

Data structure class is used to store input parameters, process the input parameters into a format more suitable for the other interacting classes and store output data from the interacting classes and the Abaqus output database.

Model database class defines the necessary Abaqus kernel commands to build the model database and submit the analysis.

ReadOdb class is utilized to open the Abaqus output database, extract the stress intensity factor values and coordinates of the corresponding nodes, process the coordinates and corresponding values, and write the obtained results to the **Data structure classes**.

Persistence class is utilized to determine the shelf database to which to save, filter the data to be saved, save the data, identify duplicate in the database and read from the database.

Analytical solutions class is utilized to calculate the analytical solution, corresponding to the designated analysis.

Visualization output database class is utilized to create an Abaqus output database for visualization of the stress intensity factors of a designated analysis.

XYPlotData class is utilized to create XYPlotData for a designated analysis.

Db data structure class is utilized to temporarily store data read from the *shelfe* database and process requests from the user.

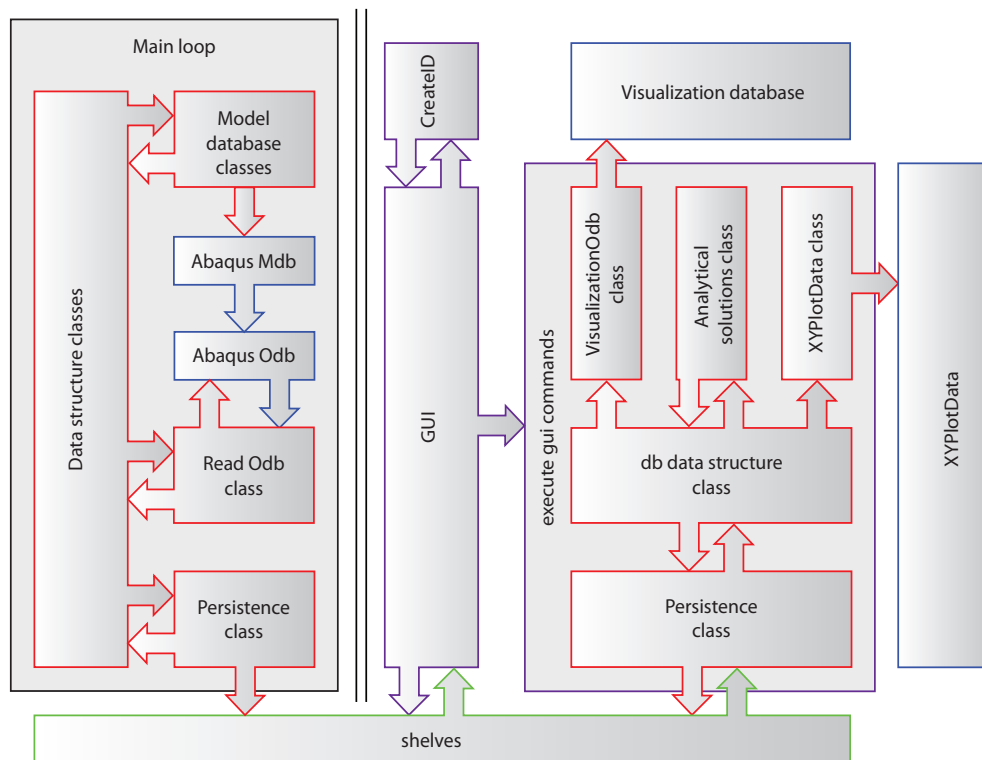


Figure 3.9: Classes interaction

3.6.2 DataStr classes

DataStr classes family is the backbone of the program. It collected input parameters, stores them in a tree structure and provides methods for manipulation of the stored parameters. Furthermore, each of the rest of the classes interacts with a **DataStr()** class by the provided interfaces.

BaseDataStr() class

The **BaseDataStr()** is the *superclass* of the **DataStr** classes family and the other members are *subclasses* of the **BaseDataStr()** class. The **BaseDataStr()** class defines the methods common with the rest of the **dataStr** classes. *Superclasses* are designated in the *subclass* definition and the *superclasses'* methods become available to the *subclass*. When a class method is called, first the method name is searched in the name space of the *subclass*, and if not found the search propagates to the *superclasses* until a method with the corresponding name is found. In case a method is not found, an exception is raised. The search algorithm enables the option for overriding or customization of *superclass* methods within the *subclass* by defining a new method with the same name. This programming technique is called *inheritance*. It is a fundamental technique in object-oriented programming (OOP) and of great utility for reduction of code duplication and increasing code reuse.

The purpose of the **BaseDataStr()** class is to provide storage and access interface that is inherited by the *subclasses*. This guarantees, that the interface and the storage structure remain consistent, throughout the program and only the required customizations are implemented in the corresponding *subclass*.

The **BaseDataStr()** class, provides methods for:

- initializing and storing input and analysis parameters,
- generating a unique model name for each simulation,
- defining the *revolutionAngle* parameter, depending on the crack type,
- determination of the analysis success,
- equal sign operator overloading.

A unique model name is created for each analysis by the **createModelName()** method. The algorithm is based on the number of seconds since the Epoch, which is obtained by the python command *time()*. The raw format of the name is *1307559473.99*, which roughly corresponds to June 6, 2011, 21:57:37. In that raw format, however, the model name is not a valid Abaqus model name, therefore, it is modified to become *1307559473dot99*, which is.

Most of the parts of the Abaqus model are defined as revolved parts and their *revolutionAngle* is different for each crack type (*embedded*, *edge*, or *surface*). The **calculateRevolutionAngle()** method specifies the *revolutionAngle* parameter.

The mesh of the FEM model type is fairly complex and is defined by a multitude of parameters, it is also being deformed during transformation. Therefore, it may happen for some parameter configuration, that the mesh may not pass the analysis checks at job submission and the analysis would fail. Therefore, mesh quality checks are performed twice, once right after the meshing of the model, before writing the input for the orphan mesh and second after the mesh transformation of the orphan mesh model. Results of the both reports are stored to the data structure, (under the *results:mesh:priorTransformation* and *results:mesh:postTransformation* keys) by the methods **setPriorMeshTransformationReport()** and **setPostMeshTransformationReport()**. The success of the analysis is set to *True* should the *failedElements* is zero for the second (post-transformation) report.

Important option to have is the ability to check whether an identical model with the same configuration of input parameters has been subject to past analysis. To facilitate the implementation, the **BaseDataStr()** class has an implementation of the equal sign overloading. The method is `__eq__()` and is executed automatically when an instance of the **BaseDataStr()** or any of its *subclasses* is compared for equality. The method verifies, whether the data structure of the class under the *input* key is equal to the compared object.

FEMdataStr() class

FEMdataStr() class is a *subclass* of **BaseDataStr()** class and inherits all of the **BaseDataStr()** methods and also defines new ones. The **FEMdataStr()** class is utilized for the *FEM analysis* type.

The essential methods of the class and their application are described below:

`__init__()` method is augmented **BaseDataStr.__init__()** method, which sets the parameter *input:analysisType* to *FEM* for identification purposes in subsequent analyses of the data.

setMidNodePosition() method sets the relative position of the middle node of the singularity at the crack tip. It is designed to assist the mesh of the model to pass the analysis checks. The midNode position is not relevant for stress intensity factors and linear elements.

createDatumsData() method creates datum parameters, for datum planes, required for partitioning the model.

calculateCrackRadiusBeforeTransformation() method identifies the radius of the crack prior mesh transformation. Initially elliptic crack is modelled as a *penny-shaped* crack, which after the mesh transformation becomes of elliptic shape. Considering the different transformation types and crack geometry parameters, this method ensures consistent input to the mesh transformation operation.

calculateCrackZoneSide() method sets the *crackZoneSide* parameter, shown in figure 3.1. It is similar to the **calculateCrackRadiusBeforeTransformation()** method, however, it determines the size of the partition for refined mesh around the crack tip.

calculateCrackTipSide() method sets the size of the *cracktipSide* parameter, shown in figure 3.1. Its value is relative to the *crackZoneSide*. The method is designed to increase the flexibility of meshing in case meshes do not pass the analysis checks.

calculateMdbGeometricParameters() method processes the geometric parameters from the *input* branch into a more suitable format for subsequent operations. Thus calculated parameters are written to the *mdb* branch of the data structure.

createPartsData() method creates the required parameters for generation of all the constituent parts of the model. Parameters are located under the *mdb:parts* branch. Under the *mdb:parts:sketchPoints* are the sketch parameters for shell and solid parts. These parts are composed of one

revolve feature. Parameters for each part correspond to a *dictionary* key, which serves as a name of the part. In addition, the method creates two more entries for the names of the *merged part* and *orphan mesh part*.

createPartitionData() method creates the required parameters for partitioning the model, depending on the crack type. Under the branch *mdb:partitionData:innerCylinderPartitions* are located parameters for partitioning the inner cylinder cells by datum plane with a designated identification number. Under the *mdb:partitionData:piePartitionsDatum* are located a number, designating which datums should be used to partition the model according to the crack type.

createPolarCoordinatesOfAPointOnEntityForASet() method created preliminary point coordinates on the *XZ* plane, for selection of edges, faces and cells, which would be organized in sets. Coordinates of the points are subsequently processed, with respect to the entity and crack type to ensure, that they are on the edges and cells or inside of the cells. Coordinates are created under the *mdb:sets:pointsProjectedOnZeroDegreePlane*. Depending on the feature, they are representing, are located under the *faces* for faces and *cells* for cells. Coordinates for edges are divided into *crossSectionEdges* for edges in *XZ* or *YZ* planes, and into *arcEdges* for edges on *XY* or parallel plane.

createAnglesForAPointOnZeroDegreePlane() method defines angles, in accordance with the crack type, which are used to calculate the final coordinates of the points for selection of the geometric features of the model.

createCompleteSetsData() method calculates the final values of the parameters required for selection of geometric features (*edges*, *faces*, *cells*, *elements* and *nodes*) and their organization in sets. First, it calls **createSetData()** method for the two types of *edges*, *faces* and *cells*. Then it calls the **createElementSetData()** and **createNodeSetData()** methods, which create element and nodal set data.

createElementSetData() method creates the required parameters for selection of elements comprising the *innerCylinder* of the orphan mesh model. Data is stored under the *mdb:sets:elementsSetData* branch of the data structure.

createNodeSetData() method writes the names of node sets for nodes contained in the *innerCylinder* of the orphan mesh model. Data is stored under the *mdb:sets:nodeSetsData* of the data structure.

createSetData() method creates the required data for geometric features of the model, utilized to create set data for *edges*, *faces* and *cells*. The method takes two arguments to identify the geometric features and read the necessary input parameters from the data structure. For each point of each geometric feature set, the method calls **calculateXYZCoordinates()** with two parameters: angle and the preliminary coordinates created by the **createAnglesForAPointOnZeroDegreePlane()** method.

calculateXYZCoordinates() method calculates and returns the final coordinates of a point on an *edge* or *face* or inside a *cell*. The point is utilized for selection of a geometric feature and organizing it in a set.

createSeedsData() method creates the required parameters to completely define seeding of the model. A complete set of seed parameters is generated for each *edge* set. Data is stored under the *mdb:seeds* branch of the data structure.

createElementTypeData() method creates element type data, for the model, according to the *elementType* input. The possible values for the input are: *linearRI*, *linearFI*, *quadraticRI* and *quadraticFI*. Corresponding element codes are as follows, for *linearRI* – **C3D8R**, **C3D6**, **C3D4**; *linearFI* – **C3D8**, **C3D6**, **C3D4**; *quadraticRI* – **C3D20R**, **C3D15**, **C3D10M**; *quadraticFI* – **C3D20**, **C3D15**, **C3D10M**. Data is stored under the *mdb:meshParameters:elementCodes* branch of the data structure.

setInnerCylinderHoleRadius() method is utilized to store the radius of the nodes on the wall of the *innerCylinder* hole of the orphan mesh model, created by deleting of the wedge elements. Parameter is stored under the *mdb:sets:nodeSetsData:radius* branch of the data structure. The parameter is accessed by the **getInnerCylinderHoleRadius()** method.

processTransformationInputData() method determines the *axis of transformation* of the mesh in accordance with the crack geometry. The *axis of transformation* coincides with the crack elliptic shape's major axis. The method also copies the *transformationType* parameter from *input:meshParameters* to *mdb:meshParameters*. The *axis of transformation* parameter is stored under the branch *mdb:meshParameters:transformationAxis*.

XFEMbaseDataStr() class

XFEMbaseDataStr() class is a *subclass* of **BaseDataStr()**. It serves as a *superclass* for **XFEMsimpleDataStr()**, **XFEMtetDataStr()** and **XFEMdataStrMP()**, which are utilized for the corresponding model types of the *XFEM* analysis types. It is, however, independent of the **FEMdataStr()** class. The purpose of **XFEMbaseDataStr()** as a *superclass* is to provide methods that are common to its *subclasses* by customization and augmentation of the **BaseDataStr()** class. Its utility is aligned with the purpose of the **DataStr** classes family.

The essential methods of the class and their application are described below:

__init__() method is an augmentation of the **BaseDataStr.__init__()** method, therefore, has the same functionality with the addition of setting the parameter *input:analysisType* to *XFEM* to identify the analysis type in subsequent data analyses.

createDatumsData() method, creates parameters defining datum planes. Data is stored to the *mdb:datumsData* branch of the data structure.

calculateMdbGeometricParameters() method processes the input geometric parameters from the *input* branch of the data structure into a more suitable format to facilitate subsequent operations. Data is stored to the *mdb:geometricParameters* branch.

createPartsData() method creates the required parameters for generation of the *crackDomain* and *crackGeometry* parts. It also writes the name of the *mergedPart* as a dictionary key. Data is stored under the *mdb:parts* branch.

createCrackPartitionPartData() method creates the required parameters to create a shell part, that is used to partition the *crackDomain* part at the crack location to create internal edges in the *crackDomain* part, to which a smaller seed size is assigned. The part geometry is dependent on the crack type. Geometrically, its shape is represented by the intersection between the crack geometry and the *crackDomain*. For *embedded* crack its shape is identical to the crack geometry. For *edge* and *surface* crack types it is sector of an ellipse. Data is stored under the *mdb:parts:crackPartitionPart* branch.

createSeedsData() method creates the complete data for seeding the model. Data is stored under the *mdb:seeds* branch.

createElementTypeData() method creates element type data for the model, according to the *elementType* input parameter. Possible values and the corresponding element codes are:

LinearTET — C3D4

LinearHexRI — C3D8R

LinearHexFI — C3D8

Data is stored to the *mdb:meshParameters:elementCodes* branch.

createCompleteSetsData() method creates the required parameters for edges of the *crackDomain* part and faces of the *crackGeometry* part. Data is stored to the *mdb:sets:setData* branch of the data structure.

setSingularityCalcRadius() method is utilized to store the *singularityCalcRadius* to *input:intractionProperties:crack:singularityCalcRadius*.

For complete specification of the *accessor* methods of the **XFEMbaseDataStr** class refer to Appendix

XFEMsimpleDataStr() class

XFEMsimpleDataStr() class is a *subclass* of the **XFEMbaseDataStr()**, which is a *subclass* of the **BaseDataStr()** class. Therefore, the **XFEMsimpleDataStr()** class inherits all the methods of both of its *superclasses*, with the customizations of the **XFEMbaseDataStr()** class. The class is utilized for the *simple* model type of the *XFEM* analysis type.

It has one only one method:

__init__() method is an augmentation of the **XFEMbaseDataStr.__init__()** method. In addition to the functionality of the base method it sets the parameter *input:modelType* to *simple* to serve as an identification of model type in subsequent analyses.

XFEMtetDataStr() class

XFEMtetDataStr() class is *subclass* of the **XFEMbaseDataStr()** class. It is similar to the **XFEMsimpleDataStr()** class with the difference that **XFEMtetDataStr()** class is utilized for *crackPartition* model type of the *XFEM* analysis type. It is also a single method class with the only method:

__init__() method is an augmentation of the **XFEMbaseDataStr.__init__()** method. In addition to the functionality of the base method it also sets the parameter *input:modelType* to *crackPartition* to serve as an identification in subsequent analyses.

XFEMdataStrMP() class

XFEMdataStrMP() class is a *subclass* of the **XFEMbaseDataStr()** class and is utilized for the *multiplePartitions* model type of the *XFEM* analysis type.

The essential methods of the class are:

__init__() method is an augmentation of the **XFEMbaseDataStr.__init__()**. In addition to the functionality of the base method it sets the *input:modelType* to *multiplePartitions* for identification in subsequent analyses.

calculateMdbGeometricParameters() method processes the input geometric parameters from the *input* branch into a more suitable form for subsequent operations. Thus calculated parameters are stored to the *mdb:geometricParameters* branch of the data structure.

createPartsData() method is an augmentation of the **XFEMbaseDataStr.createPartsData()** method. In addition to the functionality of the base method it creates data for the *smallContainer* part, in accordance to the crack type.

createParametersForLoft() method calculates coordinates of points on the circumferential edges of the *crackDomain* and *smallContainer*, used to select the edges as profiles for *loft* operation. The method calls the **calcCoordsOfCrackContainerEllipseEdges()** to find a point on the circumferential edge of the *smallContainer*. Data is stored under the *mdb:parts:sketchPoints:smallContainer* branch.

calcCoordsOfCrackContainerEllipseEdges() method calculates and returns the coordinates of a point on the circumferential edge of the *smallContainer* part. It takes two arguments: an angle of a line through the origin and the point, and the *X axis*, and *hieghtUnitVector*, which determines the sign of the *Z* coordinate.

createDatumsData() method creates the required parameters for creation of datum planes. Data is stored to the *mdb:datumsData* branch.

createAdditionalSetsData() method creates parameters for a set of the *edges* of the *smallContainer*. Data is stored under the *mdb:sets:setsData:selectBy-BoundingBoxEdges:ellipseContainerEdges* branch.

createSeedsData() method creates the required seed parameters for the model. It *redefines* the **XFEMbaseDataStr.createSeedsData()**, which creates has identical purpose, but defines different parameters. Data is stored to the *mdb:seeds* branch.

3.6.3 Model database classes

Model database classes is a family of classes, which provide methods with Abaqus kernel commands, utilized to create an Abaqus model. To each model type for *FEM* and *XFEM* analysis type corresponds a member of the **model database classes**. All classes take one argument a **DataStr class**, corresponding to the model type. The required input parameters and supporting analysis parameters are read and stored to the **DataStr class**. In addition, the **model database classes** use an internal data structure, named **self.mdb**, which is of *dictionary* type and is used to store and point to components of the Abaqus model. The organization of the **model database classes** family is as follows:

BaseCrackMdb() is a *superclass* of all other classes in the family;

FEMcrackMdb() and **FEMcrackOrphanMesh()** used to create the analysis of *FEM* type;

BaseXFEMcrackMdb() *superclass* for classes used to create *XFEM* analysis type, regardless of the model type;

XFEMcrackMdbMP() used to create *XFEM* analysis type and *multiplePartitions* model type;

SimpleXFEMcrackMdb() used to create *XFEM* analysis type and *simple* model type;

XFEMtetCrackMdb() used to create *XFEM* analysis type and *crackPartition* model type.

BaseCrackMdb() class

BaseCrackMdb() class serves as a *superclass* of all **model database classes** and provides methods used by most of the *subclasses*.

The **BaseCrackMdb()** class methods are as follows:

__init__() method initializes the class, creates the [self.mdb] variable and takes a **DataStr class**.

initializeAbaqusModel() method creates a new Abaqus model, gives it a name, generated by the **DataStr** class and deletes the generic *Model-1* form the Abaqus database.

initializeViewport() method creates a viewport named after the *modelName* to display the created model and sets *XY* plane as compass privileged plane. It also sets **self.mdb[viewport]** as a pointer to the viewport.

setVieportViewingPoint() method changes the parameters of the isometric view of the viewport, so that the *Z* axis points upwards and sets a view in the viewport **self.mdb[viewport]**.

setDisplayableObject() method takes one argument, and sets it as a *displayableObject* of the viewport.

createSolidParts() method calls the **createASolidRevolvedPart()** for each solid revolved part, specified in the **DataStr** class.

createShellParts() method calls the **createAShellRevolvedPart()** for each shell revolved part, specified in the **DataStr** class.

createASolidRevolvedPart() method creates a sketch and revolves it to create a 3D *DEFORMABLE_BODY*. The revolution angle is the angle determined by the **DataStr** class in accordance with the crack type. The created part is pointed to by the **self.mdb[parts][name of the part]**. After the part is created the method calls **createPartOrientation()** method.

createPartOrientation method takes a part as an input argument, creates a datum coordinate system of the part and calls the **createMaterialOrientation()** method, to which it passes the part.

createMaterialOrientation() method sets the material orientation of a part that takes as an input argument.

createAShellRevolvedPart() method creates a sketch and revolves it to create a 3D *DEFORMABLE_BODY*. The revolution angle is the angle determined by the **DataStr** class in accordance with the crack type. The created part is pointed to by the **self.mdb[parts][name of the part]**. After the part is created the method calls **createPartOrientation()** method.

createMergedPart() method creates a part by merging all the instances in the model assembly and gives it the name specified in the **DataStr()** class, corresponding to the *mergedPart*.

createDatums() method creates datum planes in the *rootAssembly* of the model. Datums are created according to the defined parameters in the **DataStr** class.

deleteAllInstances() method deletes all part instances from the model assembly. The method is used to clear the model of the instances, after the *mergedPart* is created.

createInstancesFromAllParts() method creates instances of all parts in the model. The method finds all the part names in the model and calls the **createInstance()** with the part name as an argument. It is used to create instances of all parts, from which the *mergedPart* is created.

createMergedPartInstance() method creates instance of the *mergedPart* by calling the **createInstance()** method and passing the *mergedPart* name. The method also sets the variable **self.mdb[mergedInstance]** to point to the created instance.

createInstance() method, takes a part name as an argument, creates instance of the part with the same name and returns the instance.

createMaterial method creates a material with elastic properties and name as specified in the **DataStr()** class.

createSection method creates a homogeneous solid section with the material name, specified in the **DataStr** class.

assignSectionToAllParts() method finds the names of all parts in the model and for each one calls the **assignSectionToPart()** with the part name as an argument.

assignSectionToMergedPart() method calls the **assignSectionToPart()** with the *mergedPart* name as an argument.

assignSectionToPart() method takes a part name as an input argument and assigns the section with name designated in the **DataStr** class.

regenerateAssembly() method calls the *regenerate()* method of the Abaqus model *rootAssembly*. The method is utilized to force Abaqus to rebuild and recalculate the model following some operations. This guarantees that subsequent operations are applied to a model that is up to date and all prior operations have been completed. In case of applying commands to a not up to date model, unexpected results may be obtained.

createStep() method creates a static step with a name specified in the **DataStr** class.

deleteHistoryOutputs() method identifies and deletes all history output requests. The method is utilized to delete the default history output request and to clear the orphan mesh model, after importing the input file.

createHistoryOutput() method creates a history output request for the crack, designating *K_FACTORS* as an output quantity and parameters defined in the **DataStr** class.

createContactInteractionProperty() method creates a contact property with name specified in the **DataStr** class and *normal behavior* as *HARD* with allowed separation of contact surfaces and *FRICITIONLESS tangential behavior*.

createGeneralContact() method creates a *standard contact* with contact property name designated in the **DataStr** class. This type of contact is utilized for the orphan mesh model to avoid designating contact surfaces, which is required by other contact types.

assignElementType() method assigns the defined in the **DataStr** elements to the model assembly.

generateMesh() method generates mesh on the *mergedInstance*.

seedEdges() method assigns a specified number of seeds to every edge of all specified *edge* sets. Seed number data is obtained from the **DataStr** class and *edge* sets are read from the **self.mdb[sets][edges]**.

verifyMesh() method performs a mesh quality verification with the *ANALYSIS.CHECKS* option, which is the mesh quality verification, that is performed automatically by Abaqus on job submission. The *meshQualityReport* command returns a dictionary with the following keys: *warningEle-*

ments, *failedElements*, *naElements* with selection mask of the corresponding elements as dictionary value, and *numElements* with a number designating the number of the elements. The mesh report is then processed so that only the number of elements corresponding to each key is returned. The importance of the report is that the analysis success can be predicted by the number of the *failedElements*. If the number of *failedElements* is not 0, the analysis will fail.

createBC() method calls the appropriate method to create the boundary conditions of the model depending on the crack type. For *embedded* crack type, the method calls **createInfiniteCylinderBC()** method. **For edge surface crack types methods are not available at the time of writing.**

createInfiniteCylinderBC() method creates a displacement constraint for each node of the external faces of the *mergedInstance*, depending on the coordinates of the node and angles γ and ω , which define the crack orientation in space and σ , which is tension magnitude. Boundary conditions are called *displacementBC-n*, where *n* is the consequent number of the BC. Nodal displacements are obtained by the method **calculateInfiniteCylinderDisplacementForNode()** and passing a node for an argument.

makeRegionForBCFromNode() method returns a *region* created by a node. The method is utilized to get a *region*, required by the *DisplacementBC()* command.

calculateInfiniteCylinderDisplacementForNode() method is utilized to calculate the displacement assigned as a boundary condition of the node. The method employs the following procedure. First, node coordinates (x , y , z) are multiplied by a rotation-transformation matrix (3.1) to obtain coordinates (x' , y' , z') corresponding to crack orientation defined by γ and ω .

$$\begin{bmatrix} \cos \gamma \cos \omega & \cos \gamma \sin \omega & -\sin \gamma \\ -\sin \omega & \cos \omega & 0 \\ \sin \gamma \cos \omega & \sin \gamma \sin \omega & \cos \gamma \end{bmatrix} \quad (3.1)$$

Next displacements are calculated by the following formulas:

$$\begin{aligned} \Delta z &= \frac{\sigma}{E} z' \\ \Delta y &= -v \frac{\sigma}{E} y' \\ \Delta x &= -v \frac{\sigma}{E} x' \end{aligned}$$

Finally (Δx , Δy , Δz) are multiplied by the inverse of the rotation-transformation matrix 3.2 to obtain the displacements at the designated nodes.

$$\begin{bmatrix} \cos \gamma \cos \omega & -\sin \omega & \sin \gamma \cos \omega \\ \cos \gamma \sin \omega & \cos \omega & \sin \gamma \sin \omega \\ -\sin \gamma & 0 & \cos \gamma \end{bmatrix} \quad (3.2)$$

createJob() method creates an analysis job for the model and setting job parameters to use multiple core CPU and memory limit for optimal performance.

submitJob() method submits the model analysis job and waits for the job completion.

closeMdb() method closes the Abaqus model database.

saveMdb() method saves the Abaqus model database.

FEMcrackMdb() class

FEMcrackMdb() class is a *subclass* of the **BaseCrackMdb()** class and therefore, inherits all of its methods. The objective of the **FEMcrackMdb()** class is to create an Abaqus model database for *FEM* analysis type of an elliptic crack, which can be of *embedded*, *edge* or *surface* type. Methods defined within the **FEMcrackMdb()** along with those inherited from the *superclass* provide functionality to initialize the model, create the necessary geometry, seed and mesh the model, and write an input file. The **FEMcrackMdb()** is designed to work with **FEMcrackOrphanMesh()** class, which is utilized to import and further process the generated input file.

Methods of the **FEMcrackMdb()** class are as follows:

createAllParts() methods calls the **createSolidParts()** and **createShellParts**, which create all of the necessary parts of the model.

partitionMergedPartInstance() method is utilized for further partitioning the *mergedPart*. The method calls **partitionInnerCylinderCells()** and **partitionContainerAsPie()**.

partitionInnerCylinderCells() method is utilized to partition the *innerCylinder* cells with datum planes parallel to the *emphXY* plane. Datum plane numbers are stored in the **DataStr** and correspond to the order of their creation in the model. The partitioning is required to obtain cells, which can be meshed with *sweep* technique.

partitionContainerAsPie() method is utilized to partition the *mergedInstance* into sectors by *YZ* and *XZ* datum planes to enable *structured* and *sweep* meshing. Datum plane numbers depend on the crack type and are read from the **DataStr** class.

createSets() method is utilized to create geometry sets for *edges*, *faces* and *cells*. The method calls the corresponding methods **createSetsForEdges()**, **createSetsForFaces()** and **createSetsForCells()**.

createSetsForEdges() method is utilized to create all *edge* sets. Set names and coordinates of a point on each edge are read from the **DataStr()** class. The method iterates through the names of the sets and for each set iterates through the corresponding *edge* points, selecting the *edges* and assigning them to the corresponding set.

createSetsForCells() method is utilized to create all *cell* sets. Its operation is analogous to the **createSetsForEdge()** method, but instead of selecting *edges*, the method selects *cells*.

createSetsForFaces() method is utilized to create all *face* sets. Its operation is analogous to **createSetsForEdges()** and **createSetsForCells()**.

createCrackInteraction() method is utilized to define the crack in the model.

First, the method defines a *crack seam* with *crackFlanks faces* set. Second, the method defines the *contourintegral* with dummy *qVectors* option. Crack parameters are read from the **DataStr()** class. Thus defined crack would probably give an error during analysis, due to the *qVectors* direction, which is chosen arbitrarily. However, the *contourIntegral* is re-defined with the proper parameters by the **FEMcrackOrphanMesh()** class. The purpose of this *contourIntegral* definition is to force Abaqus to retain some of the crack properties and geometric features during the export and import of the *orphan mesh*, which otherwise would be challenging to define.

createContactInteraction() method defines a contact interaction between the crack faces. The method defines a standard surface to surface contact interaction.

meshInstance() method is utilized to automate meshing of the model. It calls **seedEdges()**, **assignMeshControls()**, **assignElementType()** and **generateMesh()** methods.

assignMeshControls() method is utilized to assign different meshing techniques and element shapes to the cells of the model. Cells immediately surrounding the crack tip are assigned *SWEEP* meshing technique, with the default algorithm and *WEDGE* elements. Cells comprising the *inner-Cylinder* are assigned *SWEEP* meshing technique with *MEDIAL_AXIS* algorithm and *HEX_DOMINATED* elements. For the rest of the model, the default meshing technique is *STRUCTURED* is set by default by Abaqus and is not explicitly defined.

writeInputFile() method is utilized to write an input file from the constructed model, which is imported and processed by the **FEMcrackOrphan-Mesh()**. The method should be called after the model has been fully defined.

FEMcrackOrphanMesh() class

FEMcrackOrphanMesh() class is utilized to import a model from an input file and perform additional operations to complete and submit the model for analysis. It is a *subclass* of the **BaseCrackMdb()** class.

The **FEMcrackOrphanMesh()** class methods are as follows:

__init__() method is an augmentation of the **BaseCrackMdb.__init__()** method.

It takes the **DataStr()** class as an input and in addition to the method from the *superclass* defines the **self.mdb[sets]** variable.

initializeAbaqusModel() method is utilized to create an Abaqus model, import an input file with named according to the *modelName* in the **DataStr()** class, assign it to the **self.mdb[?model?]** variable and delete the generic *Model-1*. The method is a redefinition of the method with the same name from the *superclass*.

clearImportedModel() method is utilized to remove features that were employed in the **FEMcrackMdb()** class, but are no longer deemed necessary, rename necessary features, whose names were changed during the import and assign pointer variables to model features. The method calls **deleteSets()**, **renameInteractions()**, **renamePart()**, **assignVariableToPart()**, **renameInstance()** and **assignVariableToInstance()** methods.

deleteSets() method is utilized to delete the sets of the model. It reads the names of the sets from the **DataStr()**, changes the name strings to uppercase to match the modifications during the import and deletes them. By reading the set names from the **DataStr()** and not from the model *sets* repository, ensures that sets created by Abaqus for internal use are not deleted.

renameInteractions() method is utilized to correct the names of the crack, contact property, update history output requests and delete contact interaction. The method calls **renameCrack()**, **renameContactProperty()**, **renameHistoryOutput()**, **updateHistoryoutput()** and **deleteContactInteraction()** methods. The purpose of the renaming operations is to be able to refer to the features with the names that have been defined in the **DataStr()** class and to eliminate any confusion with feature names.

renameCrack() method is utilized to rectify the name of the crack, modified during the import, to correspond to the name defined in the **DataStr()** class. The method first identifies the crack feature of the model, reads the correct name from the **DataStr()** and sets the name of the feature to correspond with the one in the **DataStr()** class.

renameContactProperty() method is utilized to rectify the name of the contact interaction property. It functions in a similar fashion to the **renameCrack()** method.

renameHistoryOutput() method is utilized to rectify the name of the history output request. The method functions in a similar fashion to the **renameCrack()** and **renameContactProperty()** methods.

updateHistoryOutput() method is utilized to update the name of the contour integral in the history output request definition.

deleteContactInteraction() method is utilized to delete the standard contact interaction from the model.

renamePart() method is utilized to rectify the the name of the part, which has been modified during the import. The method functions in a similar fashion to the **renameCrack()** and **renameContactProperty()** and **renameHistoryOutput()** methods.

assignVariableToPart() method is utilized to assign the variable **self.mdb[-orphanMeshPart]** to the part of the model, which can be employed to point to the part at later stages. The method identifies the part of the model and assigns it to the specified variable.

renameInstance() method is utilized to rectify the name of the orphan mesh instance in the assembly of the model. The method functions in an analogous fashion as the **renameCrack()**, **renameContactProperty()**, **renamePart()** and **renameHistoryOutput()** methods.

assignVariableToInstance() method is utilized to assign **self.mdb[orphan-MeshInstance]** to the instance of the orphan mesh part for future reference. The method is analogous to the **assignVariableToPart()** method.

createElementSets() method is utilized to create element sets, defined in the **DataStr()** class. The method reads the element set data from the **DataStr()** and calls the **createInnerCylinderElementSet()** with arguments a set name and the corresponding parameters to filter the required elements.

createInnerCylinderElementSet() method is utilized to select elements from the model by a *bounding cylinder* and organize them in a set. Set name and the parameters defining the *bounding cylinder* are passed to the method as input arguments.

deleteCentralWedgeElements() method is utilized to delete the *WEDGE* shape elements in the *innerCylinder* cells. During mesh transformation, when the ratio of the ellipse of the crack is either large or small, the *WEDGE* shape elements along the *Z* axis may become severely distorted and corrupt the mesh quality, which may lead the analysis to fail. Therefore, it is necessary these elements to be removed and the obtained hole closed. The method calls the **selectCentralWedgeElements()** to get the labels of the elements. Next the method calls the **deleteElements-WithLabels()** method, to which passes the element labels as an input argument.

selectCentralWedgeElements() method is utilized to select the *WEDGE* elements in the *innerCylinder* cells and return their labels. The method iterates through the element sets and for each element calls the **isWedgeElement** method, passing the element and if **isWedgeElement()** returns *True*, stores the element label.

isWedgeElement() method is utilized to verify whether an element has a *WEDGE* shape and returns either *True* or *False*. The method compares the *element.type* attribute of the element to the element codes *C3D15* and *C3D6*, which correspond to quadratic and linear *WEDGE* shape elements.

deleteElementsWithLabels() method is utilized to delete elements corresponding to the passed *labels* argument. The method first creates a sequence from the *labels* argument and then deletes the elements from the orphan mesh part.

createSetForExternalNodes() method is utilized to create a node set from nodes on the top, bottom and cylinder surface of the model, to which are assigned boundary conditions. The method iterates through all nodes of the model and assigns them to the node set if they meet the criteria. If (x, y, z) are nodal coordinates then the node to be assigned to the set,

either $|z| = 1/2h$, where h is the *containerHeight* or $x^2 + y^2 = r^2$, where r is the *containerRadius*.

createSetFromInnerCylinderNodes() method is utilized to create a two node sets containing the nodes on the *innerCylinderHole* wall. Each node set contains nodes on the same side of the crack plane, so that crack would not be affected by merging the nodes of each set. First the method calls the method **findInnerCylinderElementSetWedgeElementsRadius()**, which identifies the radius of the *innerCylinderHole*. Then the method calls the **createInnerCylinderNodeSetFromElementSet()** for each element set, which creates the two node sets.

findInnerCylinderElementSetWedgeElementsRadius() method is utilized to find and store to the **DataStr()** class the radius of the *innerCylinderHole*. If (x, y, z) are coordinates of a node, the method iterates through the nodes of the element sets and finds the smallest value of $\sqrt{x^2 + y^2}$, adds to it the *selectionTolerance* value and stores it to the **DataStr()** as the *innerCylinderHole* radius.

createInnerCylinderNodeSetFromElementSet() method is utilized to assign nodes from an element set, that are no further from the Z axis than the *innerCylinderHole* radius to a node set. The method iterates through each node of the element set and compares the $\sqrt{x^2 + y^2}$ to the *innerCylinderRadius*, where (x, y, z) are the node coordinates. If $\sqrt{x^2 + y^2}$ is smaller than the *innerCylinderHole* radius, the node label is stored. Eventually a *node* set is created from the stored node labels.

applyMeshTransformation() method is utilized to transform the orphan mesh according to the specified transformation type and parameters. The method iterates through all nodes of the model and according to the transformation type calls **calculateEllipticCoordinates()**, **calculateSimpleScaleCoordinates()** or **calculateAdvancedScaleCoordinates()**, passing a node as an argument. Then the calculated coordinates are passed to **moveNode()** method, which moves the node accordingly.

calculateEllipticCoordinates() method is utilized to perform the *elliptic* transformation of the node coordinates from (x, y, z) to (x_e, y_e, z_e) . The method reads the crack parameters (a and b) and the *transformationAxis* from the **DataStr()**. Next it calculates a new set of coordinates by:

$$x_e = x \sqrt{1 + \frac{a^2 - b^2}{x^2 + y^2}}$$

$$y_e = y$$

$$z_e = z$$

if the *transformationAxis* is set to X . If the *transformationAxis* is set to

Y , the new set of coordinates are:

$$\begin{aligned}x_e &= x \\y_e &= y\sqrt{1 + \frac{a^2 - b^2}{x^2 + y^2}} \\z_e &= z\end{aligned}$$

Finally the method returns the new set of coordinates.

calculateSimpleScaleCoordinates() method is utilized to perform the *simpleScale* transformation of the node coordinates from (x, y, z) to (x_s, y_s, z_s) . The method reads the crack parameters (a and b) and the *transformationAxis* from the **DataStr()**. Next it calculates a new set of coordinates by $x_s = (a/b)x$, y_s and $z_s = z$, if the *transformationAxis* is set to X . If the *transformationAxis* is set to Y by $x_s = x$, $y_s = (a/b)y$ and $z_s = z$. Finally the method returns the new set of coordinates.

calculateAdvancedScaleCoordinates() method is utilized to perform the *simpleScale* transformation of the node coordinates from (x, y, z) to (x_a, y_a, z_a) . The method reads the crack parameters (a and b), *transformationAxis* and *crackInitialRadius* from the **DataStr()**. Next it calculates two scale factors *expansionFactor* = $a/\text{crackInitialRadius}$ and *contractionFactor* = $b/\text{crackInitialRadius}$. According to the *transformationAxis* the new set of coordinates is $x_a = x \cdot \text{expansionFactor}$, $y_a = y \cdot \text{contractionFactor}$ and $z_a = z$ if *transformationAxis* is X , or $y_a = y \cdot \text{expansionFactor}$, $x_a = x \cdot \text{contractionFactor}$ and $z_a = z$ if *transformationAxis* is Y ,

moveNode() method is utilized to edit the current coordinates of a node to a new set of coordinates, which effectively changes the nodes position in space. The method takes two input arguments a node and the new coordinates.

closeInnerCylinderHole() method is utilized to close the *innerCylinderHole* by translating and merging the nodes of the *innerCylinderWall*. The method merges the nodes from the two node sets one at a time, to ensure that the nodes from one crack flank are not merged with the nodes from the other. The procedure is implemented in a loop that calls **moveInnerCylinderHoleNodesToPlane()** method with the nodes from the set as argument and then calls **mergeNodes()**, passing the nodes of the set again. Finally the method calls **regenerateAssembly()** to update the model.

moveInnerCylinderHoleNodesToPlane() method is utilized to translate nodes, passed as an input argument. The method reads the *transformationAxis* and depending on whether the it is X or Y translates the nodes to the XZ or YZ plane.

mergeNodes() method is utilized to merge nodes, passed as input argument, within a distance from each other, defined as *mergingTolerance* in the **DataStr()** class.

redefineCrackInteraction() method is utilized to delete the old crack definition and create a new one. The crack extension direction is defined by the *CRACK_NORMAL* option.

getExternalNodes() method returns nodes, which would be assigned boundary conditions.

getCrackContainerInstance() method returns the instance of the orphan mesh model.

BaseXFEMcrackMdb() class

BaseXFEMcrackMdb() class is a *subclass* of the **BaseCrackMdb()** and is a *superclass* for **XFEMcrackMdbMP()**, **SimpleXFEMcrackMdb()** and **XFEMtetCrackMdb()** classes.

The **BaseXFEMcrackMdb()** methods are as follows:

createCrackPart() method is utilized to create the crack geometry part. The part has one feature *BaseShell* part, opposed to *BaseShellRevolve*.

createCrackAndCrackDomainInstances() method is utilized to create instances from the crack geometry and crack domain parts. The method calls **createInstance()** method to which passes the name of the *crack geometry* part. Next, the method calls the **createMergedPartInstance()** method.

createCrackPartitionPart() method is utilized to create a shell part, used to partition the *crackDomain* part at the crack location to create internal edges in the *crackDomain* part. The part geometry is dependent on the crack type. Geometrically, its shape is represented by the intersection between the *crack geometry* and the *crackDomain*. For *embedded* crack its shape is identical to the *crack geometry*. For *edge* and *surface* crack types it is an ellipse sector.

createSets() method is utilized to create a *faces* and *edges* sets and a datum coordinate system, used as a reference for the boundary conditions. The method calls **createSetsForEdges()** and **createSetsForFaces()** methods.

createSetsForEdges() method is utilized to create *edge* sets, which will be assigned seeds. Set names and parameters of the *BoundingCylinder*, which is used to select the edges are read from the **DataStr()** class.

createSetsForFaces() method is utilized to create *face* sets. The method is analogous to the **createSetsForEdges()** method.

createXFEMcrack() method is utilized to define *XFEM* crack.

createFieldOutputRequest() method is utilized to define a request for the *PHILSM* field output variable. The *PHILSM* variable is used for visualization of the crack during the post processing of the Abaqus output database.

deleteFieldOutputs() method is utilized to delete all field output requests in the model.

assignMeshControls() method is utilized to assign meshing technique to the model according to the element type. If the assigned elements are *tetrahedral*, the meshing technique is set to *FREE* and if the assigned elements are *hexahedral*, the default meshing technique is used.

seedEdges() method is used to assign seeds to the edges. Edges in all *edge* sets are seeded by size. Seed parameters are read from the **DataStr()** class.

createSetForExternalNodes() method is utilized to create a *node* set including nodes, to which are assigned boundary conditions. The method is analogous to the **FEMcrackOrphanMesh.createSetForExternalNodes()** method.

getExternalNodes() method returns the nodes in the set defined by **createSetForExternalNodes()**.

getCrackContainerInstance() method returns the instance of the *crackContainer*.

XFEMcrackMdbMP() class

XFEMcrackMdbMP() class is a *subclass* of **BaseXFEMcrackMdb()**, which is a *subclass* of **BaseCrackMdb()** and, therefore, inherits the methods of the both classes. The inherited methods including those defined in the **XFEMcrackMdbMP()** class provide functionality to create an Abaqus model database for *XFEM* analysis type of an elliptic crack of either *embedded*, *edge* or *surface* type. The model type created by the class is *multiplePartitions*

XFEMcrackMdbMP() defines the following methods:

createAllParts() method is utilized to create all the necessary parts for the model. The method calls **createCrackPart()**, **createSolidParts()**, which creates the *crackContainer* part in this case and **createSmallContainer()** methods.

createSmallContainer() method is used to create the *smallContainer* part. The *smallContainer* part is a solid part, used for partitioning of the *crackContainer*. It defines a full or a sector of an elliptic cylinder, around the crack, so that the volume of interest can be meshed with smaller elements, than the rest of the model. The part is dependent both on the crack geometric parameters and type. The axes of cross section of the *smallCylinder* are *offset* from the crack ellipse axes. Both *offset* and *height* of the cylinder are defined in the **DataStr()** class.

createInstancesForPartitioning() method is utilized to create instances, which are merged to create *mergedPart*. The method calls **createInstance()** twice, passing the *crackContainer* part name the first time and *smallContainer* part name the second time.

createLoftsOnCrackDomain() method is utilized to create loft features in the *mergedPart*, which partitions it into cells to enable meshing of the geometry. Lofts are created between the cross section edges of the *smallContainer* and the circumferential edges of the *mergedPart*.

createPiePartitions() method has analogous functionality to the **FEMcrackMdb.partitionContainerAsPie()**.

createSets() method is utilized to create *face* and *edge* sets. *Edge* sets are used for seeding the containing edges and *face* set is used in the XFEM crack definition. The method creates a datum coordinate system, which is used as a reference for the boundary conditions. The method calls **createSetsForExteriorEdges()**, **createSetsByBoundingBox()** and **createSetsForFaces()**.

createSetsForExteriorEdges() method calls the **BaseXFEMcrackMdb.createSetsForEdges()** method.

createSetsByBoundingBox() method is utilized to create *edge* set for the edges, created by partitioning with the *smallContainer*. Parameters for the selection of the edges are read from the **DataStr()** class.

assignMeshControls() method redefines the **BaseXFEMcrackMdb.assignMeshControls()** and has analogous purpose. If the assigned elements are *tetrahedral* the meshing technique is set to *FREE* and *allowMapped* setting is set to *False* and if the assigned elements are *hexahedral*, the meshing technique is set to *STRUCTURED*.

XFEMtetCrackMdb() class

XFEMtetCrackMdb() class is a *subclass* of **BaseXFEMcrackMdb()**, which is a *subclass* of **BaseCrackMdb()**. The **XFEMtetCrackMdb()** class is utilized to create an Abaqus model database for *XFEM* analysis type of an elliptic crack of either *embedded*, *edge* or *surface* type. The model created by the class is of *crackPartition* type.

XFEMtetCrackMdb() class defines the following methods:

createAllParts() method is utilized to create the parts of the model. It calls the methods **createSolidParts()** and **createCrackPart**. If the crack type is not *embedded*, the method also calls **createCrackPartition()**.

createInstancesForPartitioning() method is utilized to create instances from a selection of parts, which will comprise the *mergedPart*. If the crack type is *embedded* the method calls **createInstancesFromAllParts()**, which instances all available parts in the model. If the crack type is not *embedded*, however, the method creates instances of the *crackPartition* and *crackDomain* parts, by calling the **createInstance()** method twice and passing the *crackPartition* and *crackDomain* part names as arguments.

XFEMsimpleCrackMdb() class

The **XFEMsimpleCrackMdb()** class is a *subclass* of the **BaseXFEMcrackMdb()** class. The **XFEMsimpleCrackMdb()** class is utilized to create an

Abaqus model database for *XFEM* analysis type of an elliptic crack of either *embedded*, *edge* or *surface* type. The model created by the class is of *simple* type.

XFEMsimpleCrackMdb() class defines the following methods:

createAllParts() method is utilized to create the parts of the model. The method calls **createSolidParts()** and **createCrackPart()**.

assignSectionToCrackDomain() method is utilized to create assign section to the *crackDomain* part.

3.6.4 ReadOdb() class

ReadOdb() class is utilized to read and extract the history output data from an Abaqus output database of any combination of the model, analysis and crack types. The class takes one argument a **DataStr()** class, which defines the corresponding output database and to which the extracted and processed results are stored for further analysis.

The **ReadOdb()** class defines the following methods:

__init__() method initializes the class, assigns the **DataStr** input argument to a variable and initializes two internal variables: temporary storage and a pointer variable to the output database.

openOdb() method is utilized to open an output database, defined in the *modelName* variable of the **DataStr()** class. The opened output database is assigned a variable for future reference.

createOdbViewport() method is utilized to create a viewport to display the output database.

readHistoryOutputs() method is utilized to assign the repository with the history output data to a temporary storage variable.

extractValuesFromHistoryOutput() method is utilized to read and store value for point of each contour of the stress intensity factors and coordinates of the data point to the temporary storage. First, the method reads the number of contours that have been requested in the model definition, from the **DataStr()** class and initializes the temporary storage to match the number of contours and the stress intensity factors. Then for each *dataKey* in the history output repository calls the methods **assignSIFvalue()** and **assignCoordinates()** methods. A *dataKey* corresponds to a value in the repository and contains information identifying the value. To identify what type is the value the *dataKey* is checked against certain string patterns and the value is assigned to the appropriate place in the temporary storage.

assignCoordinates() method is utilized to assign (store) the value corresponding to the passed *dataKey*, if the *dataKey* corresponds to a coordinate value.

assignSIFvalues() method is utilized to assign (store) the value corresponding to the passed *dataKey*, if the *dataKey* corresponds to a stress intensity factor and contour number.

calculateBetas() method is used to calculate the angle β of a point on the crack and the X axis. The method iterates through the stored coordinates and calls **calculateCrackPointAngle** for each set of coordinates and then stores the angle to the temporary storage.

calculateCrackPointAngle() method is utilized to calculate the β angle and return it.

sortData() method is utilized to remove duplicate data and sort the extracted stress intensity factors and data point coordinates according to the β angle of the point.

add360DegreeDataPoint() method is utilized to create one additional point at the end of each of the sorted sequences for stress intensity factors, angles, and coordinates for *embedded* crack type. The value of the point is equal to the value of the first point for all sequences except for the β angles, where it is equal to the first β angle in the sequence + 360 degrees. The method internally checks the crack type and if it is not *embedded* skips the procedure.

averageSortedSIFs() method is utilized to create a new sequence for each stress intensity factor, where every value is an average of the same data point over a specified range of the contours. The range of averaging is read from the **DataStr()** class.

writeResultsToDataStr() method stores the sorted and processed values of the quantities to the **DataStr()** class.

getOdb() method returns the pointer to the open output database.

closeOdb() method closes the output database.

3.6.5 PersistentData() class

The **PersistentData()** class provides access to the *shelve* database for read, write and processing of the input data. The class takes two arguments, *scriptPath* – a string specifying the parent directory of the *db* directory, in which the *shelve* databases are stored, and **DataStr()** class. The class creates three *shelve* databases for each crack type and the active *shelve* depends on the crack type defined in the **DataStr()** class.

PersistentData() defines the following methods:

__init__() method is utilized to initialize internal variables for the class. It also calls the **setShelvePath()**

setShelvePath() method is utilized to set path to the *shelve* databases. It takes input argument of the *scriptPath* format.

determineActiveShelve() method is utilized to designate the full path to the active *shelve*, depending on the crack type.

setActiveShelve() method is utilized explicitly set active *shelve*. The method takes one argument, which is the crack type.

readAll() method opens the active *shelve* reads the data from the *shelve*, closes the *shelve* and returns the data.

writeToDb() method is utilized to store data to the active *shelve*. First, the method calls **prepareDataForShelving()** to extract only the necessary data from the **DataStr()**. Next it reads the model name from the **DataStr()** and sets it as a *key* under which the data will be stored to the *shelve*. Finally it writes the data to the active *shelve* and closes the *shelve*.

prepareDataForShelving() method is utilized to organize the data, which will be stored. The method creates a *dictionary* with *keys*:

input – for input parameters from the **DataStr()**

reports – for reports data from the **DataStr()**

odb – for results data from the **DataStr()**

checkForDuplicates() method is utilized to verify, whether the active *shelve* has an entry with the same *input* parameters as the **DataStr()** argument designated at the class creation. The method opens the active *shelve* and iterates through its entries. If a duplicate is found, closes the *shelve* and returns *True*. Otherwise the method closes the *shelve* and returns *False*.

getDuplicates() method is utilized to return the keys of any identical to the **DataStr()** class. The method opens the active *shelve*, iterates through its entries and stores a sequence of keys of the duplicate entries. Then the method closes the *shelve* and returns the sequence.

readKey() method is utilized to read from the active *shelve* the data, associated with a *key*, which is passed as an input argument.

3.6.6 DbDataStr() class

The **DbDataStr()** class is designed as **DataStr()** class counterpart, which serves to store and operate on the data, when postprocessing the results. An instance of the **DbDataStr()** class is created as soon as data is read from the *shelve* database. The class is an abstraction layer of the **BaseDataStr()** and internally creates an instance of the **BaseDataStr()** class and most of its methods return a call to the identically called methods of the **BaseDataStr()**. Thus created the class hides unnecessary functionality, changes to **BaseDataStr()** will not break the **DbDataStr()** and it is straightforward to define new methods. The class takes one input argument, which is the data directly read from the *shelve*.

The following methods of the **DbDataStr()** class call the identically named methods of the **BaseDataStr()** and if the method takes an argument, it is passed with the method call: **getAnalyticalResults()**, **getVisualizationResults()**, **getAnalysisType()**, **getSortedBetaAngles()**, **getSortedContourSIFs()**, **writeErrorResults()**, **getErrorResults()**, **writeAnalyticalResults()**, **writeVisualizationResults()**, **getCrackType()**, **getMaterialProperties()**, **getCrackParameters()**, **getAnalysisParameters()**, **getModelName()**, **getDataStr()**.

In addition to the afore mentioned, the **DbDataStr()** class defines the following methods:

__init__() method creates an instance of the **BaseDataStr()** and calls the **setDataStr()** and passes the input argument

writeResultRequests() method is utilized to write the requests from the graphical user interface to the data structure.

getResultRequests() method returns the requests from the GUI.

setModelName() method is utilized to overwrite the *modelName* value of the data structure.

calculateAveragedSIFs() method is used to create a new sequence for each stress intensity factor and calculate the value at each data point as an average from a specified from the gui contour range.

getSortedAveragedSIFs() method returns the sequences of the averaged stress intensity factors.

getSortedCrackCoordinates() method returns a sequence of the sorted crack coordinates.

3.6.7 AnalyticalData classes

AnalyticalData classes are a family of classes, utilized to calculate and write to the **DbDataStr()** class analytical solutions for the stress intensity factors of the crack analysis in the **DbDataStr()** class. The **AnalyticalData** class family is composed of the following classes and functions:

AnalyticalData() class

BaseAnalyticalExpressions() class

EdgeCrackAnalyticalSolutions() class

EmbeddedCrackAnalyticalSolutions() class

SurfaceCrackAnalyticalSolutions() class

miscFunctions module, containing the following functions:

- **Rfun()** — calculates R value
- **Qfun()** — calculates Q value
- **compEllipIntK()** — calculates complete Elliptic integral for a and b of a crack
- **compEllipIntE()** — calculates complete Elliptic integral for a and b of a crack

AnalyticalData() class

AnalyticalData() class is utilized to read the crack parameters and user requests from the **DbDataStr**, call appropriate methods and functions to calculate the data and write the results back to the **DbDataStr()**. the class takes one input argument the **DbDataStr()** class.

The **AnalyticalData()** class defines the following methods:

__init__() method is utilized to initialize the required parameters and classes, which are called by the other methods of the class to calculate the analytical solutions. Depending on the crack type, the method initializes the **EmbeddedCrackAnalyticalSolutions()** class for *embedded*, **SurfaceCrackAnalyticalSolutions()** class for *surface* or **EdgeCrackAnalyticalSolutions()** class for *edge* crack type and assigns it to the **self.expressions** variable. Finally the method calls the **initializeParameters()** method of the initialized class.

calculateAnalyticalResults() method is utilized to calculate and store an analytical value for the requested stress intensity factors. The method iterates through the β angles of the crack and for each β calls the **self.expressions.calculateExpressionForAngle()** with β as an input argument, which returns the calculated values.

writeAnalyticalResultsToDataStr() method is utilized to store the results obtained by **calculateAnalyticalResults()** to the **DbDataStr**.

calculateVisualizationResults() method is utilized to calculate analytical solutions with higher resolution (larger number data points) than the **calculateAnalyticalResults()**, which calculates analytical solutions for the *beta* angles of the analysis. The method calls the **self.expressions.getSolutionsForVisualization()**, which returns the results.

writeVisualizationResultsToDataStr() method is utilized to write the results obtained by **calculateVisualizationResults()** to the **DbDataStr**.

calculateErrors() method is utilized to compare the analysis results with the analytical results and calculate a quantitative estimate of the accuracy of the solution. The method calculates three types of estimates:

errors – analytical and analysis results are compared for each point of the crack and for each requested stress intensity factor. Each value is calculated as the absolute value of the difference between the analysis and the analytical solution divided by the maximum absolute value of all analytical and analysis values.

maxErrors – the maximum value of the **errors** for each stress intensity factor.

maxAbsoluteError – the maximum value of the **maxErrors**.

writeErrorsToDataStr() method is utilized to write the results obtained by **calculateErrors()** to the **DbDataStr**.

BaseAnalyticalExpressions() class

The **BaseAnalyticalExpressions()** class is a *superclass* for the **EmbeddedCrackAnalyticalSolutions()**, **SurfaceCrackAnalyticalSolutions()** and **EdgeCrackAnalyticalSolutions()** classes. The purpose of the class is to facilitate the *subclasses*, which provide methods only to evaluate the analytical solution at a point. The class takes two input arguments, **DbDataStr()** class and **SIFkeys**, which contain the names of the requested analytical values.

The **BaseAnalyticalExpressions()** defines the following methods:

__init__() method is utilized to initialize the required variables for the class.

calculateSolutionForAngle() method is utilized to calculate and return a *dictionary* containing the values for each of the requested stress intensity factors for a *beta* angle, which is passed as an input argument.

getSolutionsForVisualization() method is utilized to return the values for the requested stress intensity factors, calculated at high resolution. The method calls **calculateSolutionsForVisualization()** method and returns the calculated values.

calculateSolutionsForVisualization() method is utilized to calculate analytical solutions for the requested stress intensity factors at resolution of 1 degree and store the calculated values.

EmbeddedCrackAnalyticalSolutions() class

The **EmbeddedCrackAnalyticalSolutions()** class is a *subclass* of the **BaseAnalyticalExpressions()** class. It is designed to calculate analytical values of the stress intensity factors for *embedded* crack type.

The **EmbeddedCrackAnalyticalSolutions()** class defines the following methods:

initializeParameters() method is utilized to read crack and analysis parameters from the **DbDataStr()** class. The method also calls the **Rfun()**, **Qfun()**, **compEllipIntE()** and **compEllipIntK()** functions and stores the values.

k1() method is utilized to calculate the value of **K1** for a *beta* angle, passed as input argument.

k2() method is utilized to calculate the value of **K2** for a *beta* angle, passed as input argument.

k3() method is utilized to calculate the value of **K3** for a *beta* angle, passed as input argument.

SurfaceCrackAnalyticalSolutions() class

The **SurfaceCrackAnalyticalSolutions()** class is a *subclass* of the **BaseAnalyticalExpressions()** class. It is designed to calculate analytical values of the stress intensity factors for *surface* crack type. At the time of writing an empty class.

EdgeCrackAnalyticalSolutions() class

The **SurfaceCrackAnalyticalSolutions()** class is a *subclass* of the **BaseAnalyticalExpressions()** class. It is designed to calculate analytical values of the stress intensity factors for *edge* crack type. At the time of writing an empty class.

3.6.8 XYPlotDataFromDbEntry() class

XYPlotDataFromDbEntry() class provides methods to create *XYPlotData* in Abaqus for specified parameters. The method takes an instance of the **DbDataStr()** class as input argument and reads the required data for the *XYPlotData* from it.

The **XYPlotDataFromDbEntry()** defines the following methods:

__init__() method initialized the internal variables for the class.

createAnalyticalXYPlotData() method is utilized to create *XYPlotData* for the analytical solutions. The method creates *XYPlotData* only for the specified stress intensity factors.

createAveragedXYPlotData() method is utilized to create *XYPlotData* for the averaged analysis output data. The method creates *XYPlotData* only for the specified stress intensity factors.

createContourXYPlotData() method is utilized to create *XYPlotData* for the analysis output data. The method creates *XYPlotData* only for the specified stress intensity factors and contours.

createErrorXYPlotData() method is utilized to create *XYPlotData* for the errors between the analytical and averaged over a specified range analysis data.

createVisualizationXYPlotData() method is utilized to create *XYPlotData* for the analytical solutions for visualization, which may appear smother. The method creates *XYPlotData* only for the specified stress intensity factors.

3.6.9 VisualizationOdbFromDbEntry() class

VisualizationOdbFromDbEntry() class is utilized to create an Abaqus output database for visual representation of the stress intensity factors. Crack parameters and the analysis results are read from the **DbDataStr()** class, which is an in input argument for the class. The geometric features of the visualization are rebuilt from the analysis output to create an accurate representation of the results.

The **VisualizationOdbFromDbEntry()** defines the following methods:

__init__() method initialized the internal variables of the class, **self.data**, **self.odb** and **self.dataStr**. **self.odb** is utilized as a pointer for the newly created output database. **self.data** is utilized to store *vector* values, which define offsets of the rings of *shell* elements from the crack contour and node set names.

initializeAbaqusOdb() method is utilized to create a name for the visualization, create the output database and assign pointers to important components of the database.

initializeViewport() method is utilized to create a viewport for the output database and privileged plane for the compass

setViewportViewingPoint() method is utilized to orient the view so that the view is isometric and overwrite the *Iso* view.

setDisplayableObject() method is utilized to set the viewport to display the output database for a specific step and frame.

createMaterial() method is utilized to create an *Elastic* material with parameters read from the **DbDataStr()**.

createSections() method is utilized to create a *TrussSection* for the *truss* elements and *HomogeneousShellSection* for the *shell* elements.

createpart() method is utilized to create a part named *crackVisualization*.

createNodes() method is utilized to create the required nodes of the part. The method initializes a **nodeData** variable to store a tuple containing the node label and coordinates, for each node. The variable is passed to and returned by each method, called by **createNodes()**. This ensures that methods have a starting point, and thus node numbering is consistent. Furthermore, the variable contains the necessary information, and is utilized to create all nodes. The method calls the following methods:

createCrackFrontNodes() to create nodes for the *truss* elements, representing the crack front geometry and **K3** values;

createK1Nodes() to create nodes for the *shell* elements, representing **K1** values;

createK2Nodes() to create nodes for the *shell* elements, representing **K2** values.

Finally the method creates the nodes from the information stored in **nodeData**.

createK1Nodes() method is utilized to create node data for vertically offset from the crack front nodes. The created nodal data corresponds to nodes of equal number to the crack nodes with constant offset. The method takes two input arguments, **nodeSetName** and **nodeData**. The **nodeData** is updated with a *tuple* containing node number and coordinates for each node. Finally, each node number, created by the method, is associated with the **nodeSetName**, which is passed as an input argument, in the **self.odb** variable.

createK2Nodes() method is analogous to **createK1Nodes()**, however, it is utilized to create node data for nodes in the crack plane, which lie on the normal to the crack ellipse. The method calls **calculateCoordinatesK2EllipseNormal()** to calculate the coordinates of a node.

calculateCoordinatesK2EllipseNormal() method is utilized to calculate coordinates for a node used to create *shell* elements. Node coordinates are calculated as to lie on the intersection between the normal to the crack ellipse at *reference crack node* and an ellipse with axes equal to the corresponding axes of the crack ellipse with added *offset*. The *offset* is proportional to the minor axis of the ellipse of the crack. The method takes two input arguments: **coordinates** and **vector**. The **coordinates** argument specifies the coordinates of the *reference crack node*. The **vector** is a multiple in the calculation of the *offset* value. Larger **|vector|** results in a larger *offset*. The sign of the **vector** specifies, whether the node coordinate is inside, if *vector* is negative, or outside, if *vector* is positive, of the crack ellipse.

calculateBeta() method is utilized to calculate and return the β angle of a line through a specified point and the X axis. The method takes the (x, y) coordinates of the point.

createCrackFrontNodes() method is utilized to create node data for nodes, used to create the *truss* elements, representing the crack edge and **K3** value. The method is analogous to **createK2Nodes()** and **createK3Nodes()**, however, the node coordinates of the **nodeData** in this case, are identical to the crack node coordinates.

createElements() method is utilized to create the elements of the model. The method uses the **elementData** variable, which passes to methods, which calls to obtain the required data to create elements and **elementCounter** to keep consistent element numbers. Elements are created in three steps. Firstly the method calls **createCrackFrontElements**, to which passes **elementCounter** and gets **elementData** and **elementCounter**. Then the method uses the **elementData** to create the *T3D2 truss* elements and assigns them to an element set *K3-Elements*. Second, the method sets the **elementData** variable to an empty *tuple* and calls the methods **createOuterK2()** and **createInnerK2()**, to which passes the variables **elementData** and **elementCounter**. With the data from **elementData**, the method creates *CPS4R shell* elements and assigns them to an element set *K2-Elements*. Finally, the method sets the **elementData** variable to an empty *tuple* and proceeds as in the second step, however, the methods it calls are **createUpperK1()** and **createLowerK1()** and the set, to which the elements are assigned is *K1-Elements*.

createOuterK2() method is utilized to create the elements comprising the ring of *shell* elements in the crack plane and located on the outer side of the crack ellipse contour. The method reads the node labels for the required nodes from the **self.odb** and iterates through the number of elements, each time creating a new element data and counting the number of elements.

createInnerK2() method is analogous to **createOuterK2()** method, however, it creates element data for elements located inside the crack contour.

createUpperK1() method is analogous to the methods **createOuterK2()** and **createInnerK2**, however, it creates elements located on the cylinder with cross section the crack front and on the positive side of the Z axis.

createLowerK2() method is analogous to the **createUpperK1()** method, however, it creates elements on the negative side of the *Z* axis.

createCrackFrontElements() method is utilized to create element data for the *truss* elements of the crack front. The method iterates through the node numbers stored in the **self.odb** each time updating the **elementData** variable with the new element data and **elementCounter** with the number of the current element in the **elementData**. Finally the method returns the variables **elementCounter** and **elementData**.

createStepFrame() method is utilized to create a *step* and *frame* in the Abaqus output database, to which *field* data is associated.

createInstance() method creates an instance of the part in the output database.

createFieldOutput() method is utilized to prepare and associate the analysis results from the **DbDataStr()** for stress intensity factors of the crack to the corresponding nodes of the output database as field output. The field output created as *SCALAR* field and named *SIF*. It is created in the *step* and *frame* created by the **createStepFrame()** method.

setDefaultField() method is utilized to set the *SIF* field output as default.

saveOdb() method is utilized to save and close the output database. The database is saved in the Abaqus active directory.

reopenOdb() method is utilized to open the created output database for Abaqus to display it.

3.6.10 GUI classes

GUI classes is a name of a family of classes, designed to draw dialog boxes in Abaqus, read entries from the *shelve* database and process user input. **GUI class** family is comprised by: **SelectDb()**, **AccessDb()** and **dbAccessDialogs_plugin()** classes. The classes are registered to Abaqus by the command `getAFXApp().getAFXMainWindow().getPluginToolset().registerGuiMenuButton()` at the bottom of the **dbAccessDialogs_plugin.py**.

dbAccessDialogs_plugin() class

The **dbAccessDialogs_plugin()** class is a *subclass* of the **AFXForm()** *abstract superclass*. The **AFXForm()** class is provided by the Abaqus FOX-toolkit extension and provides the infrastructure to process **form modes**. The **AFXForm()** class defines generic methods, used by its *subclasses*, however, it might be necessary some of these methods to be customized in the *subclass* definition.

The **dbAccessDialogs_plugin()** class defines the following methods:

__init__() method is utilized to initialize the class, it takes one argument **owner**, which is of type *AFXGuiObjectManager* and is passed automatically to the class. The method also defines the name of the selected by default *shelve* database, **AFXGuiCommand**, **FXMAPFUNCS** and calls the **createKeywords()** method. The name of the *shelve* database

is updated, depending on which radio button in the *first dialog* box is selected. The **AFXGuiCommand** invokes the **readFromDb()** function from the **executeDbAccessCommands.py** module with a *dictionary* of *keywords*, which convey the user input commands. A **FXMAPFUNC** is defined to invoke a corresponding method, when it catches a message, identified by its *ID* and generated by interaction with the dialog boxes. The call to the **createKeywords()** method is to create the *keywords*, which convey requests from the user. Four **FXMAPFUNCS** are defined, three for the radio buttons of the first dialog box for selecting the crack type and one for catching the messages from the tree in the second dialog box.

onTreeSelect() method is called whenever a the corresponding **FXMAPFUNC()** catches a message, generated on user interaction with the tree of the second dialog box. The method sets the value of the **self.dataKeywords[dbKeys]** to a concatenated *string* of the selected items in the tree of the second dialog box. For the purpose the method iterates members of the variable **self.selectableTreeItemIDs** and checks if the item is selected. If the item is selected the corresponding database key is concatenated to the *string* value of the **AFXStringKeyword**.

getModelName() method is utilized to split the value of the **dbKeys** *keyword* and return the last member of the resulting tuple.

onEmbeddedButton() method is called whenever the corresponding **FXMAPFUNC()** catches a message, generated on user selecting the *Embedded crack* radio button. The method modifies the values of the **db** and **activeDb** to reflect the changes in the user interface. To create the value of the **db** value the method calls **getDbPath()**.

onSurfaceButton() method is analogous to the **onEmbeddedButton**, however, it is called when the user selects *Surface crack* radio button.

onEdgeButton() method is analogous to the **onEmbeddedButton** and **onSurfaceButton**, however, it is called when the user selects *Edge crack* radio button.

createKeywords() method is utilized to create a *dictionary* of *keywords* – **self.dataKeywords**, which is structured in the following way:

dbKeys entry contains an **AFXStringKeyword** with value equal to a concatenated *string* of the selected *shelve* database keys from the tree of the second dialog box.

activeDb entry contains an **AFXStringKeyword** with value equal to *shelve* database name, which is named identically to the crack type.

db entry contains an **AFXStringKeyword** with value equal to the full path including the *shelve* name.

thisDir entry contains an **AFXStringKeyword** with value equal to the value of the **thisDir** variable, a *string* with the directory containing the module of the class.

analytical entry contains a *dictionary* with keys **K1**, **K2** and **K3** associated with an **AFXBoolKeyword**. The value of the **AFX-BoolKeyword** is altered in accordance to the state of the corresponding check box is marked in the *Analytical data* section of the second dialog box.

analysis entry is similar to the **analytical**, however, the **analysis** corresponds to the check boxes in the *Analysis data* section.

contoursToAverage entry contains an **AFXStringKeyword** with value equal to a concatenated *string* of the selected entries in the *Contours to average* section.

includeContours entry contains an **AFXBoolKeyword** associated with the *Include contour data* check box.

XYPlotData entry contains an **AFXBoolKeyword** associated with the *XYPlotData* check box.

VisualizationOdb entry contains an **AFXBoolKeyword** associated with the *VisualizationOdb* check box.

printData entry contains an **AFXBoolKeyword** associated with the *printData* check box.

getDbPath() method is utilized to create and return the directory path including the name of the active *shelve* database.

getFirstDialog() method is used internally to generate the *first dialog box*, by creating an instance of the class for the dialog box. The method returns the *first dialog box* instance

getNextDialog() method is used internally to generate the following dialog box. The method takes one argument, an instance of the previous dialog box. For the purposes of the program, the method generates the second dialog box, creating an instance of the class for the second dialog box.

doCustomChecks() method is utilized to verify the validity of the selected options in the second dialog box. The method verifies that at least one *shelve* database key and entry of the *Select contours to average* is selected. Otherwise an error message is displayed.

okToCancel() method is used internally to close the dialog box.

SelectDb() class

The **SelectDb()** class is a *subclass* of the **AFXDataDialog()** class, which is a *superclass* for all dialog boxes, which collect data from the user. The **SelectDb()** defines the first dialog box, in which the user selects the crack type and respectively database, which will be the object of analysis for the second dialog box.

The class has only one method **__init__()**, which takes one argument an instance of the **dbAccessDialogs_plugin()** class.

AccessDb() class

The **AccessDb()** class is a *subclass* of the **AFXDataDialog()** class. The **AccessDb()** defines the second dialog box, in which the user selects the one or more database entries from the tree to analyze and designates the options for post processing. The tree in the dialog box is generated when an instance of the class is created and, therefore, reflects the current *shelve* database entries. The class takes two input arguments **dbAccessDialogs_plugin()** and the path to the active *shelve* database.

The **AccessDb()** class defines the following methods:

__init__() method is utilized to initialize the dialog box. The method calls the **createWidgets()**, which creates the widgets of the dialog box.

createWidgets() method is utilized to create the layout of the dialog box and call methods to create the rest of the widgets. The method calls **createTreeWidget()**, **createDataOptionsWidgets()**, **createContoursOptionsWidgets()** and **createOutputOptionsWidgets()**.

createOutputOptionsWidgets() method is utilized to create the check box widgets:

- *XYPlotData*
- *Print Data structure*
- *Visualization Odb*

createContoursOptionsWidgets() method is utilized to create the *Separate contours* group box widget and the *Include contour data* check box widget.

createDataOptionsWidgets() method is utilized to create check box widgets associated with the *dictionary keys* and corresponding *AFXBoolKeyword* of the **dataKeywords[analytical]** and **dataKeywords[analysis]** variables from the **dbAccessDialogs_plugin()** class. The number of the check box widgets and their names is controlled by the contents of the two variables.

createTreeWidget() method is utilized to build the tree widget and creates its structure from the *shelve* database entries. The tree branches represent model parameter, progressively narrowing down the selection of possible models, down to the model name. The tree root entries are the analysis types *FEM* and *XFEM*, which are propagated with the available entries in the corresponding *shelve* database. All of the tree items are disabled and thus not selectable, with the exception of model names of the simulations that have been completed successfully. A record of the selectable tree entries is kept and utilized in the **dbAccessDialogs_plugin()** class to update the respective **dataKeywords[dbEntries]**. The method creates the *FEM* and *XFEM* tree entries, opens and iterates through the active *shelve* database calling the **createEntryID.createID()** function to create a unique *ID* for the entry and passes it to **createTreeItems()** method. Finally the method closes the *shelve* database.

createTreeItems() method is utilized to create the structure of the tree widget. The tree entries are organized in *hierarchical pairs* of *parameter name* entry, which groups its corresponding *value* entries available in the *shelve* database. *Value* entries are further propagated with *hierarchical pairs* until the model name is reached. To ensure, the consistency of the tree structure, each tree entry is assigned a unique *key*, which determines the parent/child relationship of the entries. The method iterates the sorted keys of the unique entry *ID* and calls **createTreeEntry()** once to create the *parent parameter name entry* and second time to create the *value entry*.

createTreeEntry() method is utilized to identify the *parent* of a new entry and create the entry under the *parent*. The entry is made selectable only if it is a *modelName* and its **analysisSuccess** variable is *True*. The method also keeps the record of selectable entries, which is utilized by the **dbAccessDialog.plugin()** to keep track of the selected tree entries.

3.6.11 CreateID function family

The **CreateID** is a family of three functions in the **createEntryID.py** module, utilized to create a *unique ID* for a *shelve* database entry. The family is composed of three functions: **createID()**, **createIDfem()** and **createIDxfem()**.

createID() function

The **createID()** function is called by the **AccessDb.createTreeWidget()** to create a *unique ID* for an entry from a *shelve* database. The function calls either **createIDfem()** or **createIDxfem()**, according to the *analysis type* of the model. Finally the function returns the *unique ID*.

createIDfem() function

The **createIDfem()** function generates a unique *ID* for a *shelve* database entry, based on the input parameters of the model. The function is designed to operate on input data for *FEM* analysis type. The **ID** is a *dictionary* with keys of format *01_parameter name* for consistent sorting. The corresponding *value* is a combination of the parameters and their values. The *dictionary key* is utilized in the generation of the *parent* entries of the hierarchy and the *values* of the corresponding *child* entry.

createIDxfem() function

The **createIDxfem()** function is similar to the **createIDfem()**, however, it operates on input data for *XFEM* analysis type.

3.6.12 Execute gui commands functions

The **execute gui commands** is a family of functions, designed to call the required classes and methods, according to user requests. The functions are defined in the **executeDbAccessCommands.py**. The following functions are defined in the module: **readFromDb()**, **prepareDbDataStr()**, **appendPath()**, **createXYPlots()**, **printData()** and **createVisualizationOdb()**.

readFromDb() function

The **readFromDb()** function is utilized to process the *dataKeywords*, which are passed as an input argument by the **dbAccessDialogs_plugin()**, when the *Create* button of the *second dialog* box is pressed. First, the method calls the function **appendPath()** to make the required modules available in the system path. Second, the method extracts the *shelve* keys from the *dataKeywords[dbKeys]* string in a *tuple*. Next, the method iterates through the keys, reads the corresponding entry from the *shelve* database and calls the **prepareDbDataStr()** functions, which returns an *instance* of the **DbDataStr()** class. Then the instance is passed to **createXYPlots()**, **printData()** and **createVisualizationOdb()** if the corresponding *dataKeywords* are *True*.

prepareDbDataStr() function

The **prepareDbDataStr()** function is utilized to create an instance of the **DbDataStr()** class. The function takes three arguments as input **data**, which is the data read from the *shelve* database, **requests**, *dictionary* with the requests from the user and **dbKey**, which is the model name. Firstly the method creates an *instance* of the **DbDataStr()** class and then, calls the appropriate **DbDataStr()** class methods to write the **requests** and the **dbKey** value as a model name to the class.

appendPath() function

The **appendPath()** function is utilized to append the directory containing the required modules to the **sys.path**, which is a record of directories, where Abaqus searches during import.

createXYPlots() function

The **createXYPlots()** function is utilized to call the **XYPlotDataFromDbEntry()** and its methods to create *XYPlotData* for the passed *instance* of the **DbDataStr()** class.

printData() function

The **printData()** function is utilized to print the contents of the passed *instance* of the **DbDataStr()** class.

createVisualizationOdb() function

The **createVisualizationOdb()** function is utilized to create an Abaqus output database for visualization of the stress intensity factors from the passed **DbDataStr()** class *instance*. The method creates an *instance* of the **VisualizationOdbFromDbEntry()** class and calls the required methods to create the output database.

3.6.13 Main loop

The **main loop** name corresponds to modules defining functions to create and analyze a model database, extract the results from the output database and

write to the corresponding *shelve* database. Parameters for the model database are defined as range of values, which define a combination of input parameters. A function iterates through each configuration of input parameters and proceeds with the creation, analysis and results processing of the model. To avoid duplication of analyses and to be able to resume in case of an interruption, the *shelve* database entries are compared with the current input parameters before the creation of the model database. If a duplicate is detected the loop jumps to the next parameter configuration, until the configuration is unique for the *shelve* database. The **main loop** is comprised of four modules corresponding to each model type:

femCrackLoop.py is utilized to create a *FEM* analysis type.

xfemCrackLoop.py is utilized to create a *XFEM* analysis type and *crack-Partition* model type.

xfemCrackMPLoop.py is utilized to create a *XFEM* analysis type and *multiplePartitions* model type.

xfemSimpleCrackLoop.py is utilized to create a *XFEM* analysis type and *simple* model type.

Chapter 4

Results

4.1 Introduction

The program developed in the current project is capable of handling automated analysis of elliptic cracks. The only limitation is imposed by the available computational resources. The chapter covers the following points:

- element type comparison for *FEM* analysis type
- investigation of the optimal size of the cylinder
- mesh convergence analysis for *FEM* analysis type
- comparison of the mesh transformations for the *FEM* analysis type
- mesh and singularity radius convergence study for *XFEM* analysis type
- comparison of the accuracy of the models of *XFEM* analysis type
- comparison between *FEM* and *XFEM* results
- visualization of stress intensity factors

4.2 Procedure

The analysis of the results is performed in several steps. In each step of the analysis the optimum value of the analyzed parameter is selected and fixed for the consecutive step of the analysis, thus reducing the amount of parameters and narrowing the possible configurations to the optimal. As a starting point for the analysis the model of type *crackNormal* with *elliptic* mesh transformation is selected, for which is known to give the most accurate results.

1. Evaluation of the accuracy for each element type for *FEM* analysis type. Results of the stress intensity factors obtained for *linear full integration*, *linear reduced integration*, *quadratic reduced integration* and *quadratic full integration* elements are analyzed. Further, simulations are performed with the element type, which gives the smallest error.

2. Investigation of the optimal size of the cylinder containing the crack. Dimensions of the cylinder significantly influence the results for the stress intensity factors. In addition, the analytical solutions are for elliptic cracks in infinite medium. Therefore, it is crucial to estimate and limit the influence of the size of the cylinder on the final results.
3. Mesh convergence analysis for the *FEM* analysis, performed only for the selected element types.
4. Comparison of the mesh transformation types for otherwise identical meshes of the *FEM* analysis type.
5. Mesh and singularity radius convergence study for the different models of the *XFEM* analysis type. Only the optimal model dimensions, obtained are considered.
6. Comparison of the accuracy of the *XFEM* model types.
7. Comparison is made between *FEM* and *XFEM* results.
8. Review of the stress intensity factors visualization technique developed in the project.
9. Discussion of the results

4.3 Delimitations

Results in this chapter are generated for $\gamma = 30^\circ$ and $\omega = 60^\circ$, applied remote stress $\sigma = 100$. All the calculations for the *FEM* and *XFEM* analyses are performed for 5 contours.

Values obtained by averaging over contours 2, 3 and 4 are presented in this chapter. This simplification streamlines the generation of the results, however, it may degrade the accuracy, although, this effect should be limited and manifest itself mostly as additional noise to the solution.

Apart from the averaging, no additional processing operations have been performed on the results, which have been read from the Abaqus output database.

4.4 Element type comparison

As a starting point for the analysis of the element accuracy are the four simulations in table 4.1. Direct comparisons of the stress intensity factors are shown in figure 4.1 for K_I , figure 4.2 for K_{II} and figure 4.3 for K_{III} . Errors between the simulation and analytical values for the stress intensity factors are shown in figure 4.4 for K_I , figure 4.5 for K_{II} and figure 4.6 for K_{III} .

Comparing the results from table 4.1, the maximum error is less than 14% and *quadratic reduced integration* element appears to give the most accurate results. Graphs, however, reveal that the *quadratic* elements introduce more noise in the solution. Nevertheless, the *quadratic reduced integration* elements are selected for the next step in the analysis.

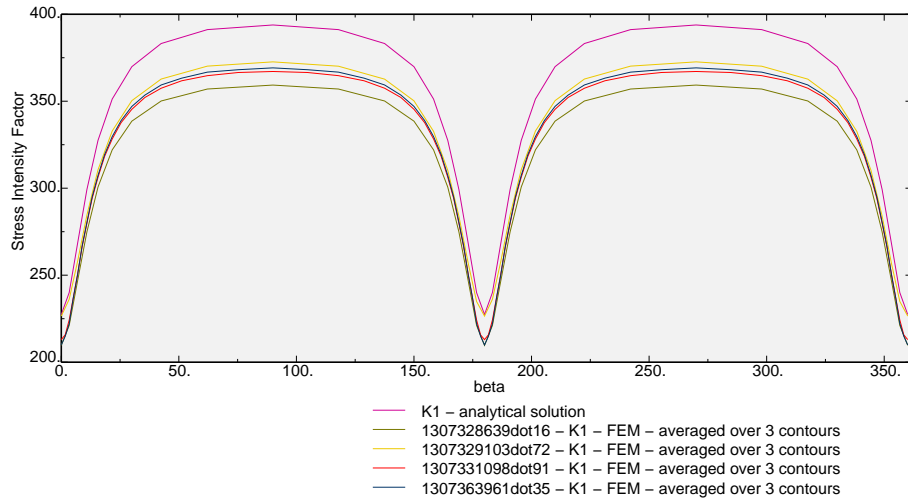


Figure 4.1: Comparison of values for K_I obtained for *crackNormal* model type with different element types and *elliptic* transformation

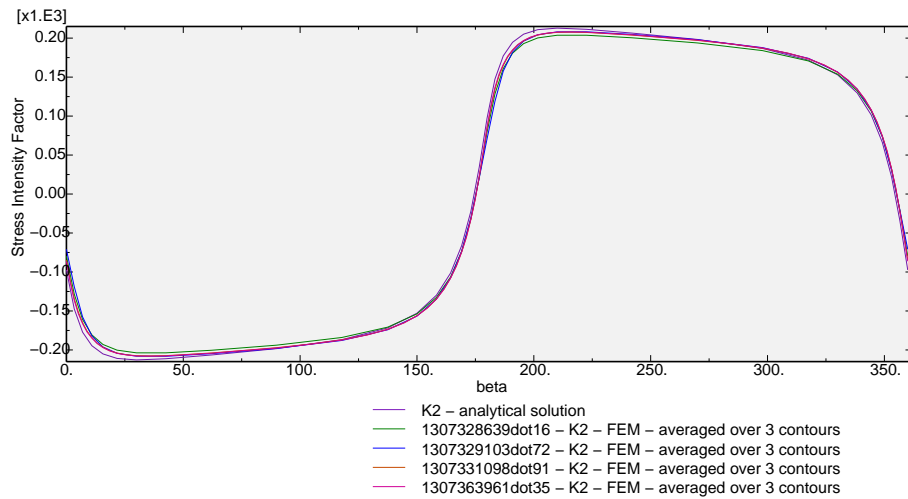


Figure 4.2: Comparison of values for K_{II} obtained for *crackNormal* model type with different element types and *elliptic* transformation

ID	mesh transform	element type	crack ratio	max error [%]		
				K_I	K_{II}	K_{III}
1307331098dot91	elliptic	quadraticFI	3	6.79	6.55	12.62
1307363961dot35	elliptic	quadraticRI	3	6.36	5.92	12.45
1307329103dot72	elliptic	linearRI	3	5.39	13.41	11.76
1307328639dot16	elliptic	linearFI	3	8.77	8.89	13.65

Table 4.1: Models included in the element type study

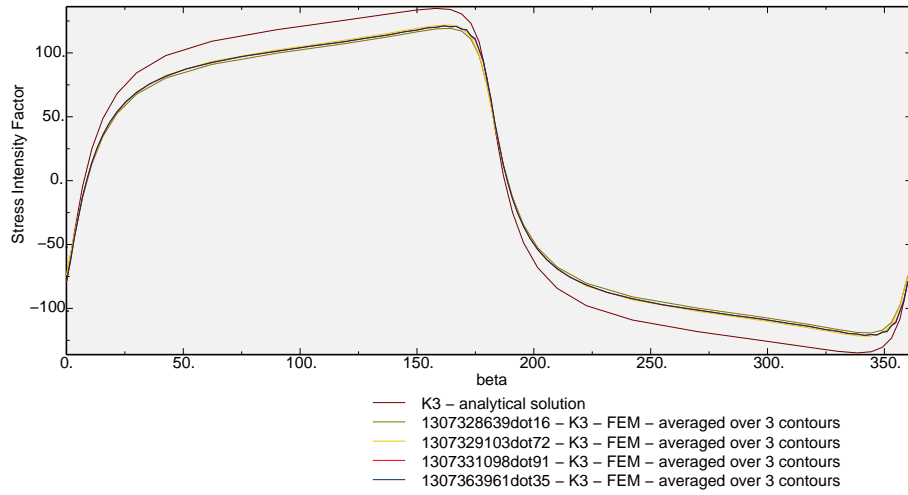


Figure 4.3: Comparison of values for K_I obtained for *crackNormal* model type with different element types and *elliptic* transformation

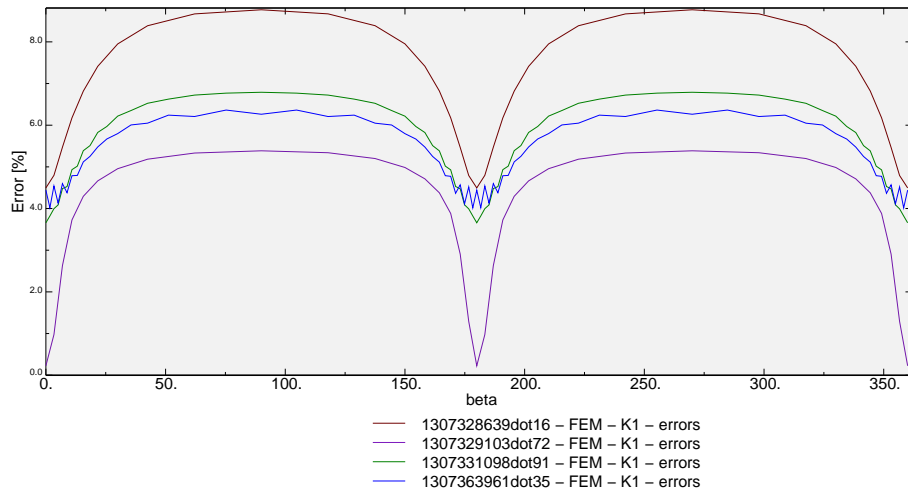


Figure 4.4: Comparison of errors for K_I obtained for *crackNormal* model type with different element types and *elliptic* transformation

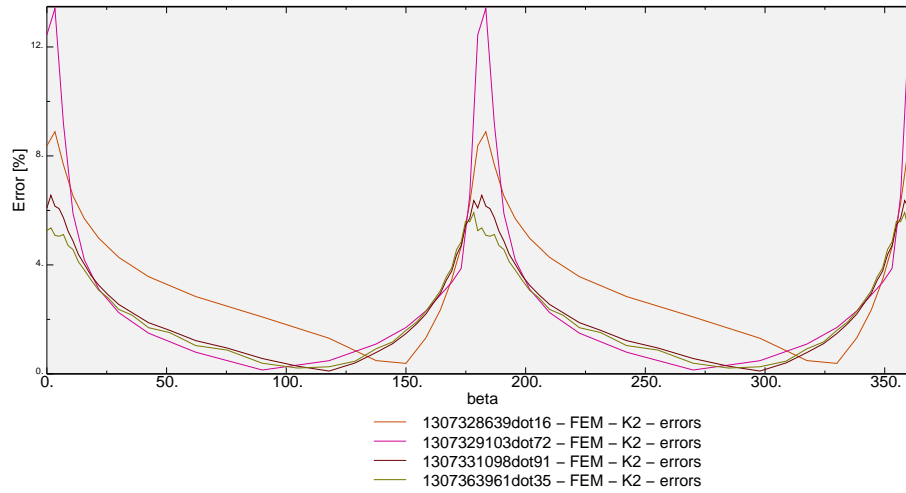


Figure 4.5: Comparison of errors for K_{II} obtained for *crackNormal* model type with different element types and *elliptic* transformation

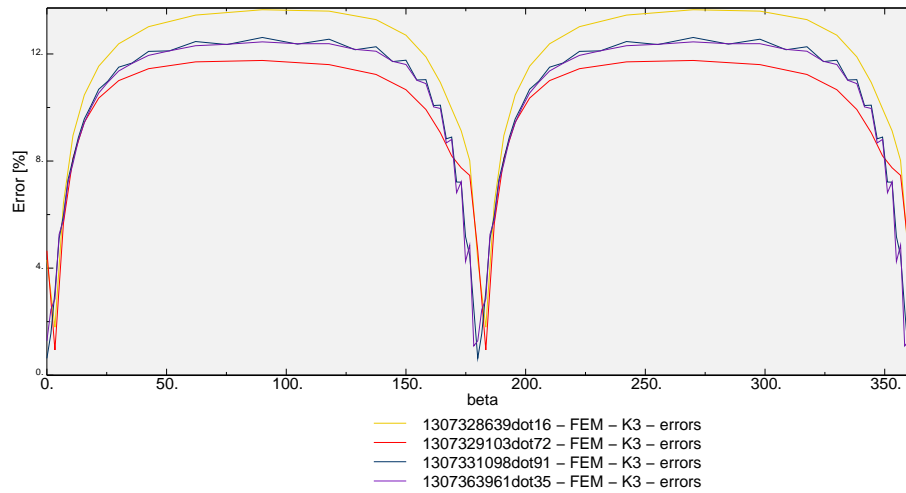


Figure 4.6: Comparison of errors for K_{III} obtained for *crackNormal* model type with different element types and *elliptic* transformation

4.5 Analysis of the influence of the cylinder dimensions

The analysis of the influence of the cylinder dimensions is performed by comparison of the maximum error for each of the stress intensity factor for different cylinder dimensions. The total number of simulations includes all the configurations with cylinder height and radius of: 40, 80, 120, 200, 300, including the configuration of a cylinder with height and radius of 100. The results are shown in figure 4.7 for K_I , figure 4.8 for K_{II} and figure 4.9 for K_{III} .

In addition, figure 4.10 illustrates the errors along the crack for the K_I stress intensity factor, figure 4.11 for K_{II} and figure 4.12 for K_{III} . Details about these simulations are presented in table 4.2.

Results prove the expected tendency of increased accuracy with increased dimensions of the cylinder. However, the dependence is not linear and is most pronounced for the height. Regarding the stress intensity factors, the trend is most pronounced for K_I , however, errors for K_{II} and K_{III} slightly increase after a certain point.

Finally, the optimal dimensions for a cylinder with a crack with $a = 30$ and $b = 10$ are:

$$\begin{aligned} & \text{height} = 200 \\ & \text{and} \\ & \text{radius} = 120 \end{aligned}$$

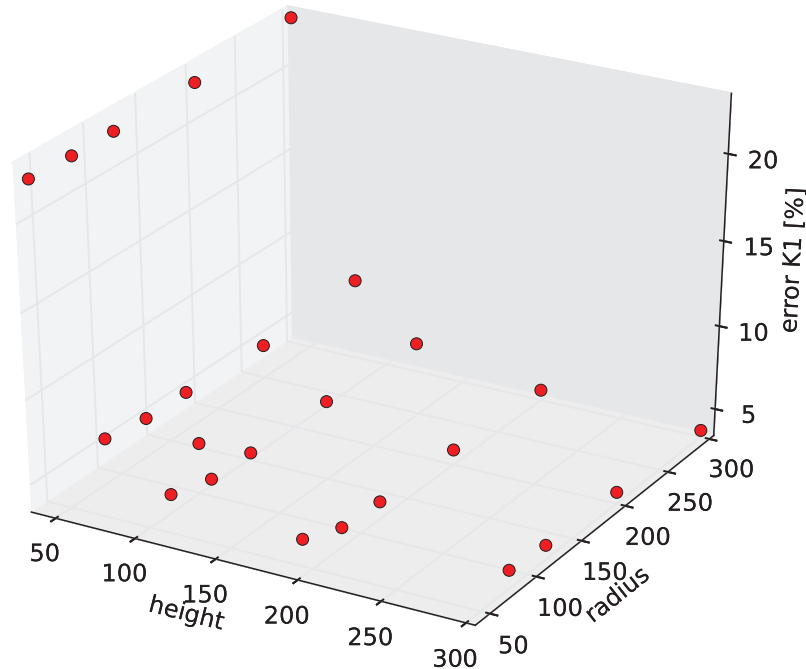


Figure 4.7: Convergence study for cylinder dimensions against the maximum errors for K_I

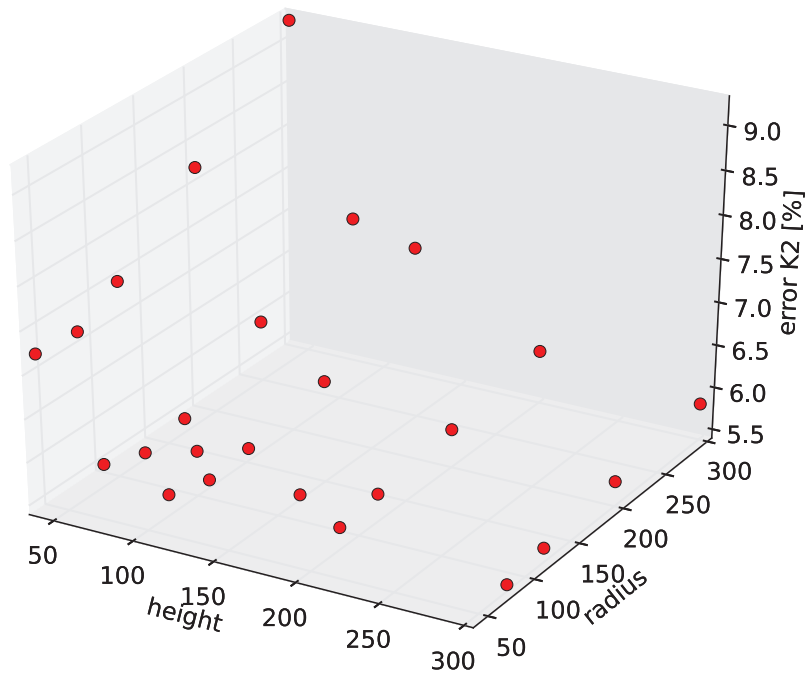


Figure 4.8: Convergence study for cylinder dimensions against the maximum errors for K_{II}

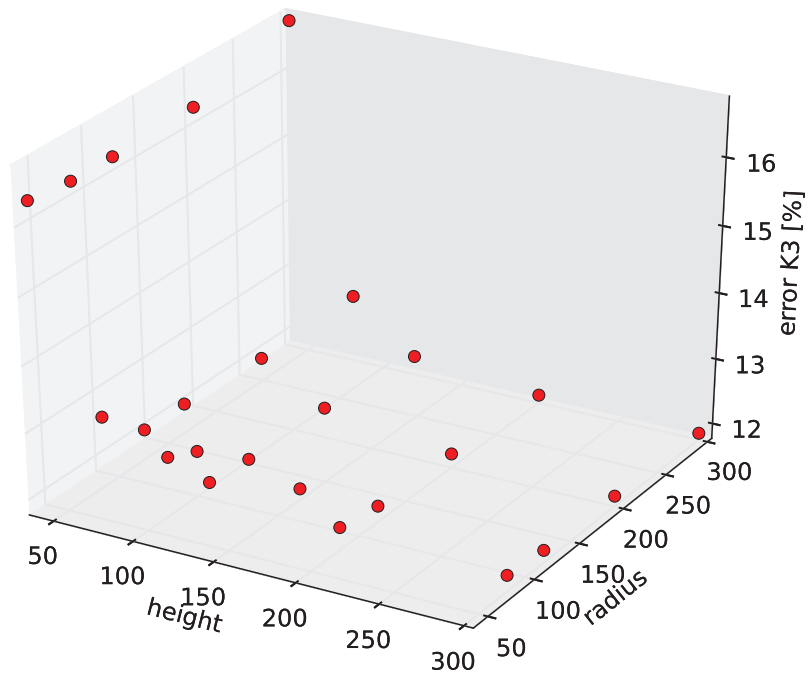


Figure 4.9: Convergence study for cylinder dimensions against the maximum errors for K_{III}

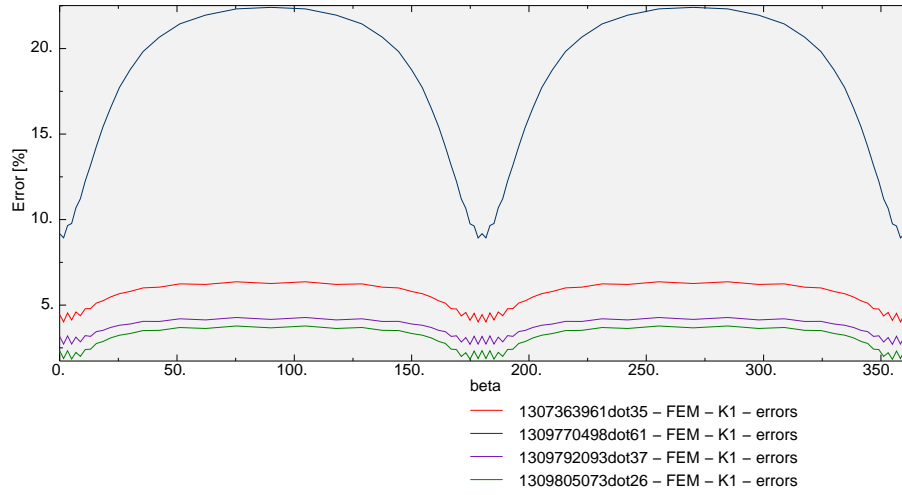


Figure 4.10: Comparison of errors for K_I along the crack front for different cylinder dimensions

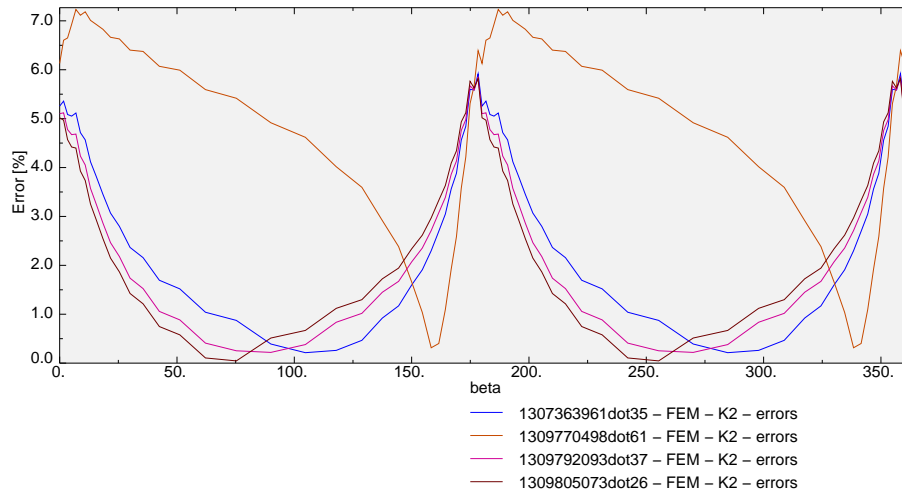


Figure 4.11: Comparison of errors for K_{II} along the crack front for different cylinder dimensions

ID	cylinder		max error [%]		
	height	radius	K_I	K_{II}	K_{III}
1309805073dot26	300	300	3.78	5.82	11.87
1309792093dot37	200	200	4.27	5.84	11.98
1307363961dot35	100	100	6.36	5.92	12.45
1309770498dot61	40	40	22.41	7.23	16.359

Table 4.2: Models in figures 4.10, 4.11 and 4.12

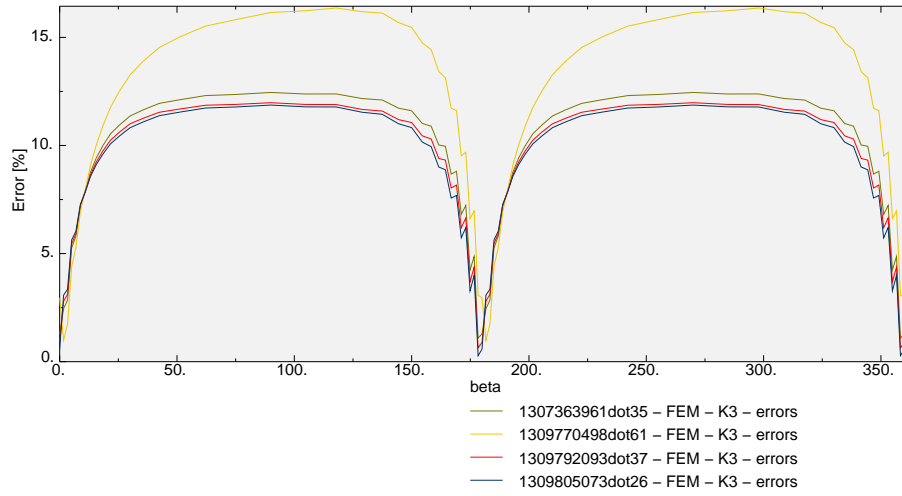


Figure 4.12: Comparison of errors for K_{III} along the crack front for different cylinder dimensions

4.6 Mesh convergence analysis

In this section the influence of the mesh refinement is analyzed by comparing different mesh densities for *linear reduced integration* and *quadratic reduced integration* elements. Analysis is performed for model with dimensions defined in section 4.5 and *elliptic* mesh transformation.

4.6.1 Mesh convergence analysis with quadratic reduced integration elements

Models included in the study are presented in table 4.3. According to table 4.3 the maximum errors of the stress intensity factors are almost independent of the mesh density.

For more complete representation, graphs of the errors for the stress intensity factors for some extreme cases, along the crack front are shown in figure 4.13 for K_I , figure 4.14 for K_{II} and figure 4.15 for K_{III} .

Although, maximum errors of the evaluated stress intensity factors is relatively constant, higher mesh density corresponds to a solution with less noise.

ID	seeds				max error [%]		
	czm	czt	ar	cr	K_I	K_{II}	K_{III}
1309848413dot98	5	5	3	5	failed analysis checks		
1309840073dot36	3	5	12	5	4.93	5.91	11.91
1309850324dot89	5	5	12	5	4.33	5.74	12.04
1309842434dot45	5	3	3	5	failed analysis checks		
1309837868dot7	3	3	12	5	4.82	5.91	11.93
1309837554dot03	3	3	5	5	5.05	5.94	11.85
1309843793dot24	5	3	12	5	4.38	5.8	12.07
1309837418dot02	3	3	3	5	failed analysis checks		
1309842855dot88	5	3	5	5	4.54	6.09	11.98
1309789759dot25	5	5	9	5	4.41	5.72	12.01
1309839557dot28	3	5	5	5	5.17	6.01	11.84
1309848923dot31	5	5	5	5	4.54	6.0	11.98
1309839345dot21	3	5	3	5	failed analysis checks		

Table 4.3: Models with *quadratic reduced integration* elements included in the mesh convergence study

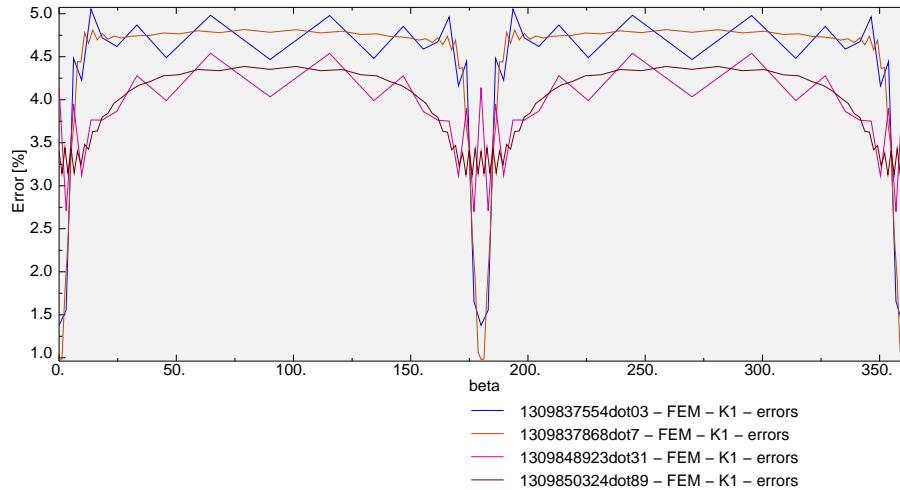


Figure 4.13: Comparison of errors for K_I along the crack front for different mesh densities of *quadratic reduced integration* elements

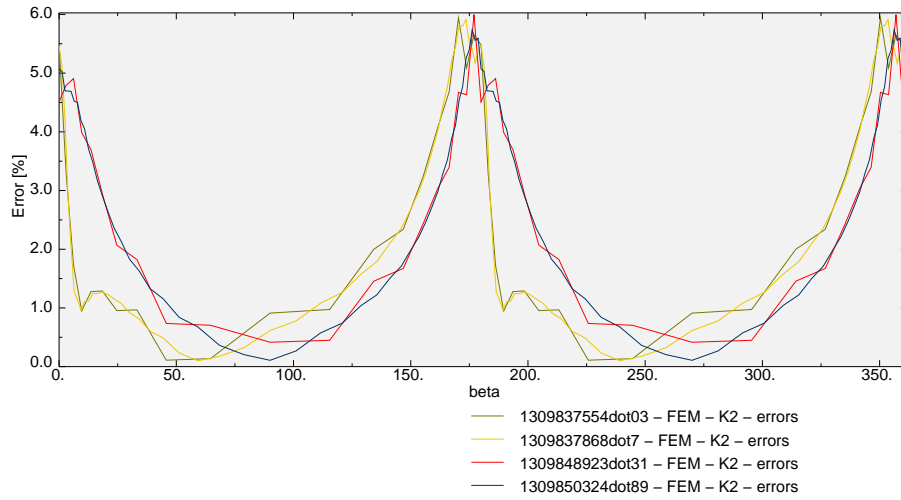


Figure 4.14: Comparison of errors for K_{II} along the crack front for different mesh densities of *quadratic reduced integration* elements

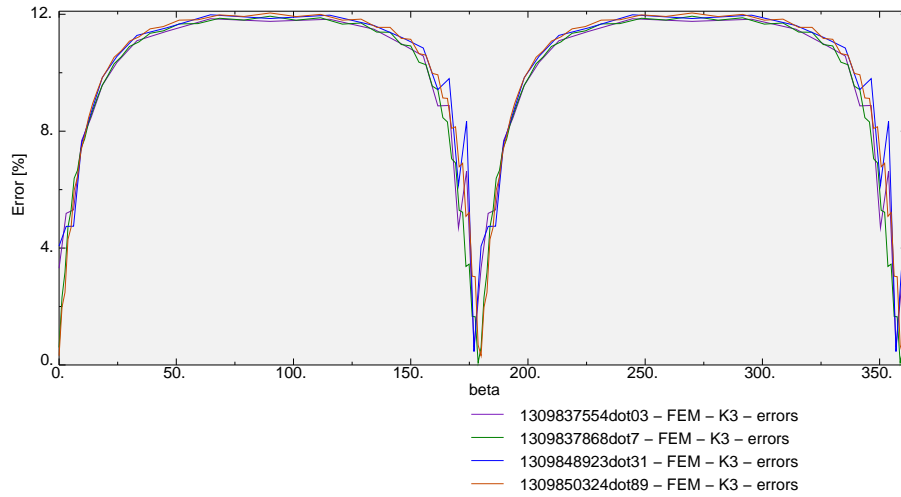


Figure 4.15: Comparison of errors for K_{III} along the crack front for different mesh densities of *quadratic reduced integration* elements

ID	seeds				max error [%]		
	czm	czr	ar	cr	K_I	K_{II}	K_{III}
1309835867dot25	5	5	5	5	3.85	12.75	11.6
1309835491dot63	5	3	15	5	3.48	13.68	11.26
1309835163dot74	5	3	3	5	5.56	14.23	12.9
1309834706dot86	3	3	12	5	9.16	32.28	16.3
1309836322dot15	5	5	15	5	3.31	13.89	11.12
1309835814dot17	5	5	3	5	5.53	14.17	12.74
1309835202dot98	5	3	5	5	4.02	12.74	11.75
1309835270dot46	5	3	12	5	3.52	13.49	11.28
1309834845dot13	3	5	3	5	4.47	25.13	12.22
1309834682dot92	3	3	5	5	7.05	26.93	13.14
1309834763dot64	3	3	15	5	9.26	31.98	16.27
1309835011dot44	3	5	15	5	11.01	34.24	17.4
1309834661dot92	3	3	3	5	3.34	24.22	12.43
1309834907dot25	3	5	12	5	10.88	34.14	17.43
1309834869dot43	3	5	5	5	8.49	29.03	14.0
1309835969dot28	5	5	12	5	3.35	13.72	11.15

Table 4.4: Models with *linear reduced integration* elements included in the mesh convergence study

4.6.2 Mesh convergence analysis with linear reduced integration elements

Models included in the study are presented in table 4.4. Contrary to the results in section 4.6.1, maximum errors of the stress intensity factors exhibit strong mesh density dependence, especially for the K_{II} factor.

For more complete representation, graphs of the errors for the stress intensity factors for some extreme cases, along the crack front are shown in figure 4.16 for K_I , figure 4.17 for K_{II} and figure 4.18 for K_{III} .

In conclusion, the simulation with ID *1309835867dot25*, table 4.4 provides the optimal balance between accuracy and mesh size, from the performed simulations.

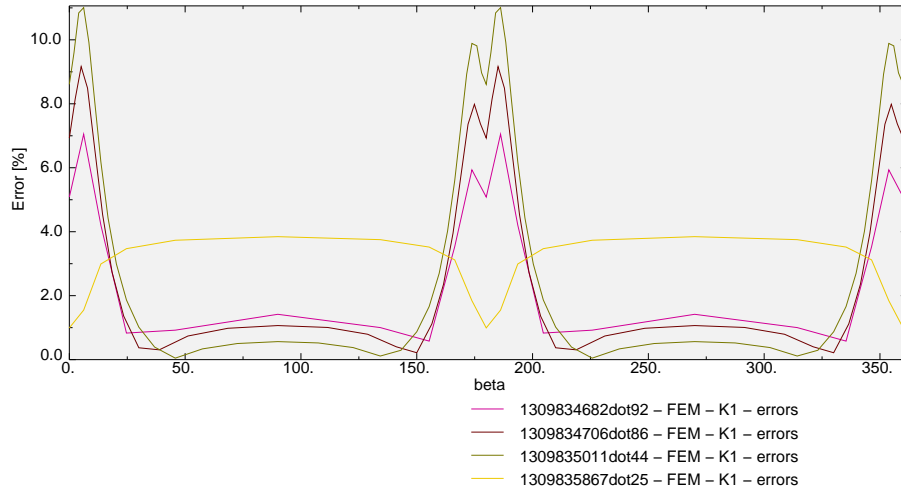


Figure 4.16: Comparison of errors for K_I along the crack front for different mesh densities of *linear reduced integration* elements

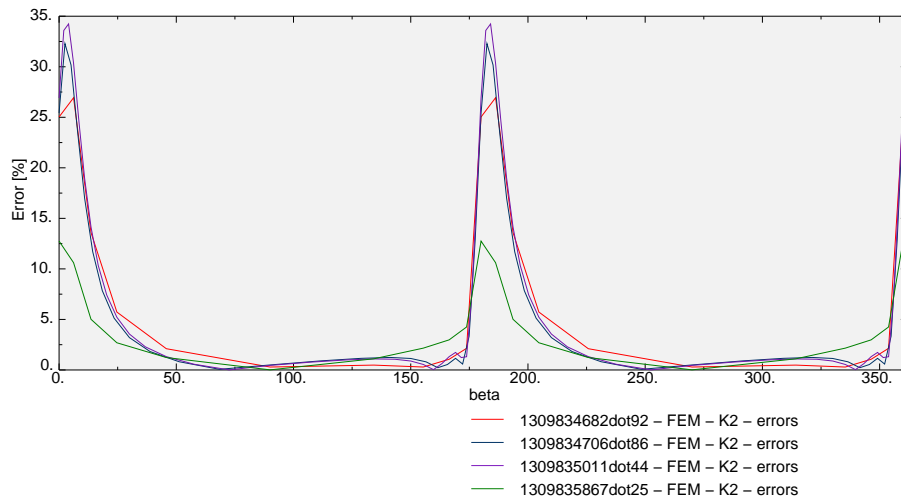


Figure 4.17: Comparison of errors for K_{II} along the crack front for different mesh densities of *linear reduced integration* elements

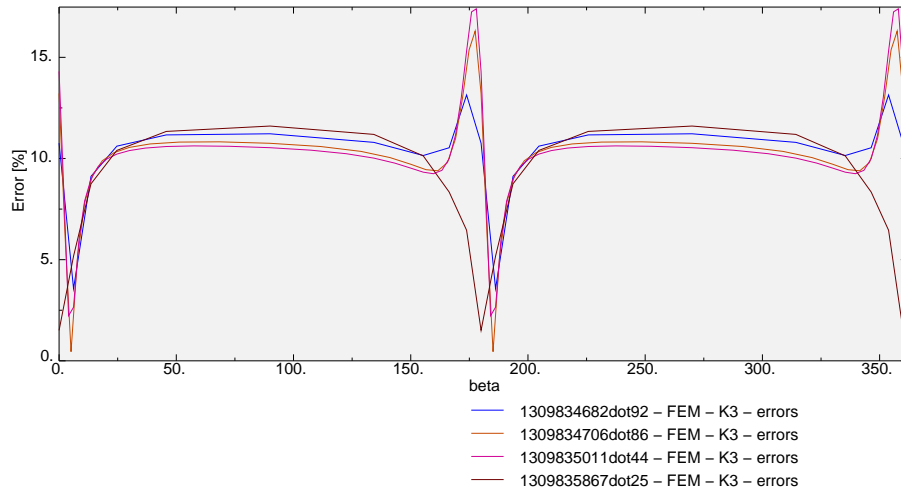


Figure 4.18: Comparison of errors for K_{III} along the crack front for different mesh densities of *linear reduced integration* elements

4.7 Comparison between mesh transformations

4.7.1 Comparison between *elliptic* and *simpleScale* mesh transformations

The accuracy of evaluation of stress intensity factors obtained from models with *elliptic* and *simpleScale* mesh transformations is compared. The comparison is made with both *linear reduced integration* and *quadratic reduced integration* elements. For the comparison, cylinder dimensions and mesh configurations obtained in sections 4.5 and 4.6 are used. Models included in the comparison are presented in table 4.5. Graphs for the maximum errors are illustrated in figure 4.28 for K_I , figure 4.29 for K_{II} and figure 4.30 for K_{III} .

Results from the comparison of a crack with aspect ratio 3 are shown in figure 4.19 for K_I , figure 4.20 for K_{II} and figure 4.21 for K_{III} . For cracks with ratios 5 and 10, results from the comparison are shown in figures 4.22, 4.23, 4.24, 4.25, 4.26, 4.27.

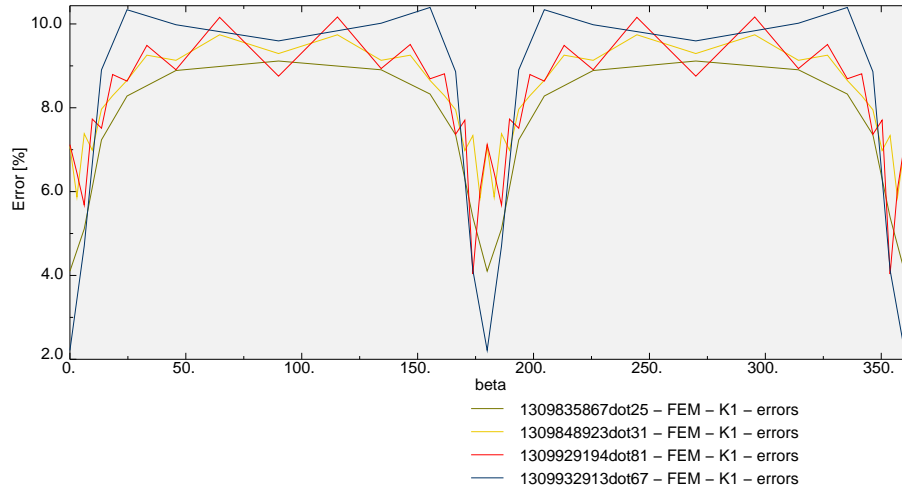


Figure 4.19: Comparison of errors for K_I for *elliptic* and *simpleScale* mesh transformation along the crack front for crack with aspect ratio of 3

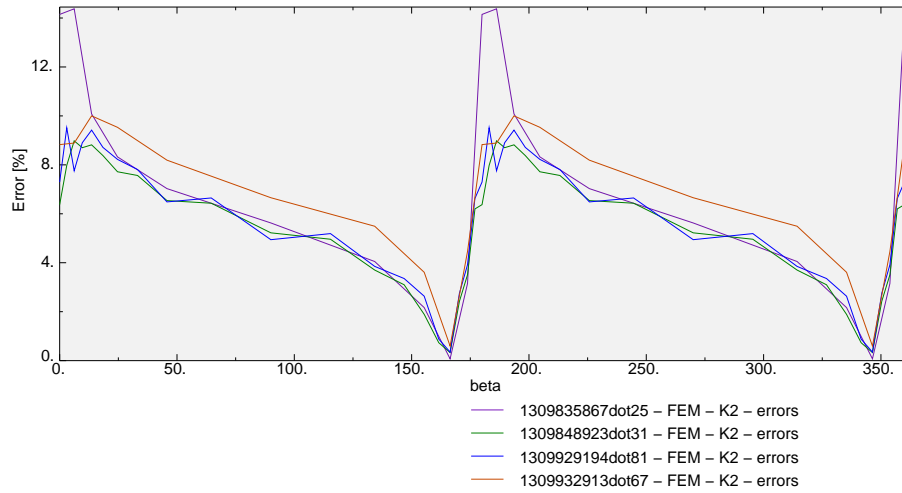


Figure 4.20: Comparison of errors for K_{II} for *elliptic* and *simpleScale* mesh transformation along the crack front for crack with aspect ratio of 3

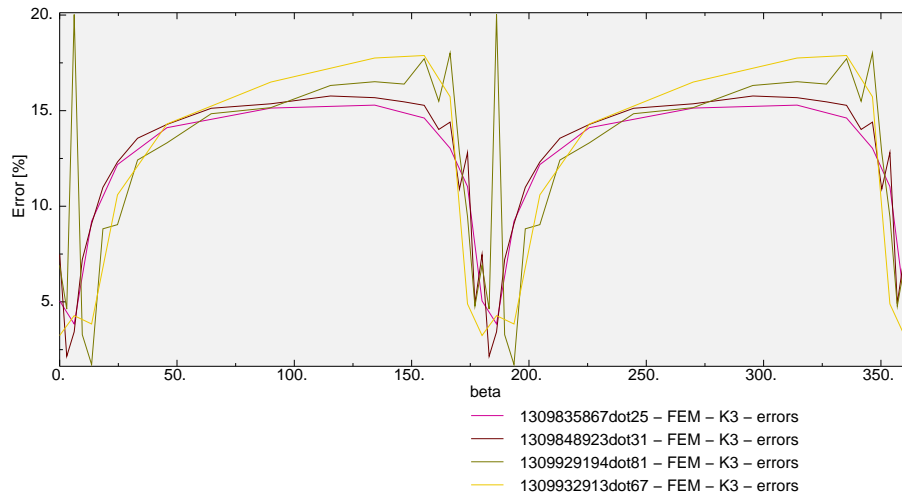


Figure 4.21: Comparison of errors for K_{III} for *elliptic* and *simpleScale* mesh transformation along the crack front for crack with aspect ratio of 3

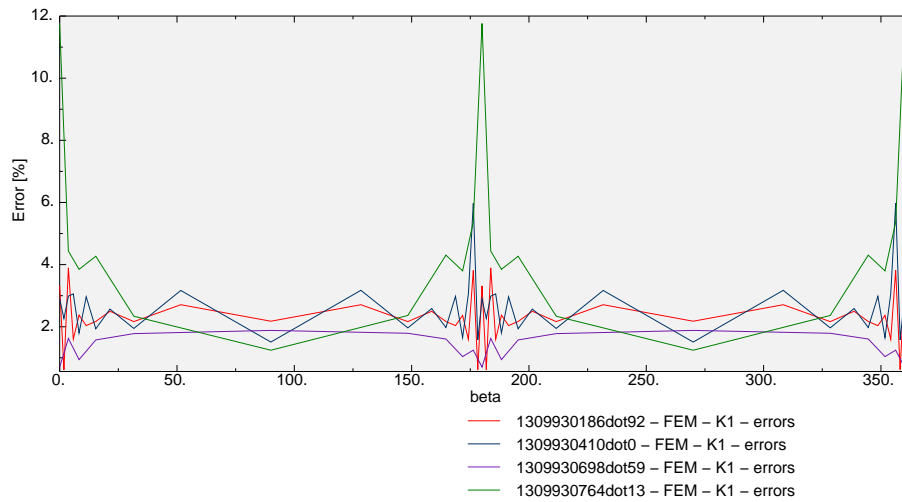


Figure 4.22: Comparison of errors for K_I for *elliptic* and *simpleScale* mesh transformation along the crack front for crack with aspect ratio of 5

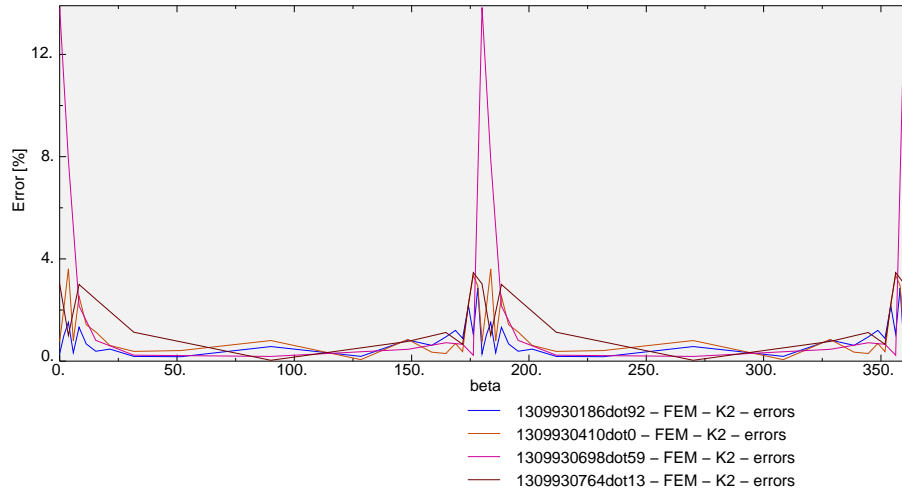


Figure 4.23: Comparison of errors for K_{II} for *elliptic* and *simpleScale* mesh transformation along the crack front for crack with aspect ratio of 5

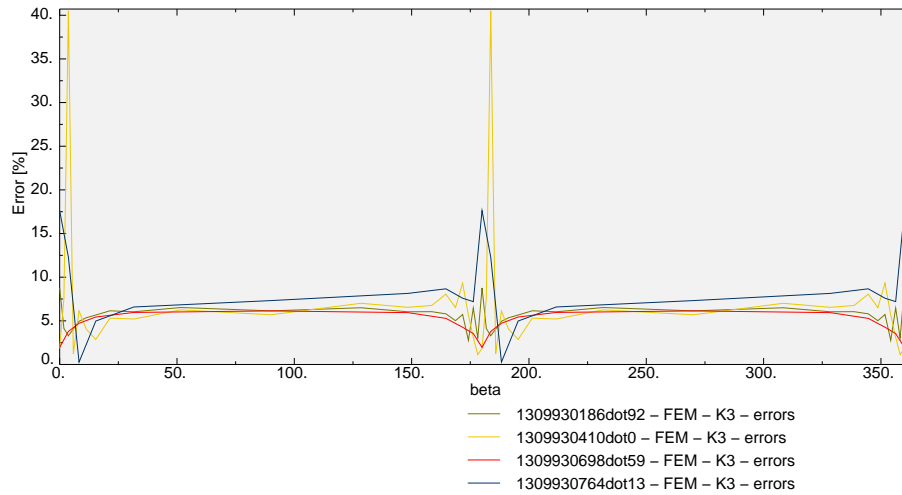


Figure 4.24: Comparison of errors for K_{III} for *elliptic* and *simpleScale* mesh transformation along the crack front for crack with aspect ratio of 5

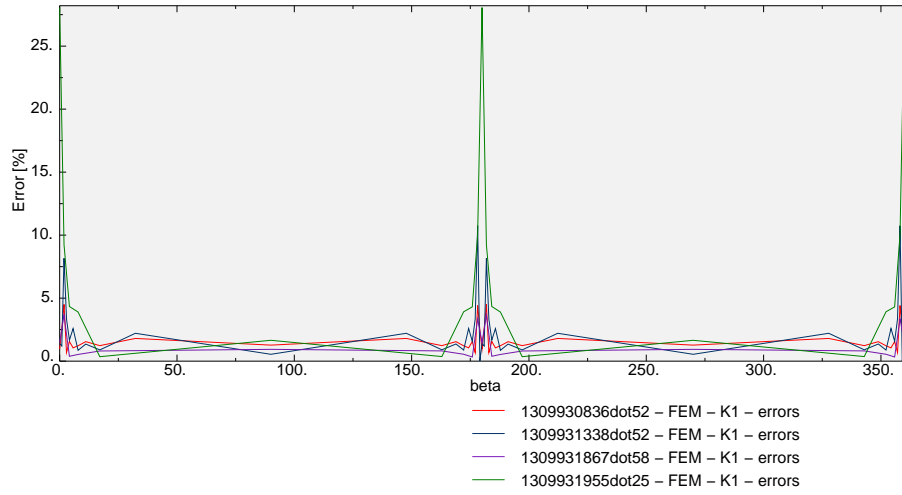


Figure 4.25: Comparison of errors for K_I for *elliptic* and *simpleScale* mesh transformation along the crack front for crack with aspect ratio of 10

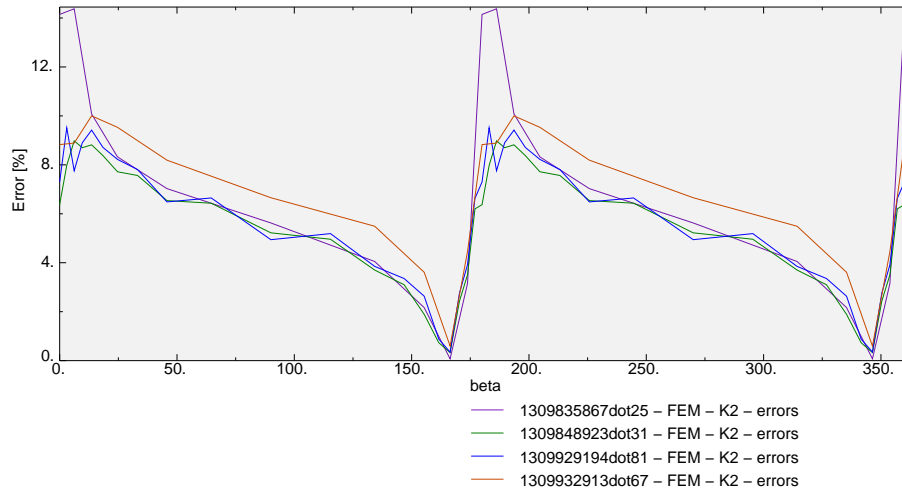


Figure 4.26: Comparison of errors for K_{II} for *elliptic* and *simpleScale* mesh transformation along the crack front for crack with aspect ratio of 10

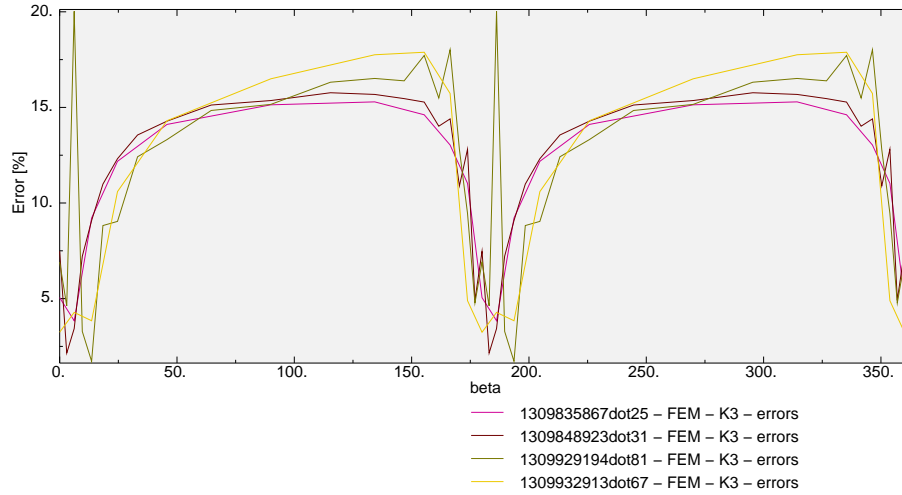


Figure 4.27: Comparison of errors for K_{III} for *elliptic* and *simpleScale* mesh transformation along the crack front for crack with aspect ratio of 10

ID	mesh transform	element type	crack ratio	max error [%]		
				K_I	K_{II}	K_{III}
1309929194dot81	simpleScale	quadRI	3	4.99	6.45	19.97
1309932913dot67	simpleScale	linearRI	3	5.71	7.1	13.78
1309835867dot25	elliptic	linearRI	3	3.85	12.75	11.6
1309848923dot31	elliptic	quadRI	3	4.5	6.0	11.98
1309930698dot59	elliptic	linearRI	5	1.88	13.84	6.14
1309930186dot92	elliptic	quadRI	5	3.9	2.86	8.77
1309930764dot13	simpleScale	linearRI	5	11.76	3.46	17.62
1309930410dot0	simpleScale	quadRI	5	5.97	3.61	40.51
1309931867dot58	elliptic	linearRI	10	3.65	13.85	2.41
1309930836dot52	elliptic	quadRI	10	4.51	4.32	27.5
1309931955dot25	simpleScale	linearRI	10	28.07	4.7	32.01
1309931338dot52	simpleScale	quadRI	10	10.75	8.31	45.54

Table 4.5: Models included in the comparison of mesh transformations

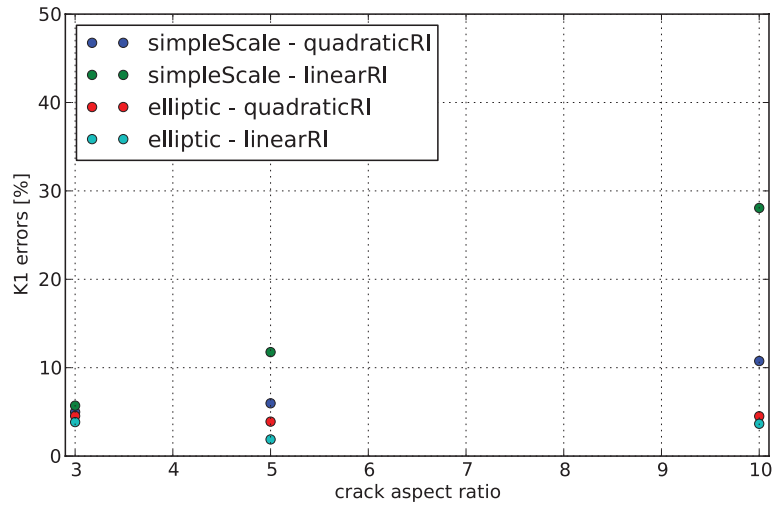


Figure 4.28: Comparison of the maximum errors for K_I for *elliptic* and *simpleScale* mesh transformations for crack with aspect ratios of 3, 5 and 10

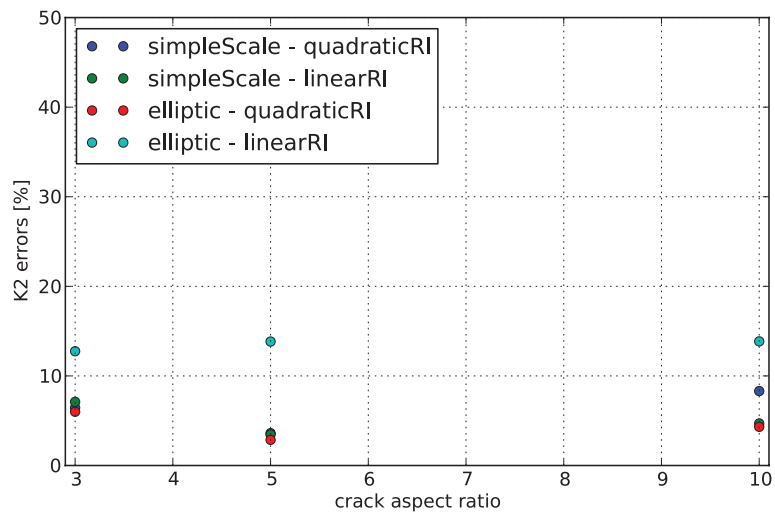


Figure 4.29: Comparison of the maximum errors for K_{II} for *elliptic* and *simpleScale* mesh transformations for crack with aspect ratios of 3, 5 and 10

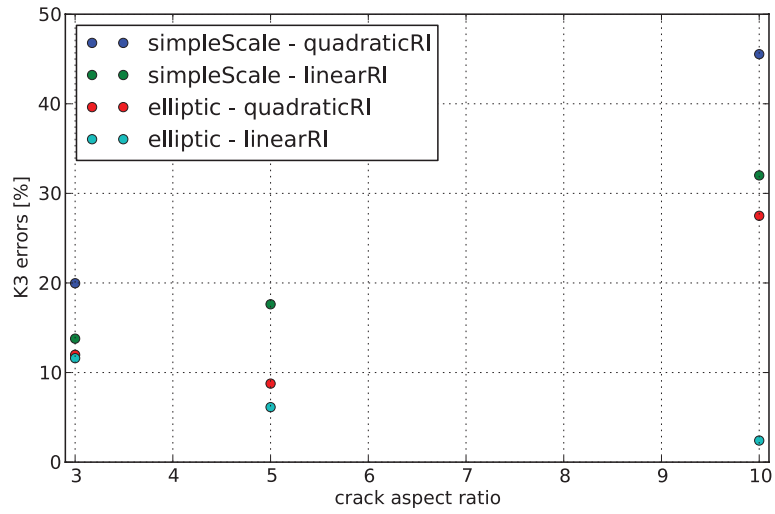


Figure 4.30: Comparison of the maximum errors for K_{III} for *elliptic* and *simpleScale* mesh transformations for crack with aspect ratios of 3, 5 and 10

4.7.2 *advancedScale* mesh transformation

The *advancedScale* mesh transformation in its present implementation proved to give unreliable results. The problem can be tracked to the merging on nodes of the *innerCylinder*. The procedure works reliably for *elliptic* and *simpleScale* mesh transformations, however, is not reliable for *advancedScale*. Therefore, results for this particular transformation are not considered and is not advisable to be used until the algorithm is fixed.

4.8 XFEM results

4.8.1 Mesh and singularity radius convergence study

The accuracy of the *XFEM* solution, in addition to mesh density, depends on the *singularity calculation radius*. It determines which elements, located radially in the vicinity of the crack front would be included in the calculation of the singularity. Judging from the results, it may have a significant impact on the accuracy of the results.

The convergence study is carried out on models with dimensions, determined in section 4.5 and crack aspect ratio of 3.

Results for the K_{II} stress intensity factor have consistently been calculated with the opposite to the analytical solution sign and errors are in the vicinity of 200%.

Convergence study for the *crackPartition* model

The *crackPartition* model type is meshed with *linear tetrahedral elements*, which are generally perceived as inferior to hexahedral elements and require dense meshes to converge.

Models in the convergence study are presented in table 4.6. Results for K_I stress intensity factors are shown in figure 4.31, K_{II} in figure 4.32, K_{III} in figure 4.33.

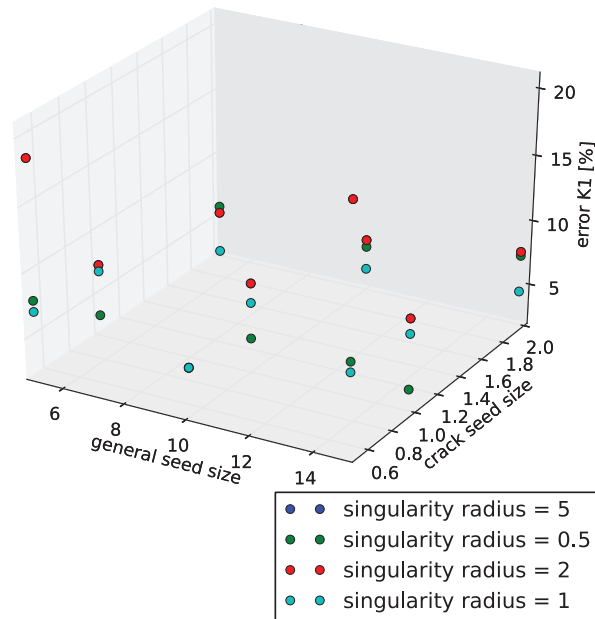


Figure 4.31: Convergence study for *crackPartition* XFEM model for K_I stress intensity factor

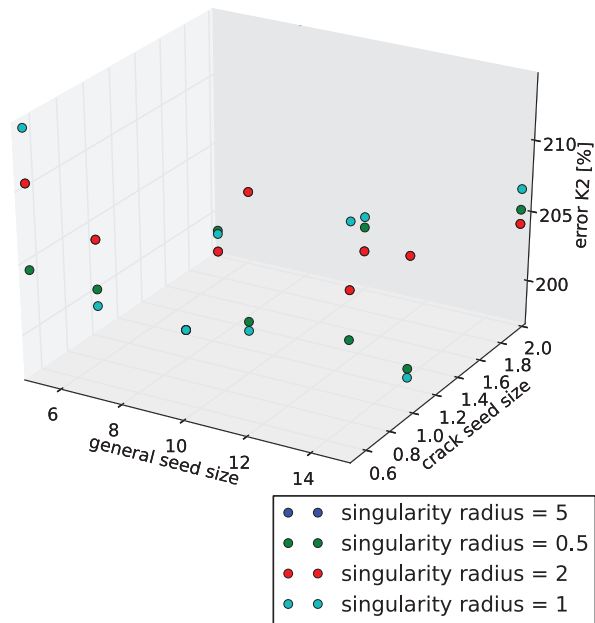


Figure 4.32: Convergence study for *crackPartition* XFEM model for K_{II} stress intensity factor

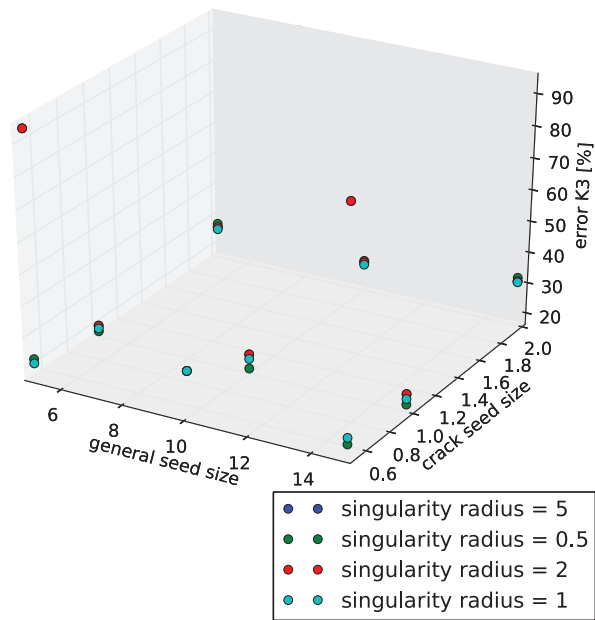


Figure 4.33: Convergence study for *crackPartition* XFEM model for K_{III} stress intensity factor

ID	singularity radius	seed size		max error [%]		
		general	crack	K_I	K_{II}	K_{III}
1309881638dot61	0.5	5	0.5	7.9	204.57	22.75
1309867375dot36	0.5	5	1	3.48	200.22	17.89
1309861189dot43	0.5	5	2	5.89	198.75	37.41
1309888005dot75	0.5	10	0.5	5.68	203.0	31.3
1309869569dot74	0.5	10	1	4.53	200.51	17.77
1309862320dot31	0.5	10	2	5.31	201.45	26.11
1309890615dot21	0.5	15	0.5	9.12	205.0	20.7
1309870282dot26	0.5	15	1	3.53	199.86	18.56
1309862604dot44	0.5	15	2	7.32	205.19	31.94
1309877851dot66	1	5	0.5	7.05	214.25	21.36
1309866047dot71	1	5	1	6.94	199.0	18.84
1309860508dot44	1	5	2	2.25	198.5	25.59
1309887212dot44	1	10	0.5	5.68	203.0	31.3
1309869302dot8	1	10	1	7.3	199.86	20.91
1309862186dot35	1	10	2	3.53	202.21	24.83
1309890029dot56	1	15	0.5	8.33	212.85	22.79
1309870142dot52	1	15	1	7.8	199.23	20.36
1309862530dot48	1	15	2	4.49	206.65	30.46
1309874034dot54	2	5	0.5	18.55	210.53	94.47
1309864682dot98	2	5	1	7.45	203.82	19.76
1309859802dot52	2	5	2	5.39	197.16	26.31
1309886494dot28	2	10	0.5	5.68	203.0	31.3
1309869048dot44	2	10	1	8.8	209.58	22.39
1309862054dot23	2	10	2	5.84	199.68	25.65
1309889469dot37	2	15	0.5	20.78	208.35	94.26
1309869997dot09	2	15	1	8.96	207.7	21.95
1309862457dot59	2	15	2	7.62	104.18	30.81
1309870420dot11	5	5	0.5	18.55	210.53	94.47
1309862678dot81	5	5	1	7.45	203.82	19.76
1309859167dot16	5	5	2	5.39	197.16	26.31
1309885742dot85	5	10	0.5	5.68	203.0	31.3
1309868759dot33	5	10	1	8.8	209.58	22.39
1309861904dot84	5	10	2	5.84	199.69	25.65
1309888886dot84	5	15	0.5	20.78	208.35	94.27
1309869835dot18	5	15	1	8.98	207.7	21.95
1309858154dot86	5	15	2	7.62	204.18	30.81

Table 4.6: Models of type *crackPartition* included in the convergence study

ID	singularity radius	seed size		max error [%]		
		general	container	K_I	K_{II}	K_{III}
1309986788dot06	0.5	10	1	37.37	221.32	23.25
1309984483dot97	0.5	10	2	37.37	221.32	23.25
1309987175dot79	0.5	20	1	56.44	327.06	33.83
1309985293dot77	0.5	20	2	56.44	327.27	33.83
1309986877dot41	1	10	1	31.39	208.08	28.56
1309984680dot36	1	10	2	31.39	208.08	28.56
1309987100dot02	1	15	1	55.84	221.56	31.71
1309985152dot52	1	15	2	55.84	221.56	31.71
1309987202dot14	1	20	1	39.2	264.25	25.7
1309985340dot47	1	20	2	39.2	264.25	25.7
1309986968dot52	2	10	1	16.35	199.61	28.96
1309984881dot75	2	10	2	16.35	199.61	28.96
1309987134dot36	2	15	1	27.22	216.11	30.81
1309985220dot46	2	15	2	27.22	216.11	30.81
1309987226dot5	2	20	1	14.42	195.64	19.08
1309985392dot83	2	20	2	14.42	195.64	19.09

Table 4.7: Models of type *multiplePartitions* included in the convergence study

Convergence study for the *multiplePartitions* model

The *multiplePartitions* model is meshed with *linear hexahedral reduced integration* elements. The models in the convergence study are presented in table 4.7.

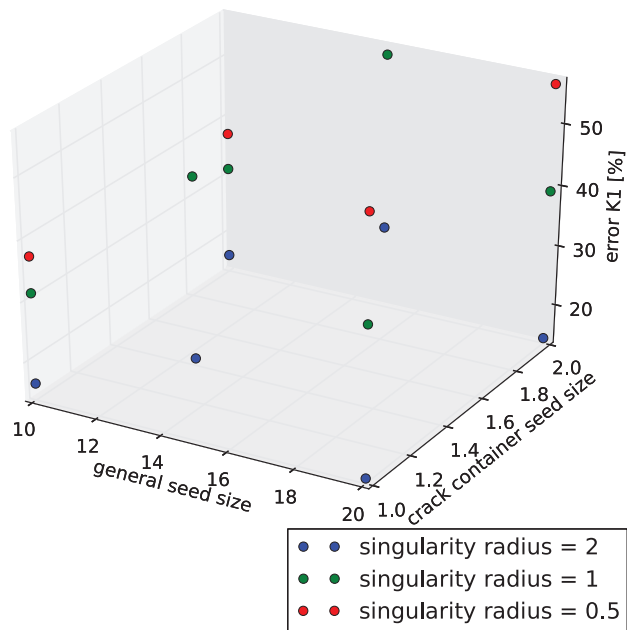


Figure 4.34: Convergence study for *multiplePartitions* XFEM model for K_I stress intensity factor

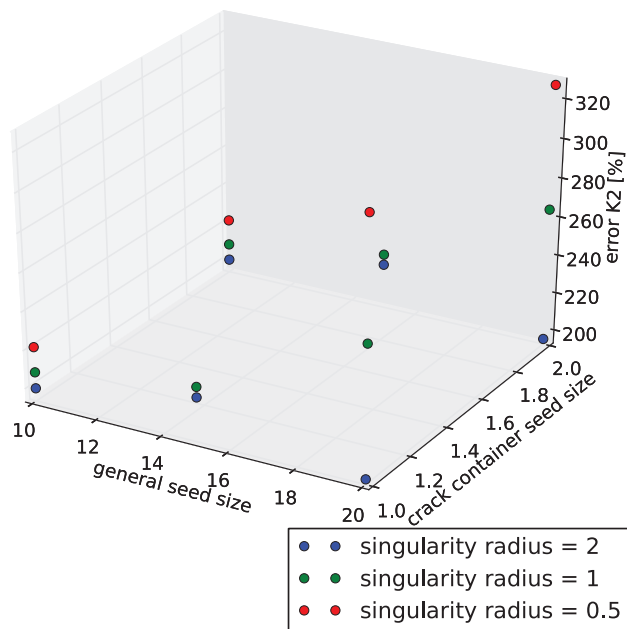


Figure 4.35: Convergence study for *multiplePartitions* XFEM model for K_{II} stress intensity factor

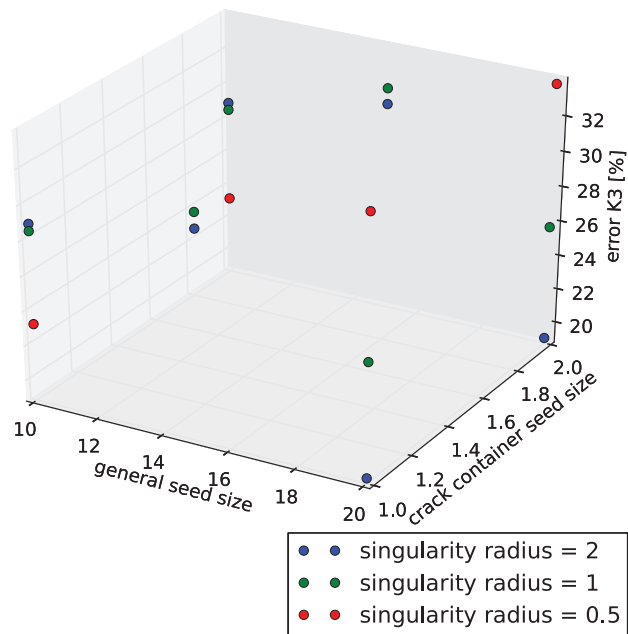


Figure 4.36: Convergence study for *multiplePartitions* XFEM model for K_{III} stress intensity factor

Convergence study for the *simple* model

The *simple* model is meshed with *linear hexahedral reduced integration* elements. The models in the convergence study are presented in table 4.8.

ID	singularity radius	seed size	max error [%]		
			K_I	K_{II}	K_{III}
1310135264dot81	1	4	28.13	215.56	28.67
1309907173dot28	1	5	12.27	210.25	37.22
1309907898dot52	1	10	39.02	167.13	33.73
1310133138dot24	2.5	4	21.58	210.3	33.56
1309906614dot41	2.5	5	16.94	204.39	42.01
1309907836dot46	2.5	10	42.12	169.7	33.5
1310131219dot07	5	4	21.85	210.3	33.56
1309906107dot27	5	5	16.06	204.07	42.61
1309907767dot41	5	10	42.12	169.7	33.5

Table 4.8: Models of type *simple* included in the convergence study

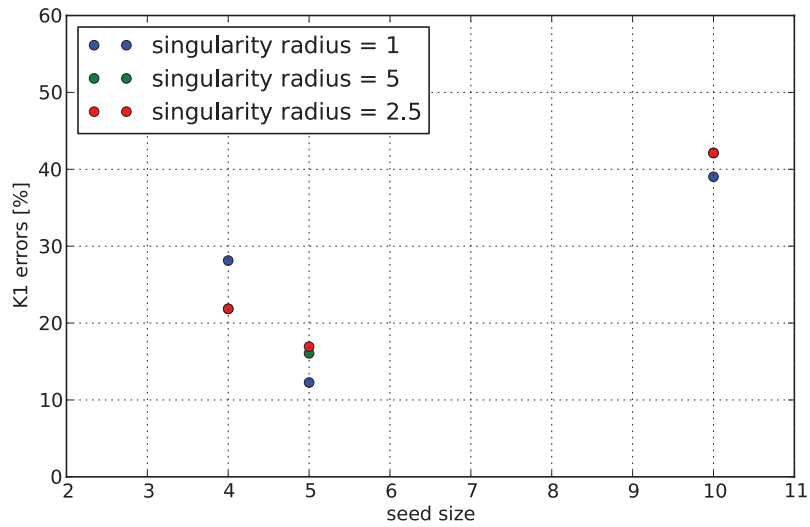


Figure 4.37: Mesh and singularity radius convergence for K_I

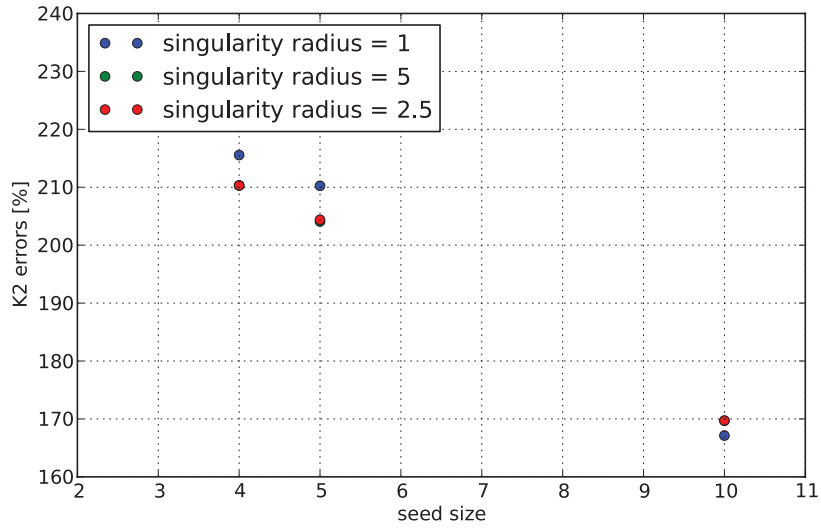


Figure 4.38: Mesh and singularity radius convergence for K_{II}

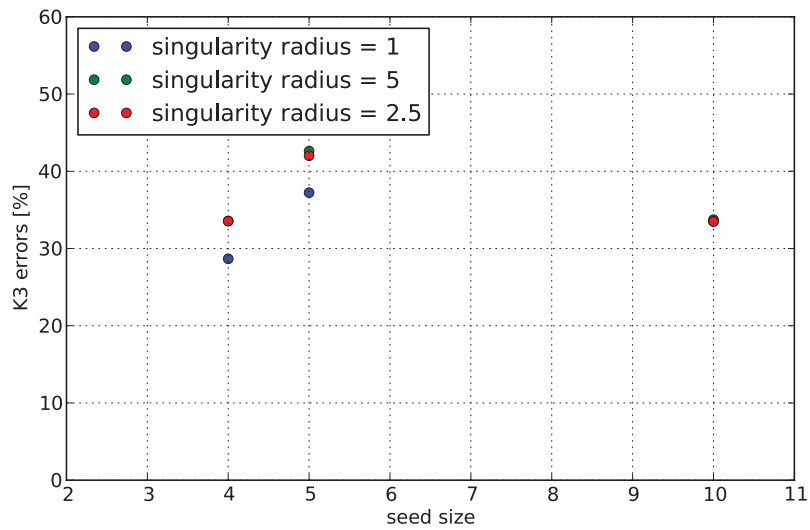


Figure 4.39: Mesh and singularity radius convergence for K_{III}

4.8.2 Comparison of the values and errors of the calculated stress intensity factors by *XFEM*

Accuracy of the *crackPartition*, *multiplePartitions* and *simple* model types is compared. Models included in the study are presented in table 4.9. The models are selected on the basis of the best accuracy for a given model type. The selection, however, does not guarantee, that the number of evaluations of the stress intensity factors is equal. Furthermore, the contrary is true and the number of points for evaluation of the stress intensity factors varies significantly with the different model types. Nevertheless, the comparison would be useful to give a general notion of what accuracy can be expected and what strategy may be give optimal results in future studies.

Comparison of the stress intensity factors along the crack front are illustrated in figure 4.40 for K_I , figure 4.41 for K_{II} and figure 4.42 for K_{III} . Errors of the stress intensity factors are illustrated in figure 4.43 for the K_I , figure 4.44 for K_{II} and figure 4.45 for K_{III} .

Stress intensity factors, calculated with *XFEM* show considerable noise and the *maximum error* value is not a precise measure for the overall accuracy. This is especially true for model *1309888886dot84*, which has a very high peak, which leads to high value of the *maximum error*.

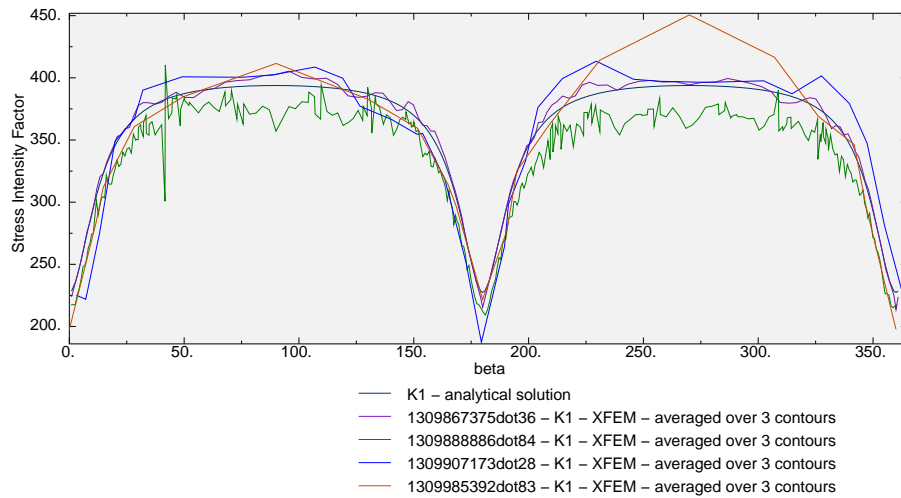


Figure 4.40: Comparison of the calculated values for K_I along the crack front for the different *XFEM* model types

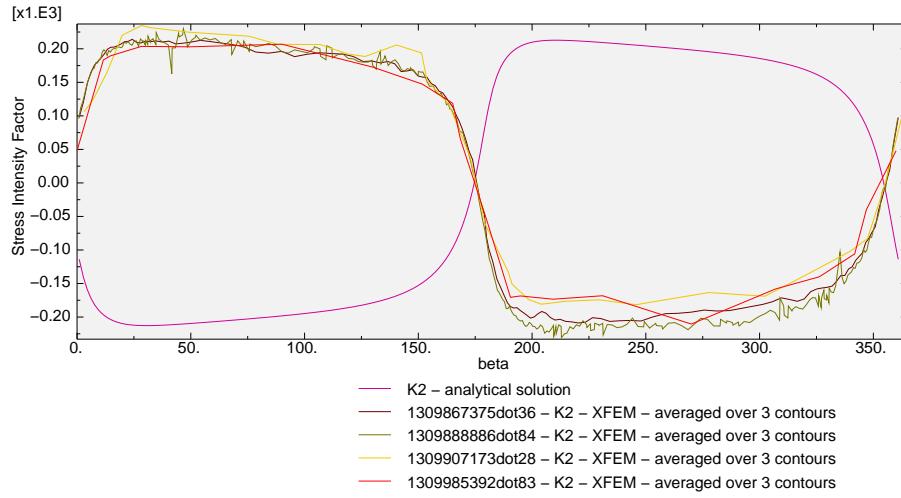


Figure 4.41: Comparison of the calculated values for K_{II} along the crack front for the different $XFEM$ model types

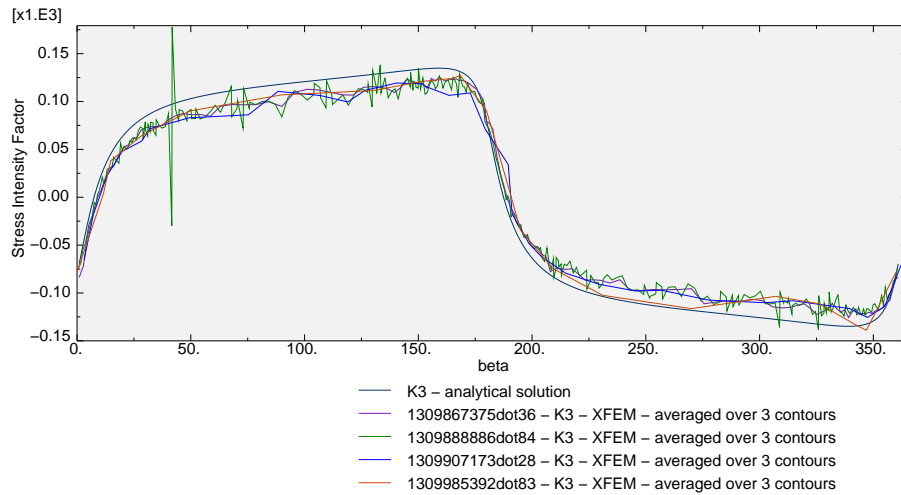


Figure 4.42: Comparison of the calculated values for K_{III} along the crack front for the different $XFEM$ model types

ID	sing. radius	seed size			max error [%]		
		general	crack	cont.	K_I	K_{II}	K_{III}
1309985392dot83	2	20	—	2	14.42	195.64	19.08
1309867375dot36	0.5	5	1	—	3.48	200.22	17.89
1309888886dot84	5	15	0.5	—	20.78	208.35	94.27
1309907173dot28	1	5	—	—	12.27	210.25	37.23

Table 4.9: Models included in the comparison of the accuracy of the different $XFEM$ model types

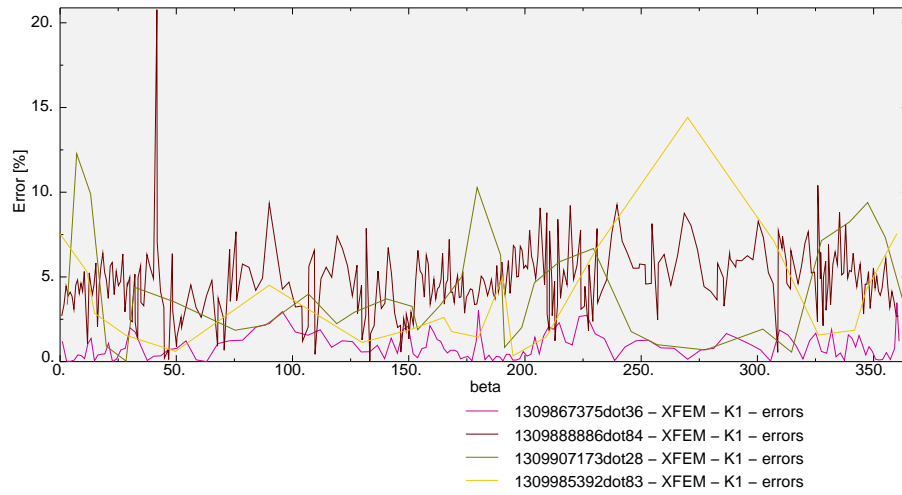


Figure 4.43: Errors of the calculated values for K_I along the crack front for the different *XFEM* model types

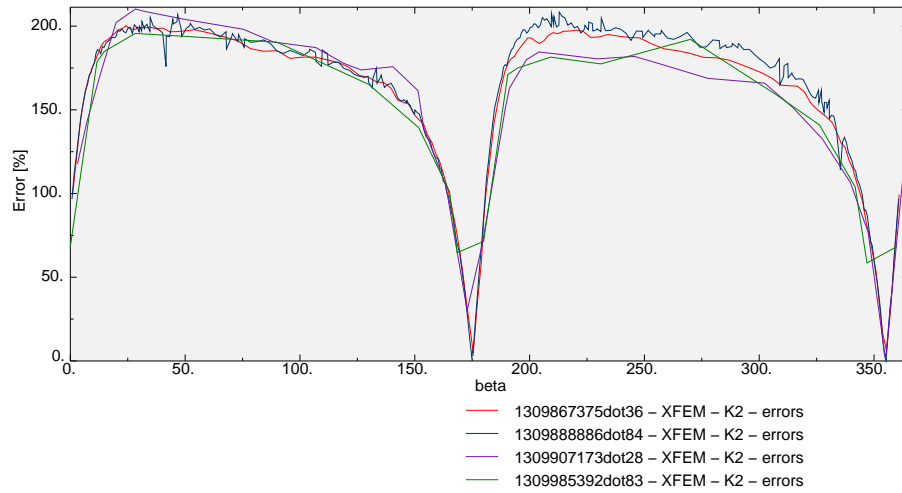


Figure 4.44: Errors of the calculated values for K_{II} along the crack front for the different *XFEM* model types

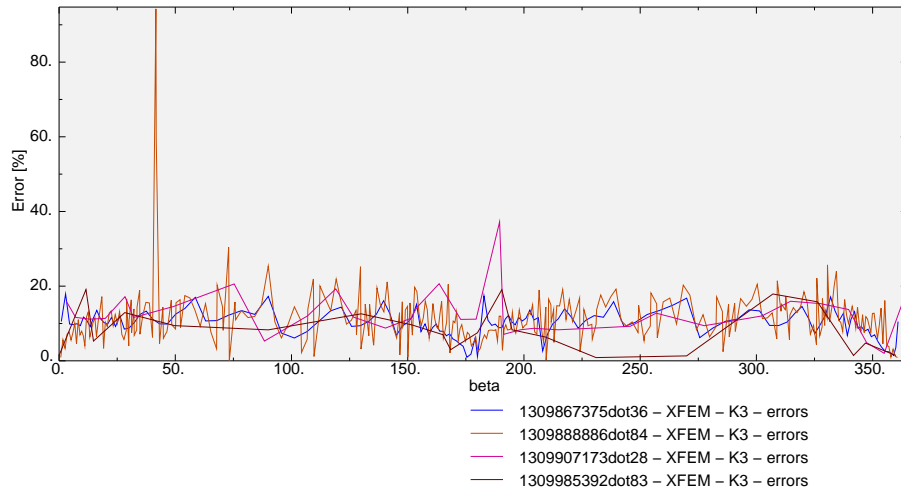


Figure 4.45: Errors of the calculated values for K_{III} along the crack front for the different $XFEM$ model types

4.8.3 Comparison between FEM and $XFEM$ results

The obtained results for the stress intensity factors from FEM and $XFEM$ analyses are compared in this section. Comparison is performed for cracks with aspect ratios of 3, 5 and 10. The included models are of types *crackNormal* with *elliptic* mesh transformation and *quadratic reduced integration* elements and *crackPartition* with *linear tetrahedral* elements. The comparison is performed for models with cylinder dimensions determined in section 4.5, regardless of the crack aspect ratio. Therefore, it could be expected that the comparison performed for crack aspect ratio of 3 to be the most representative.

The comparison is limited to K_I and K_{III} stress intensity factors, as the results for K_{II} from the $XFEM$ analysis are calculated with opposite signs.

Comparison for crack aspect ratio of 3 K_I is illustrated in figure 4.46, for K_{III} in figure 4.47 and errors along the crack front in figure 4.48. For crack with aspect ratio of 5, K_I is illustrated in figure 4.49, K_{III} in figure 4.50 and errors in figure 4.51. For crack with aspect ratio of 10, K_I is illustrated in figure 4.52, K_{III} in figure 4.53 and errors in figure 4.54. Finally, models included in the comparison are listed in tables 4.10 and 4.11.

Results of the comparison prove that the $XFEM$ and FEM models have comparable accuracy for K_I and K_{III} stress intensity factors. The decrease in accuracy of the K_I and K_{III} for the $XFEM$ analysis for crack aspect ratios of 5 and 10 could be due to a requirement for a cylinder with larger dimensions to better represent the infinite medium. The mesh transform, however, increases the dimensions of the cylinder, which may have influence, which is not accounted for. Regarding the K_{II} values calculated with $XFEM$ have the opposite sign.

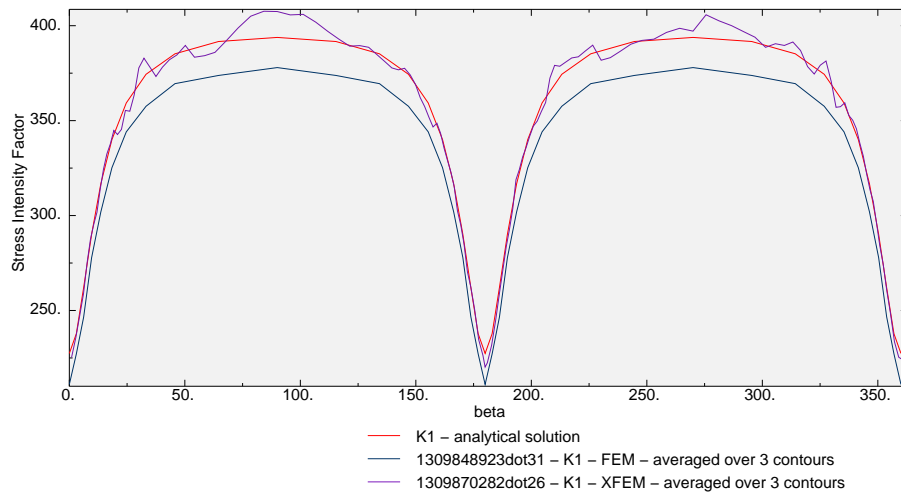


Figure 4.46: Comparison between the calculated values for K_I by *FEM* and *XFEM* along the crack front for crack with aspect ratio of 3

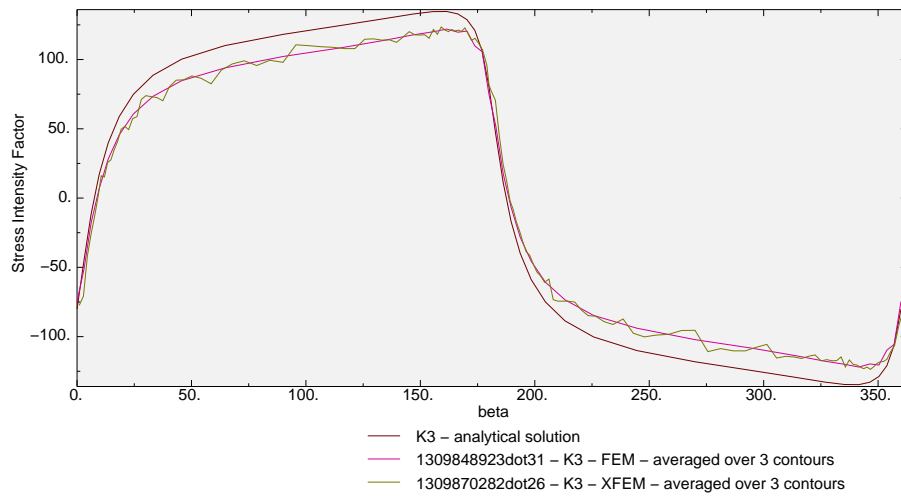


Figure 4.47: Comparison between the calculated values for K_{III} by *FEM* and *XFEM* along the crack front for crack with aspect ratio of 3

ID	crack ratio	seeds				max error [%]		
		czm	cZr	ar	cr	K_I	K_{II}	K_{III}
1309848923dot31	3	5	5	5	5	4.54	6.0	11.99
1309930186dot92	5	5	5	5	5	3.9	2.86	8.77
1309930836dot52	10	5	5	5	5	4.51	4.32	27.5

Table 4.10: *FEM* models included in the comparison of the accuracy with *XFEM* models

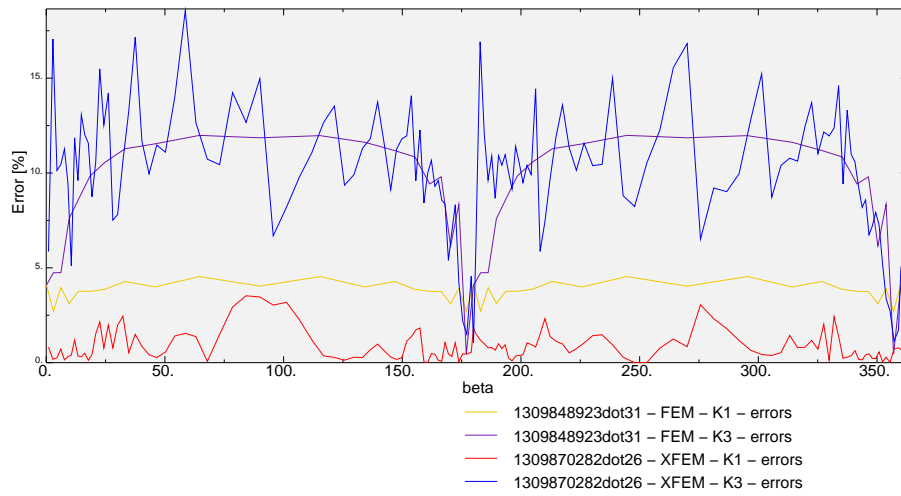


Figure 4.48: Comparison between the calculated errors for K_{III} by *FEM* and *XFEM* along the crack front for crack with aspect ratio of 3

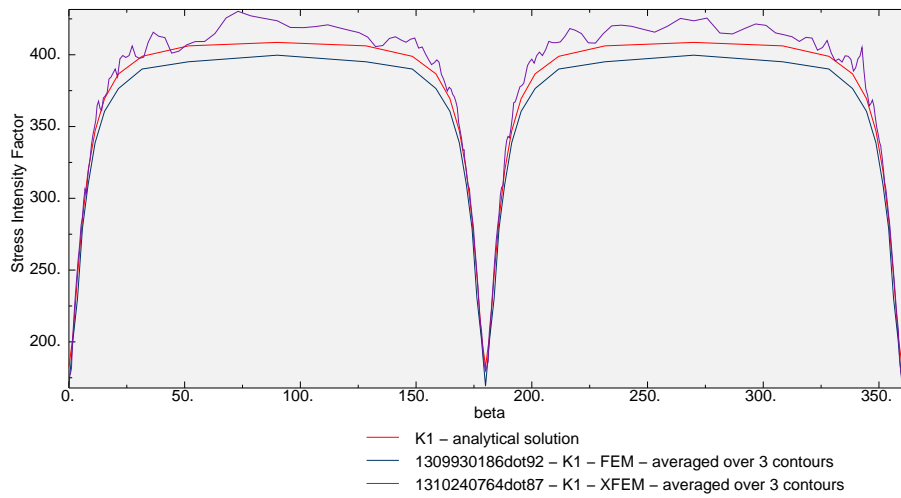


Figure 4.49: Comparison between the calculated values for K_I by *FEM* and *XFEM* along the crack front for crack with aspect ratio of 5

ID	crack ratio	seeds		max error [%]		
		general	crack	K_I	K_{II}	K_{III}
1309870282dot26	3	15	1	3.53	199.86	18.56
1310240764dot87	5	15	1	7.0	200.66	15.89
1310240980dot74	10	15	1	7.86	202.52	14.09

Table 4.11: *XFEM* models included in the comparison of the accuracy with *FEM* models

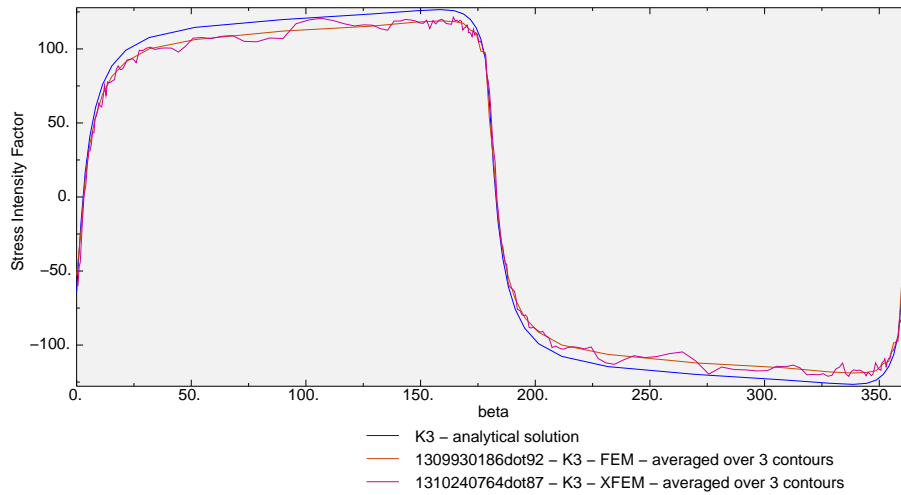


Figure 4.50: Comparison between the calculated values for K_{III} by *FEM* and *XFEM* along the crack front for crack with aspect ratio of 3

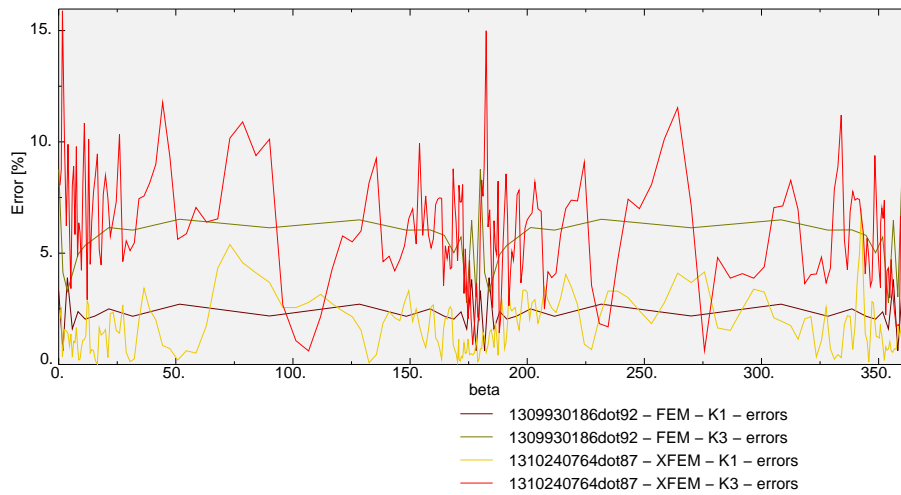


Figure 4.51: Comparison between the calculated errors for K_{III} by *FEM* and *XFEM* along the crack front for crack with aspect ratio of 5

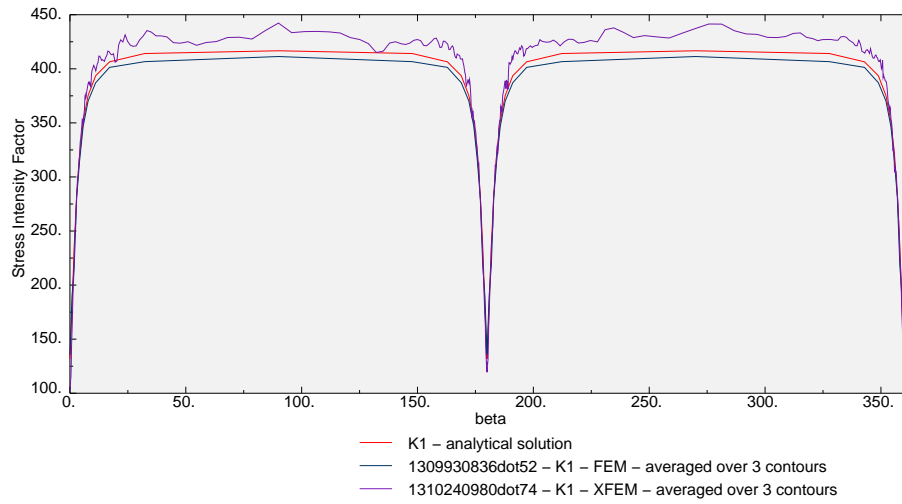


Figure 4.52: Comparison between the calculated values for K_I by *FEM* and *XFEM* along the crack front for crack with aspect ratio of 10

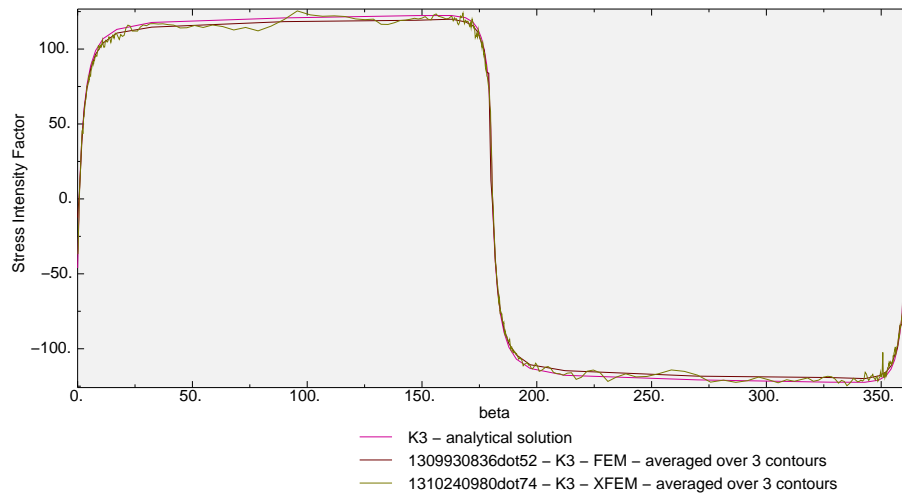


Figure 4.53: Comparison between the calculated values for K_{III} by *FEM* and *XFEM* along the crack front for crack with aspect ratio of 10

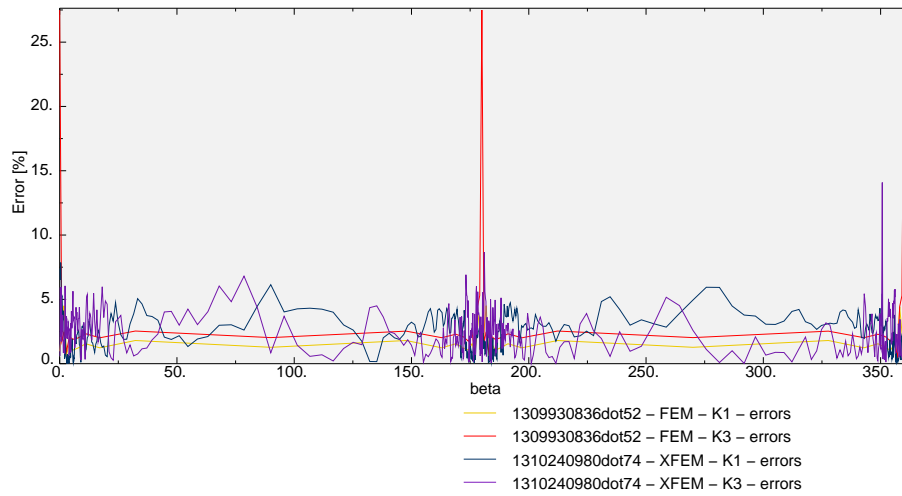


Figure 4.54: Comparison between the calculated errors for K_{III} by FEM and $XFEM$ along the crack front for crack with aspect ratio of 10

ID	crack ratio	analysis type	model type	figure
1309848923dot31	3	FEM	<i>crackNormal</i>	4.55
1309869569dot74	3	XFEM	<i>crackPartition</i>	4.56
1310240764dot87	5	XFEM	<i>crackPartition</i>	4.57
1310240980dot74	10	XFEM	<i>crackPartition</i>	4.58
1309907898dot52	3	XFEM	<i>simple</i>	4.59

Table 4.12: Visualization of models

4.9 Visualization of the stress intensity factors

In this section are presented visualizations of the stress intensity factors for cracks with aspect ratios of 3, 5 and 10 and FEM and $XFEM$ analyses. Models are listed in table 4.12 and illustrated in figures 4.56, 4.58, 4.57, 4.55 and 4.59.

The visualization can also be utilized as a verification tool. For instance, figure 4.59 is a visualization of a $XFEM$ *simple* model type with seed size of 10. The visualization, clearly illustrates the accuracy of the approximation.

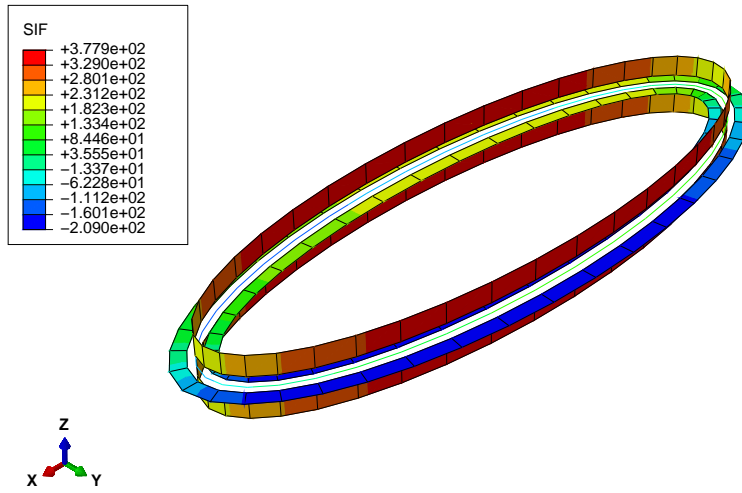


Figure 4.55: Visualization of the *1309848923dot31* FEM model with crack aspect ratio 3

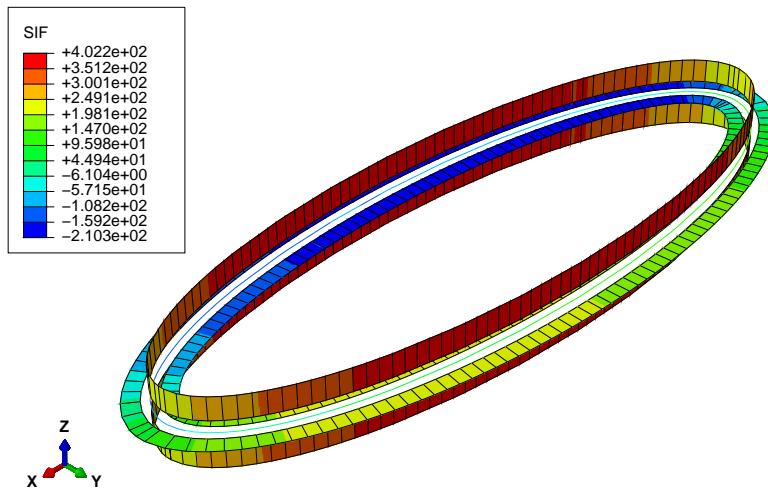


Figure 4.56: Visualization of the *1309869569dot74* XFEM model with crack aspect ratio 3

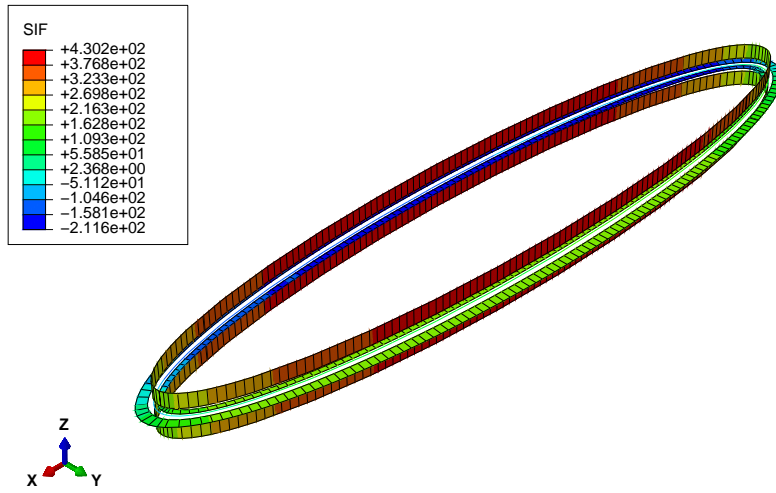


Figure 4.57: Visualization of the $1310240764dot87$ XFEM model with crack aspect ratio 5

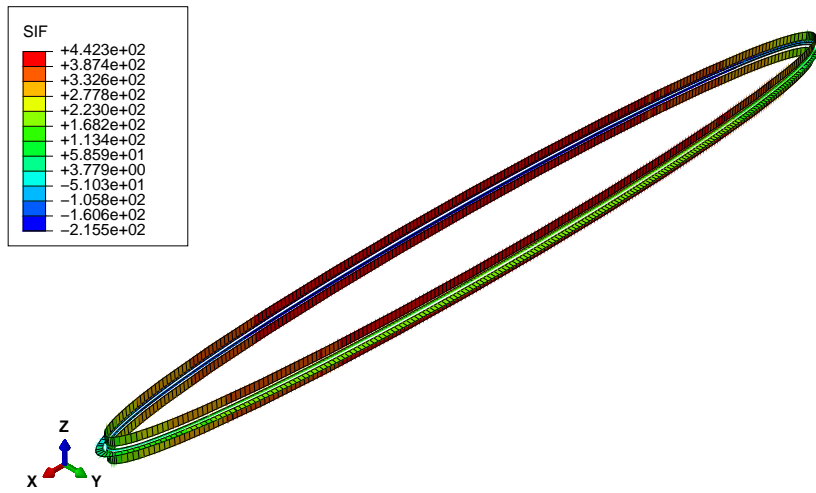


Figure 4.58: Visualization of the $1310240980dot74$ XFEM model with crack aspect ratio 10

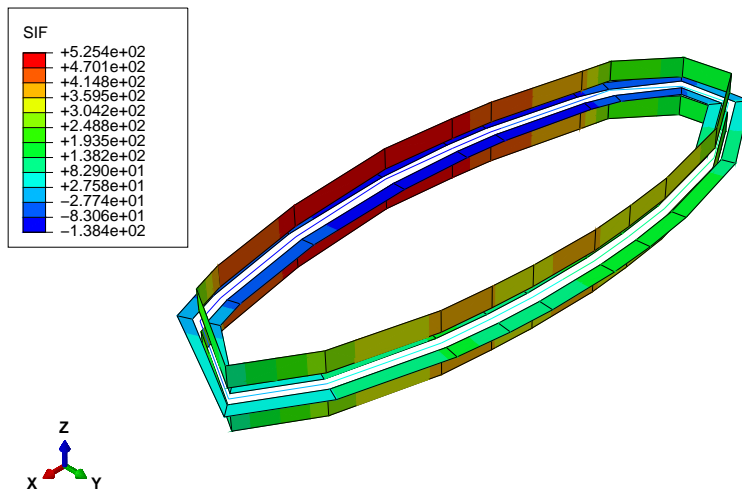


Figure 4.59: Visualization of the *1309907898dot52* XFEM model with crack aspect ratio 3

Chapter 5

Conclusion

5.1 Introduction

The present project is an attempt to facilitate the analysis of elliptic cracks by providing a framework, which is capable of generating, analyzing, extracting the calculated values from the output database, writing the results to a custom *shelve* database and visualizing the results.

The program automates the described process and the created *shelve* database, which is a valuable knowledge base containing calculations for cracks with different parameters.

5.2 Summary of results

From the results in chapter 4 can be concluded that the *crackNormal* model type with *quadratic reduced integration* elements and *elliptic* mesh transformation would give the most consistent results. Comparable accuracy can also be achieved also with *linear reduced integration* elements, however, they should be used with meshes with higher density. Noise in the *FEM* solution can be reduced by increasing the mesh density, a viable option is also using *linear reduced integration* elements with a fine mesh.

XFEM can also be used successfully to analyze elliptic cracks, however, at the moment of writing, Abaqus has only an *XFEM* implementation with *linear* elements. Results prove that the accuracy of the *XFEM* solution is less consistent than the accuracy of the conventional *FEM* performed with *quadratic reduced integration* elements and has considerably more noise. Therefore, a dense mesh is generally required for accurate evaluation of stress intensity factors. In addition, with the increase of the crack aspect ratio the number of elements increase in the mesh, resulting in a more computationally expensive solution.

The mesh independent formulation of *XFEM* is a considerable advantage, however, to improve accuracy, use of dense mesh in the vicinity of the singularity is strongly advisable.

The visualization technique proposed can also be especially convenient as a diagnostic tool for verification of the *XFEM* approximation of the crack geometry as shown in figure 4.59.

5.3 Implications for practice and recommendations

The developed program in the project significantly facilitates modeling and analysis of embedded cracks. In addition, the developed visualization technique considerably improves representation of stress intensity factors by mapping the values to coordinates in three dimensional space.

Both *FEM* and *XFEM* model databases can be employed in a larger analysis by means of submodeling.

In addition, the program can be of utility for convergence studies for optimal mesh and analysis technique for a particular case. The convergence study can be executed on the model databases created by the program and then the results applied as a guidance in analysis of larger models.

Furthermore, the program can be utilized to facilitate the selection of optimal combination of seed size and singularity radius for an *XFEM* analysis, by performing a convergence study, similar to the one discussed in section 4.8.1 and designing a mesh for the analysis with the obtained parameters.

Use of results of the present project and the developed program are a good starting point for further analyses and fashion it is used would mostly depend on the specific analysis. However, my personal recommendation is to automate the analysis as feasible, the amount of parameters is vast and extensive analysis without automation may prove particularly challenging and unfeasible if performed manually. For instance, even creating a graph from the history output of the stress intensity factors for an *XFEM* analysis, without automation may prove quite challenging.

5.4 Implications for further development

The program for the project in its current state should provide a sound foundation for further development. Furthermore, it has been designed with scalability in mind and can be extended in a variety of ways.

5.4.1 Modeling automation

A major feature, would be an automated procedure to analyze cracks by submodeling, which would facilitate significantly parametric studies and optimization.

5.4.2 Results processing and optimization

One possibility for further functionality is the development of algorithms to further analyze results and find parameter configurations, which meet a certain criteria.

5.4.3 Other functionality

A more trivial development is to include results for *J*-integral and other fracture mechanics parameters.

5.5 Conclusion

In conclusion, the project attempted to create a self-contained and automated framework, built upon Abaqus software for modeling, analysis, results storage and visualization of elliptic cracks. As a result, the framework allows to analyze stress intensity factors, calculated by *FEM* and *XFEM* and compare their values with analytical solutions. The obtained results, comparisons between analysis types and convergence studies are presented in chapter 4. Furthermore, results prove, that *XFEM* is a promising development for stress intensity factors, although, the issue with opposite sign for K_{II} has not been resolved.

The introduced visualization technique, would come as a useful representation and diagnostic tool in analyzing *XFEM* crack geometry approximation, as well as to improve representation of stress intensity factors or other fracture mechanics parameter.

Bibliography

- [1] Y. Abdelaziz and A. Hamouine. A survey of the extended finite element. *Computers & Structures*, 86(11-12):1141–1151, June 2008.
- [2] W.E. Anderson. An engineer views brittle fracture history. *Boeing report*, 1960.
- [3] A. O Ayhan. Three-Dimensional fracture analysis using tetrahedral enriched elements and fully unstructured mesh. *International Journal of Solids and Structures*, 2010.
- [4] Ivo Babuska and Manil Suri. The p- and h-p versions of the finite element method, an overview. *Computer Methods in Applied Mechanics and Engineering*, 80(1-3):5–26, June 1990.
- [5] T. Belytschko, R. Gracie, and G. Ventura. A review of extended/generalized finite element methods for material modeling. *Modelling and Simulation in Materials Science and Engineering*, 17:043001, 2009.
- [6] James Chen, Xianqiao Wang, Huachuan Wang, and James D. Lee. Multiscale modeling of dynamic crack propagation. *Engineering Fracture Mechanics*, 77(4):736–743, March 2010.
- [7] C. Colombo, M. Guagliano, and L. Vergani. A numerical analysis of flat internal cracks under mixed mode loading. *Theoretical and Applied Fracture Mechanics*, 50(1):66–73, August 2008.
- [8] H. G. deLorenzi. On the energy release rate and the j-integral for 3-D crack configurations. *International Journal of Fracture*, 19(3):183–193, July 1982.
- [9] Hachmi Ben Dhia and Olivier Jamond. On the use of XFEM within the arlequin framework for the simulation of crack propagation. *Computer Methods in Applied Mechanics and Engineering*, 199(21-22):1403–1414, April 2010.
- [10] V. I. Fabrikant. The stress intensity factor for an external elliptical crack. *International Journal of Solids and Structures*, 23(4):465–467, 1987.
- [11] R. Forman and J. Beek. Fracture mechanics and fatigue crack growth analysis software.
- [12] M. Guagliano and M. Pau. An experimental-numerical approach for the analysis of internally cracked railway wheels. *Wear*, 265(9-10):1387–1395, October 2008.

- [13] M. Guagliano, L. Vergani, and M. Vimercati. Determination of stress intensity factors for three-dimensional subsurface cracks in hypoid gears. *Engineering Fracture Mechanics*, 73(14):1947–1958, September 2006.
- [14] T. K. Hellen. *How To Undertake Fracture Mechanics Analysis with Finite Elements*. NAFEMS Ltd, 2001 edition.
- [15] T. K Hellen. On the method of virtual crack extensions. *International Journal for Numerical Methods in Engineering*, 9(1):187–207, January 1975.
- [16] Thomas Hettich, Andrea Hund, and Ekkehard Ramm. Modeling of failure in composites by X-FEM and level sets within a multiscale framework. *Computer Methods in Applied Mechanics and Engineering*, 197(5):414–424, January 2008.
- [17] A. R. Ingraffea. Introduction to FRANC2D, FRANC2D/L and FRANC3D, May 2004.
- [18] M. K. Kassir and George C. Sih. *Three-dimensional crack problems: a new selection of crack solutions in three-dimensional elasticity*. Noordhoff International Pub., 1975.
- [19] Zentech Ltd. State-of-the-art software for 3D fracture mechanics simulation, 2008.
- [20] Mark Lutz. *Learning Python*. O’Reilly Media, 4 edition, October 2009.
- [21] Robert C. Martin. *Clean Code: A Handbook of Agile Software Craftsmanship*. Prentice Hall, 1 edition, August 2008.
- [22] J. M. Melenk and I. Babuska. The partition of unity finite element method: Basic theory and applications. *Computer Methods in Applied Mechanics and Engineering*, 139(1-4):289–314, December 1996.
- [23] Prof Soheil Mohammadi. *Extended Finite Element Method: for Fracture Analysis of Structures*. Wiley-Blackwell, 1 edition, April 2008.
- [24] B. Nuller, M. Kachanov, and E. Karapetian. On the stress intensity factor for the elliptical crack. *International Journal of Fracture*, 92:17–20, July 1998.
- [25] D. M. Parks. A stiffness derivative finite element technique for determination of crack tip stress intensity factors. *International Journal of Fracture*, 10(4):487–502, December 1974.
- [26] H. Rajaram, S. Socrate, and D. M. Parks. Application of domain integral methods using tetrahedral elements to the determination of stress intensity factors. *Engineering Fracture Mechanics*, 66(5):455–482, July 2000.
- [27] Johann Rannou, Nathalie Limodin, Julien Rethore, Anthony Gravouil, Wolfgang Ludwig, Marie-Christine Baietto-Dubourg, Jean-Yves Buffiere, Alain Combescure, Francois Hild, and Stephane Roux. Three dimensional experimental and numerical multiscale analysis of a fatigue crack. *Computer Methods in Applied Mechanics and Engineering*, 199(21-22):1307–1325, April 2010.

- [28] M. Schollmann, M. Fulland, and H. A. Richard. Development of a new software for adaptive crack growth simulations in 3D structures. *Engineering Fracture Mechanics*, 70(2):249–268, January 2003.
- [29] Abaqus Version. 6.10 documentation. *Dassault Systemes Simulia Corporation*, 2010.
- [30] John Zelle. *Python Programming: An Introduction to Computer Science*. Franklin, Beedle & Associates Inc, 2nd revised edition edition, September 2010.